DEVELOPMENT OF ALGORITHMICALLY PRIORITIZED METHODS FOR GENERALIZED NATURAL PRODUCT SYNTHESIS

BY

CLAIRE LILLIAN WOLFE SIMONS

DISSERTATION

Submitted in partial fulfillment of the requirements
for the degree of Doctor of Philosophy in Chemistry
in the Graduate College of the
University of Illinois Urbana-Champaign, 2021

Urbana, Illinois

Doctoral Committee:

Professor Martin D. Burke, Chair
Professor Wilfred A. van der Donk
Professor Douglas A. Mitchell
Associate Professor Jian Peng

ABSTRACT

The synthesis of small molecule natural products has long captivated the attention of chemists and has generally proceeded via custom solutions to specific molecules. We propose to instead utilize a human guided algorithm to analyze a building block approach to natural products and identify key methodologies. Additionally, the stereochemical make up around each coupling can be used to help guide the creation of a substrate table. Herein we report the use of an algorithm to systematically fragment all linear natural product, conduct an optimization to choose the smallest set of blocks required to cover >75% of natural product chemical space, and establish a list of impactful couplings. We then selected one of the couplings and used a data driven substrate scope to guide methodological development that covered the predetermined substrates.

TABLE OF CONTENTS

CHAPTER 1

INTRODUCTION

Big, complex, multi-dimensional problems are hard for humans to solve. We generally have to break large problems down into smaller pieces and work through the pieces sequentially, applying and modifying our solutions where we can or creating new ones where we can't. Computers on the other hand, excel at handling massive amounts of data at a time, but still fall short of human creativity and innovation. This has resulted in many examples of computer science being used for discovering solutions for very targeted problems, but not for identifying what narrowly focused problems within a larger complex problem are worth solving. We believe that computer science can be used to help humans understand the full scope of these kinds of multi-dimensional problems and identify the specific areas of research for which the combination of solutions would provide a solution to the multi-dimensional problem.

The field of genomics is a powerful example of this approach being used time and again beginning with the Human Genome Project, where algorithms and compute power were essential for bringing together genes already discovered as well as filling in the gaps.[1–4] This interface of computer and human abilities has continued to enable more rapid understanding of both individual genes and complex multi-gene phenomena. For example, the BLAST algorithm can now be used to rapidly characterize a gene of unknown function, and genome-wide association studies performed on thousands of individuals first established links between collections of genetic variants and increased risk of complex psychiatric disorders.[5] The advantages of systematic science have similarly been leveraged in understanding RNA, proteins,[6] and human gut microbes.[7]

1-1 AUTOMATION AND MODULARITY: POWERFUL APPROACHES TO SYNTHESIS

Computers are not the only machines that have greatly enabled human innovation. Machinery enabling automation was a significant contributor to the industrial revolution, with inventions like the "spinning jenny"[8] and Fourdrinier machine[9] greatly increasing the output and consistency of quality of yarn and paper, respectively. Today, so many of the things we utilize are made in an automated fashion that 'hand-made' is frequently a notable quality of an object. Automation has also made its way into the world of chemistry with development of fully or partially automated processes for key chemicals of interest, whether to help with the speed of synthesis, the scale of synthesis, or the handling of dangerous and/or sensitive materials.[10] Eli Lily utilized automation to synthesize 24kg of prexasertib monolactate monohydrate for clinical trials,[11] while automation of the synthesis of radio labels for PET scans enables on site and on demand synthesis of the correct dose of radioactive compounds with short half-lives.[12]

In addition to automation, modularity is another concept that has been drastically beneficial to production on both the macro and micro scale. Henry Ford's assembly line is perhaps the most famous example of the power of modular building-block based construction[13] and modular construction is as ubiquitous as automation in the products of today.[14] Chemists and biochemists have also exploited modular construction in the synthesis of macromolecules: peptides are composed of 20 amino acids, DNA and RNA are composed of 5 nucleotides, and even sugar chemistry—though more complex due to the large number of sugar monomers and the ability to introduce branching—is still enabled by the modular construct of oligosaccharides. By adding blocks one at a time any desired sequence can be made. For the sequential addition of one block at a time to occur without side products, a bifunctional building block with reversible protection

of one terminus is required. After coupling of the first two blocks occurs a deprotection reveals a new active terminus to couple with the next (**Figure 1-1**). For amino acids that breakthrough came in 1932 with Bergman's and Zervas' creation of the carbobenzoxy (Z) protecting group for the N-
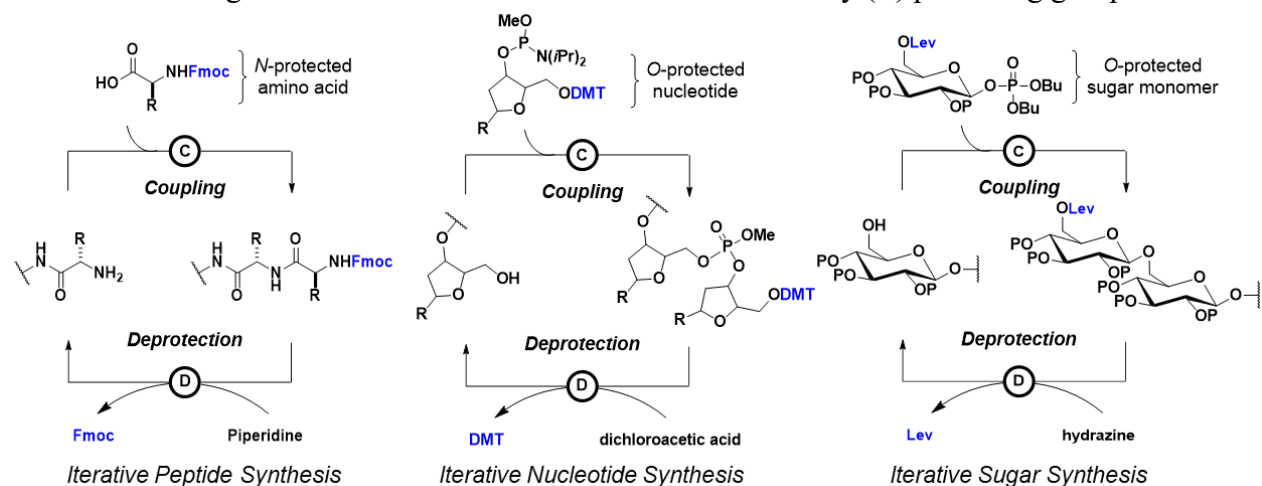

Figure 1-1 Iterative synthetic platforms for peptides, oligonucleotides, and oligosaccharides

terminus.[15] Its harsh conditions for deprotection limited its use, and 20 years later Carpino's development of the acid labile tert-butyloxycarbonyl (Boc) group[16] all but replaced it. Carpino also contributed the base labile 9-fluorenylmethoxycarbonyl (Fmoc) group[17] in 1970, which was then popularized by Sheppard's[18] and Meienhofer's[19] independent reports of its use. Due to their mild and orthogonal deprotection conditions Boc and Fmoc continue to see wide use and further development today.[20,21] Both oligonucleotide and oligosaccharide synthesis have applied similar strategies to enable the growth of monomers into oligomers in a controlled and precise fashion.[22,23]

Many types of small molecules, particularly aromatic compounds, have also been made through this modular and iterative approach. Functionalized naphthalenes have seen a wide variety of uses as pharmaceuticals, liquid crystals, organic dyes, and plastic additives.[23–25] In 2015, Kwon and coworkers described a phosphine-mediated multicomponent cascade reaction with a 1,2-dialdehyde and an ethyl allenoate, where a subsequent oxidation reveals another dialdehyde allowing for iteration.[26] Polyacenes have great value as semiconductors but become increasingly

difficult to access synthetically as they get larger. Utilizing iterative Diels-Alder to build a precursor of the desired size followed by aromatization and oxidations reactions allowed the Bettinger group to synthesize and study octacene and nonacene.[27]

Rather than identifying monomers that could be iteratively assembled to make useful substances, one could consider which chemical reactions would be well suited to iteration. The rapidly expanding scope and stereospecificity of cross-coupling reactions for the synthesis of carbon-carbon and carbon-heteroatom bonds makes such couplings attractive candidates for iterative assembly.[28] The Suzuki-Miyaura and Buchwald-Hartwig couplings in particular can employ non-toxic and shelf-stable building blocks, be highly efficient and stereospecific, and proceed under mild reaction conditions with high levels of functional group tolerance. Importantly, the ability of the N-methyliminodiacetic acid (MIDA) ligand to reversibly attenuate the reactivity of boronic acids allows iterative cycles of coupling and deprotection to sequentially assemble bifunctional MIDA boronates while preventing undesired oligomerization (**Figure 1-2** *left*).[29] With this iterative cross coupling (ICC) approach, all of the functional groups, oxidation states,

Figure 1-2 *Left* Iterative cross coupling platform utilizing MIDA boronates *Right* Examples of molecules made with ICC

4
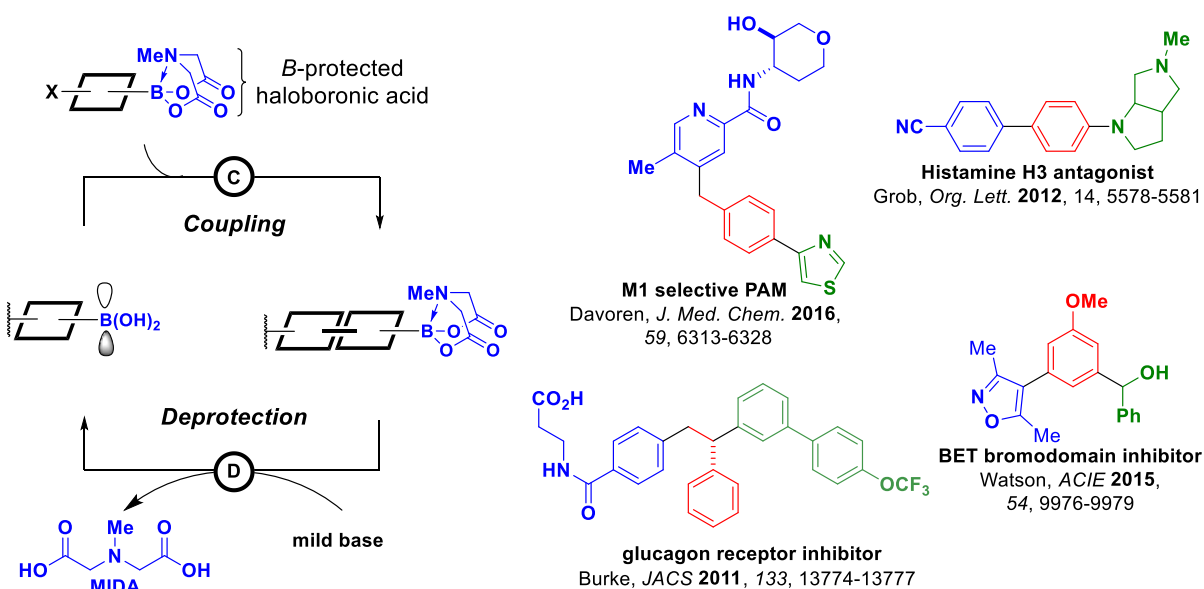
and stereochemistry required for natural product assembly are pre-installed in the blocks (**Figure 1-2** *right*).

1-2 NATURAL PRODUCTS IMPORTANCE TO SOCIETY AND THE HISTORY OF THEIR SYNTHETIC DEVELOPMENT

Of small molecules, natural products have arguably had the greatest impact on our lives. They represent or inspired more than half of all human medicines, a third of all crop protectants, many of the safest food preservatives, and the most highly informative biological probes (**Figure 1-3**). For example, artemisinin helps nearly 400 million
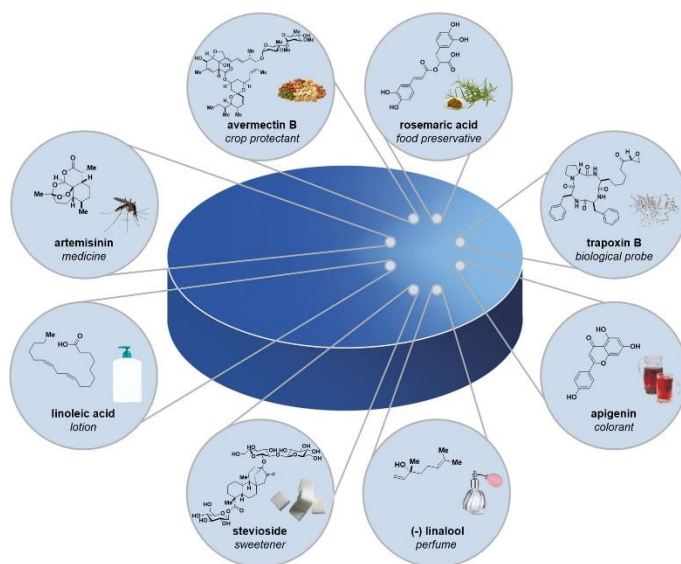

Figure 1-3 Natural products serve a wide array of purposes in both research and everyday life

people survive or prevent infections with malaria each year,[30] abamectin helps protect more than a billion tons of food each year,[31] and trapoxin enabled the discovery of human histone deacetylase enzymes, which helped launch the field of epigenetics.[32] Natural products also make the world more wonderful to see, smell, taste, and feel by serving as many of the most popular colorants, perfumes, seasonings, and lotions used in everyday life around the globe.[33]

Because of their capacity for function and the frequent difficulty of isolating them from producing organisms, the synthesis of small molecule natural products has long captivated the attention of chemists. Total syntheses of natural products have historically been highly customized to each target—a slow and specialist-dependent process—resulting in an ad hoc selection of

methodological problems. Impactful methodologies certainly have arisen from the design of customized synthetic routes including the Corey-Bakshi-Shibata reduction, which was developed for the synthesis of PGF2α,[34] and carbodiimide-based reactions for the formation of peptide bonds, which was first utilized in the synthesis of penicillin.[35] Additionally, the discovery of interesting reactivity and its optimization for broad application has led to many impactful methods such as olefin metathesis. While methods such as these have turn out to be broadly useful, the majority remain more narrowly applicable.

Thinking back to the success of a modular approach to the synthesis of other biomolecules, one must wonder why this approach has yet to be widely adopted for small molecule natural products. There has certainly been success in iterative approaches to specific subclasses of or motifs within natural products. Chiral auxiliaries in combination with iterative aldol reactions have been widely used in polypropionate synthesis,[36–39] while the allylboration work of Brown and coworkers has provided access to the 1,3-polyol motif of polyketides.[40–42] More recently the Aggarwal group has very successfully leveraged iterative chain extension of boronic esters to create challenging Csp^3 rich natural products with excellent stereospecificity.[43–45] Our group has utilized our MIDA boronate platform
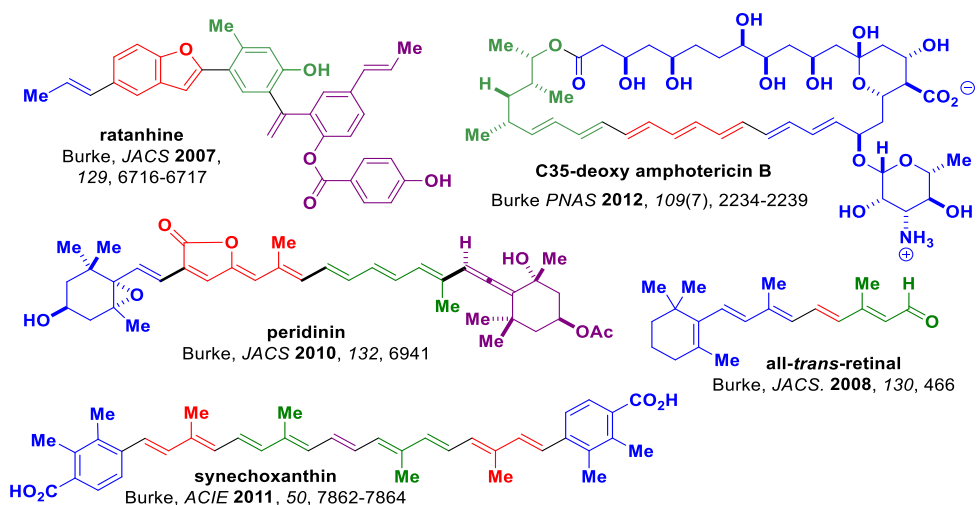

Figure 1-4 Natural products made through ICC

to synthesis a variety of natural products from carotenoids[46,47], to chromophores[48], to lignans,[49]

even leveraging the modularity to easily create derivatives[50] (**Figure 1-4**). While all impressive advances in iterative and modular synthesis of natural products and similar to the humble beginnings of solid phase synthesis, the current power of iterative peptide or oligonucleotide synthesis hint at the still untapped potential within natural products.

1-3 PROMISING EVIDENCE FOR A NEW APPROACH FOR GENERALIZED NATURAL PRODUCT SYNTHESIS

I believe the limitations of humans to consider the full scope of the problem due to the significant increase in complexity of natural products comparted to other biomolecules have prevented natural product synthesis from keeping pace with said biomolecules. But if the power of computers to process immense amounts of data can be brought in to assist chemists, I believe more general and impactful methodologies can be identified and worked on. There are several promising lines of evidence that point to the possibility of a modular and iterative synthetic approach that could be applied widely across natural products.

First, most natural products are derived from one or more of four biosynthetic pathways, each of which employs common coupling chemistry to iteratively assemble a small number of highly versatile bifunctional building blocks: polyterpenes from isopentenyl and dimethylallyl pyrophosphate, polyketides from malonyl coenzyme A (CoA) and methylmalonyl CoA, polyphenylpropanoids from 4-coumaroyl-CoA and malonyl CoA, and fatty acids from malonyl CoA (**Figure 1-5**). This building block-based biosynthesis leads to significant structural similarities within and between these four major biosynthetic classes. For example, fatty acids, polyketides, and polyphenylpropanoids all utilize malonyl CoA in their iterative assembly, suggesting that these three biosynthetic classes have evolutionarily homologous enzymes that
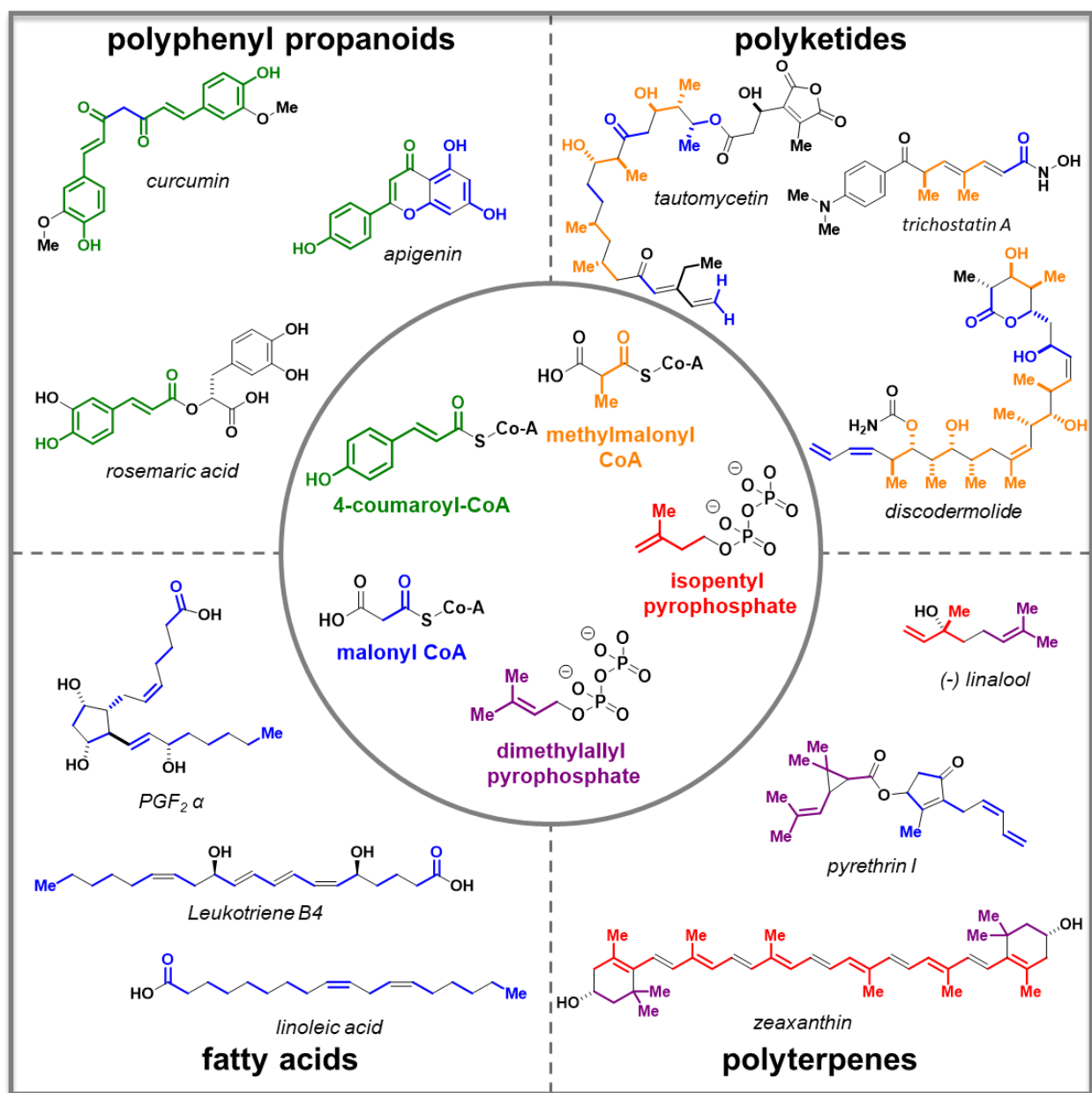
Figure 1-5 The four classes of small molecule natural products made through iterative carbon-carbon bond formation can be biosynthetically tracked back to a small set of blocks.

underwent divergent evolution.[51–56] Even the most topologically complex macrocyclic and/or polycyclic natural products are typically biosynthesized via the same iterative building block assembly processes to make linear precursors which are then (poly)cyclized. Additionally, similar to the conservation of functional protein domains, many functional domains in natural products have been reused and repurposed throughout evolution, leading to the conservation of many

structural subunits.[57] As most natural products bind proteins, the limited number of common protein folds suggests reciprocated evolutionary constraints on the structures of proteins and natural products.

An investigation into the possibility of identifying common building blocks and the chemistry required for their assembly was undertaken by former group member Eric Woerly with a small subset of natural products called polyenes. Polyenes are defined by their long section of conjugated double bonds and are present in all four classes of small molecule natural products and can be made through a variety of biosynthetic pathways. Considering just the polyene section, 15 motifs were identified that covered greater than 75% of all 2,839 polyene natural products. Breaking the motifs down into bifunctional MIDA boronates revealed that theoretically only five blocks and one coupling would be required for their assembly. However, due to the realities of organic synthesis, it was determined and then demonstrated that 12 blocks and one coupling reaction were sufficient to cover most of the polyene chemical space[58] (**Figure 1-6**).
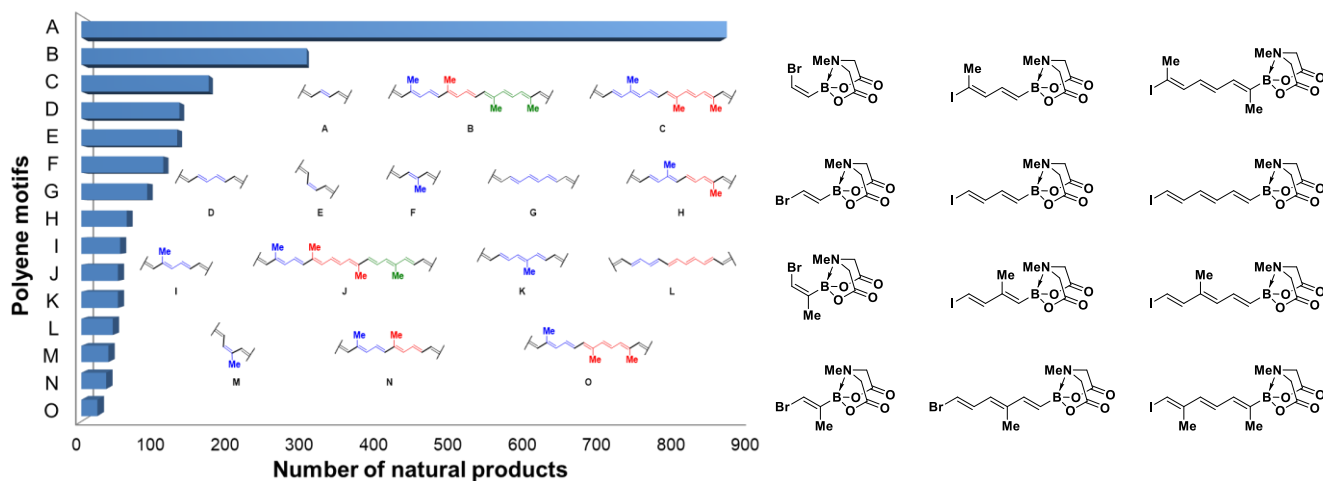
Figure 1-6 Manual analysis of 2839 polyene natural products reveals a collection of motifs A-O which cover 75% polyene space which can be covered with only 12 building blocks.

One of the most powerful reasons for pursuing a modular approach is its easy adaption to automation. Because a modular approach with its limited building blocks and reactions is a

polypeptides   **oligonucleotides**   **oligosaccharides**
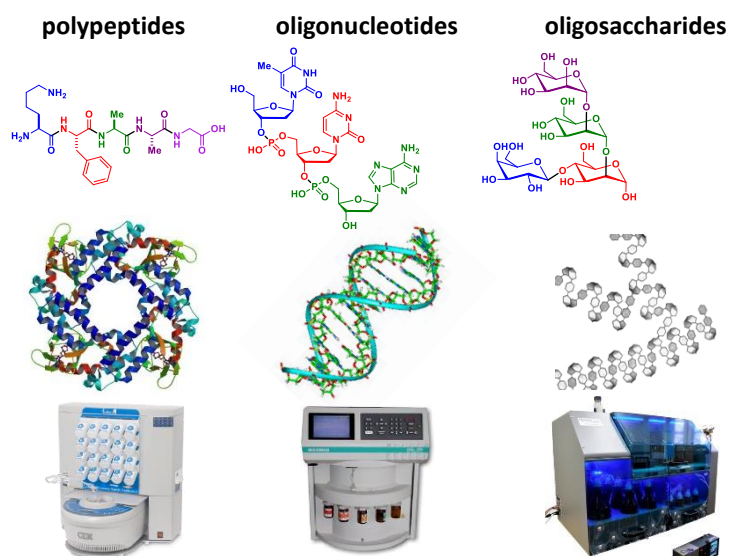
Figure 1-7 Automated synthesizers for polypetides, oligonucleotides, and oligosaccharides

bounded space, the number of functions a machine must be able to accomplish to replace a synthetic chemist is drastically reduced. The success of this combination of automation and modularity into an automated synthesizer are evident in peptides and oligonucleotides, and increasingly in oligosaccharides (**Figure 1-7**). For peptides and oligonucleotides, great strides in their automation have been made since the pioneering work of Merrifield[59] and Caruthers[60] respectively. Automated bench top synthesizers accessible to non-specialists and on-demand synthesis and shipping are available for both peptides and oligonucleotides, which has accelerated and democratized the discovery of new molecular functions in those spaces. Seeberger has made great strides in development of automated oligosaccharides synthesis, which requires substantially more building blocks than either peptides or oligosaccharides.[61–63]

Our group has pioneered an automated synthetic machine to complement our MIDA boronate platform. One of the most challenging parts of automating natural products is that the blocks don't all have a common handle like the larger biomolecules do. Such a common handle is vital for the creation of a common purification step, and in most cases is utilized to attach to a solid support allowing for easy washing away of all waste products. Fortuitously for us, MIDA boronates have a uniform binary elution property on silica where a low percentage methanol in

ether solution does not move them from the baseline while THF elutes them easily. This allows for a catch and release type purification. With such a common purification strategy in hand, automation of a
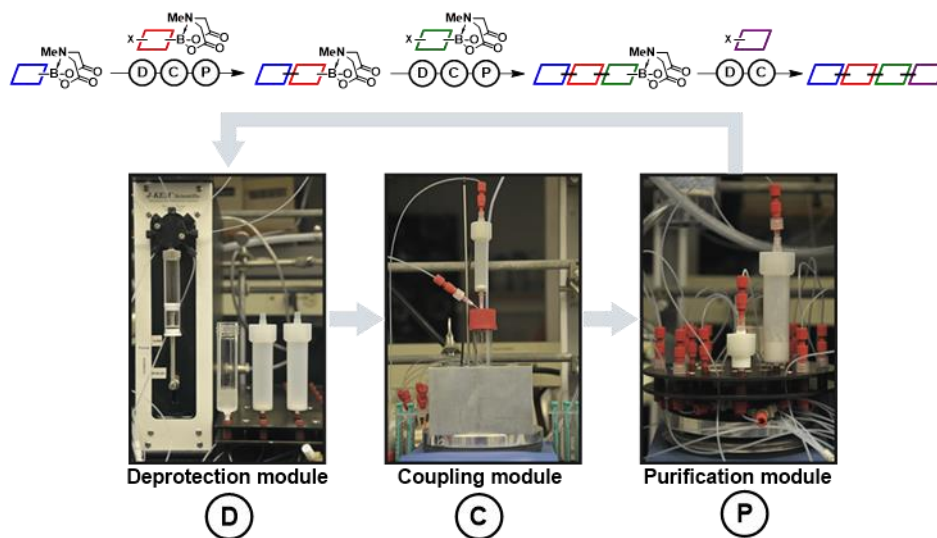
Figure 1-8 Automated synthesizer developed in our lab to perform ICC with MIDA boronates

deprotect, couple, purify cycle was achieved (**Figure 1-8**). The automated synthesizer was used to make a collection of small molecules, both natural products and other targets, and even several linear precursors of natural products which were then cyclized manually.[64]

With such a collection of promising evidence for the ability to create a modular and automatable platform for generalized small molecule natural product synthesis, we decided to tackle just such a problem. Knowing that the scope of this problem was too large for us—or any human—to handle alone, we needed to bring in power of computers. We needed an algorithm that brought the full power of computer science, but still allowed for input and direction from human chemical expertise, something not common in many of the current powerful black box chemistry algorithms.

1-4 REFERENCES

(1)   Abdellah, Z.; Ahmadi, A.; Ahmed, S.; Aimable, M.; Ainscough, R.; *et al.* Finishing the Euchromatic Sequence of the Human Genome. *Nature* **2004**, *431* (7011), 931–945. https://doi.org/10.1038/nature03001.

(2)   Craig Venter, J.; Adams, M. D.; Myers, E. W.; Li, P. W.; Mural, R. J.; *et al.* The Sequence of the Human Genome. *Science* **2001**, *291* (5507), 1304–1351. https://doi.org/10.1126/science.1058040.

(3)   Lander, E. S.; Linton, L. M.; Birren, B.; Nusbaum, C.; Zody, M. C.; *et al.* Initial Sequencing and Analysis of the Human Genome. *Nature* **2001**, *409* (6822), 860–921. https://doi.org/10.1038/35057062.

(4)   White, O.; Dunning, T.; Sutton, G.; Adams, M.; Venter, J. C.; Fields, C. A Quality Control Algorithm for DNA Sequencing Projects. *Nucleic Acids Research* **1993**, *21* (16), 3829–3838. https://doi.org/10.1093/nar/21.16.3829.

(5)   Geschwind, D. H.; Flint, J. Genetics and Genomics of Psychiatric Disease. *Science*. American Association for the Advancement of Science September 25, 2015, pp 1489–1494. https://doi.org/10.1126/science.aaa8954.

(6)   Cravatt, B. F.; Simon, G. M.; Yates, J. R. The Biological Impact of Mass-Spectrometry-Based Proteomics. *Nature*. Nature Publishing Group December 13, 2007, pp 991–1000. https://doi.org/10.1038/nature06525.

(7)   Gill, S. R.; Pop, M.; DeBoy, R. T.; Eckburg, P. B.; Turnbaugh, P. J.; Samuel, B. S.; Gordon, J. I.; Relman, D. A.; Fraser-Liggett, C. M.; Nelson, K. E. Metagenomic Analysis of the Human Distal Gut Microbiome. *Science* **2006**, *312* (5778), 1355–1359. https://doi.org/10.1126/science.1124234.

(8)   Guest, Richard. *A Compendious History of the Cotton Manufacture : Richard Guest.*; F. Cass and C°,: London :, 1968.

(9)   *Papermaking in Britain 1488–1988 : A Short History*; Bloomsbury Academic, 1988. https://doi.org/10.5040/9781474284943.

(10)   Trobe, M.; Burke, M. D. The Molecular Industrial Revolution: Automated Synthesis of Small Molecules. *Angewandte Chemie - International Edition*. Wiley-VCH Verlag April 9, 2018, pp 4192–4214. https://doi.org/10.1002/anie.201710482.

(11)   Cole, K. P.; Groh, J. M. C.; Johnson, M. D.; Burcham, C. L.; Campbell, B. M.; Diseroad, W. D.; Heller, M. R.; Howell, J. R.; Kallman, N. J.; Koenig, T. M.; May, S. A.; Miller, R. D.; Mitchell, D.; Myers, D. P.; Myers, S. S.; Phillips, J. L.; Polster, C. S.; White, T. D.; Cashman, J.; Hurley, D.; Moylan, R.; Sheehan, P.; Spencer, R. D.; Desmond, K.; Desmond, P.; Gowran, O. Kilogram-Scale Prexasertib Monolactate Monohydrate Synthesis under Continuous-Flow CGMP Conditions. *Science* **2017**, *356* (6343), 1144–1151. https://doi.org/10.1126/science.aan0745.

(12)   Reischl, G.; Ehrlichmann, W.; Bieg, C.; Solbach, C.; Kumar, P.; Wiebe, L. I.; MacHulla, H. J. Preparation of the Hypoxia Imaging PET Tracer [18F]FAZA: Reaction Parameters and Automation. *Applied Radiation and Isotopes* **2005**, *62* (6), 897–901. https://doi.org/10.1016/j.apradiso.2004.12.004.

(13)   Hounshell, D. A. *From the American System to Mass Production, 1800-1932: The Development of Manufacturing Technology in the United States*; 1985.

(14) Ryu, D. D. Y.; Nam, D.-H. REVIEW Recent Progress in Biomolecular Engineering. **2000**. https://doi.org/10.1021/bp088059d.

(15) Bergmann, M.; Zervas, L. Über Ein Allgemeines Verfahren Der Peptid-Synthese. *Berichte der deutschen chemischen Gesellschaft (A and B Series)* **1932**, *65* (7), 1192–1201. https://doi.org/10.1002/cber.19320650722.

(16) Carpino, L. A. Oxidative Reactions of Hydrazines. II. Isophthalimides. New Protective Groups on Nitrogen. *Journal of the American Chemical Society* **1957**, *79* (1), 98–101. https://doi.org/10.1021/ja01558a026.

(17) Carpino, L. A.; Han, G. Y. The 9-Fluorenylmethoxycarbonyl Function, a New Base-Sensitive Amino-Protecting Group. *Journal of the American Chemical Society* **1970**, *92* (19), 5748–5749. https://doi.org/10.1021/ja00722a043.

(18) Atherton, E.; Fox, H.; Harkiss, D.; Logan, C. J.; Sheppard, R. C.; Williams, B. J. A Mild Procedure for Solid Phase Peptide Synthesis: Use of Fluorenylmethoxycarbonylamino-Acids. *Journal of the Chemical Society, Chemical Communications* **1978**, No. 13, 537–539. https://doi.org/10.1039/C39780000537.

(19) Chang, C.-D.; Meienhofer, J. SOLID-PHASE PEPTIDE SYNTHESIS USING MILD BASE CLEAVAGE OF NαFLUORENYLMETHYLOXYCARBONYLAMINO ACIDS, EXEMPLIFIED BY A SYNTHESIS OF DIHYDROSOMATOSTATIN. *International Journal of Peptide and Protein Research* **2009**, *11* (3), 246–249. https://doi.org/10.1111/j.1399-3011.1978.tb02845.x.

(20) Li, W.; O'brien-Simpson, N. M.; Hossain, M. A.; Wade, J. D. The 9-Fluorenylmethoxycarbonyl (Fmoc) Group in Chemical Peptide Synthesis - Its Past, Present, and Future. **1942**. https://doi.org/10.1071/CH19427.

(21) Ragnarsson, U.; Grehn, L. Dual Protection of Amino Functions Involving Boc. *RSC Advances*. Royal Society of Chemistry November 7, 2013, pp 18691–18697. https://doi.org/10.1039/c3ra42956c.

(22) Sonveaux, E. Protecting Groups in Oligonucleotide Synthesis. *Methods in molecular biology (Clifton, N.J.)*. Humana Press 1994, pp 1–71. https://doi.org/10.1007/978-1-59259-513-6_1.

(23) Ghosh, B.; Kulkarni, S. S. Advances in Protecting Groups for Oligosaccharide Synthesis. *Chemistry - An Asian Journal*. John Wiley and Sons Ltd February 17, 2020, pp 450–462. https://doi.org/10.1002/asia.201901621.

(24) Harvey, R. G. *Polycyclic Aromatic Hydrocarbons | Wiley*; Wiley-VCH: New York, 1997.

(25) De Koning, C. B.; Rousseau, A. L.; Van Otterlo, W. A. L. *Modern Methods for the Synthesis of Substituted Naphthalenes*.

(26) Zhang, K.; Cai, L.; Jiang, X.; Garcia-Garibay, M. A.; Kwon, O. Phosphine-Mediated Iterative Arene Homologation Using Allenes. *Journal of the American Chemical Society* **2015**, *137* (35), 11258–11261. https://doi.org/10.1021/jacs.5b07403.

(27) Anthony, J. E. The Larger Acenes: Versatile Organic Semiconductors. *Angewandte Chemie International Edition* **2008**, *47* (3), 452–483. https://doi.org/10.1002/anie.200604045.

(28)   Lehmann, J. W.; Blair, D. J.; Burke, M. D. Towards the Generalized Iterative Synthesis of Small Molecules. *Nature Reviews Chemistry*. Nature Publishing Group February 7, 2018, pp 1–20. https://doi.org/10.1038/s41570-018-0115.

(29)   Gillis, E. P.; Burke, M. D. A Simple and Modular Strategy for Small Molecule Synthesis: Iterative Suzuki-Miyaura Coupling of B-Protected Haloboronic Acid Building Blocks. *Journal of the American Chemical Society* **2007**, *129* (21), 6716–6717. https://doi.org/10.1021/ja0716204.

(30)   WHO | World Malaria Report 2014. *WHO* **2015**.

(31)   Gerwick, B. C.; Sparks, T. C. Natural Products for Pest Control: An Analysis of Their Role, Value and Future. *Pest Management Science* **2014**, *70* (8), 1169–1185. https://doi.org/10.1002/ps.3744.

(32)   Taunton, J.; Hassig, C. A.; Schreiber, S. L. A Mammalian Histone Deacetylase Related to the Yeast Transcriptional Regulator Rpd3p. *Science* **1996**, *272* (5260), 408–411. https://doi.org/10.1126/science.272.5260.408.

(33)   Corey, E. J.; Noyori, R. A Total Synthesis of Prostaglandin F2α (Dl) from 2-Oxabicyclo[3.3.0]Oct-6-En-3-One. *Tetrahedron Letters* **1970**, *11* (4), 311–313. https://doi.org/10.1016/S0040-4039(00)61816-6.

(34)   Madison, W. S. J.; Duff, W.; Allen, S. *THE TOTAL SYNTHESIS OF PENICILLIN V*.

(35)   Paterson, I.; Scott, J. P. Polyketide Library Synthesis: Iterative Assembly of Extended Polypropionates Using (R)- and (S)-1-(Benzyloxy)-2-Methylpentan-3-One. *Tetrahedron Letters* **1997**, *38* (42), 7441–7444. https://doi.org/10.1016/S0040-4039(97)01751-6.

(36)   Atzrodt, J.; Derdau, V.; Kerr, W.; Reid, M. Applications of Hydrogen Isotopes in the Life Sciences. *Angewandte Chemie International Edition* **2017**, 1–26. https://doi.org/10.1002/(ISSN)1521-3773.

(37)   Evans, D. A.; Nelson, J. V.; Vogel, E.; Taber, T. R. Stereoselective Aldol Condensations via Boron Enolates. *Journal of the American Chemical Society* **1981**, *103* (11), 3099–3111. https://doi.org/10.1021/ja00401a031.

(38)   Crimmins, M. T.; Chaudhary, K. Titanium Enolates of Thiazolidinethione Chiral Auxiliaries: Versatile Tools for Asymmetric Aldol Additions. *Organic Letters* **2000**, *2* (6), 775–777. https://doi.org/10.1021/ol9913901.

(39)   Brown, H. C.; Bhat, K. S.; Randad, R. S. B-Allyldiisopinocampheylborane: A Remarkable Reagent for the Diastereoselective Allylboration of a-Substituted Chiral Aldehydes. *Journal of Organic Chemistry* **1987**, *52* (2), 319–320. https://doi.org/10.1021/jo00378a042.

(40)   Brown, H. C.; Bhat, K. S. Enantiomeric (Z)- and (E)-Crotyldiisopinocampheylboranes. Synthesis in High Optical Purity of All Four Possible Stereoisomers of β-Methylhomoallyl Alcohols. *Journal of the American Chemical Society*. American Chemical Society 1986, pp 293–294. https://doi.org/10.1021/ja00262a017.

(41)   Brown, H. C.; Bhat, K. S. Chiral Synthesis via Organoboranes. 7. Diastereoselective and Enantioselective Synthesis of Erythro- and Threo-ß-Methylhomoallyl Alcohols via Enantiomeric

(Z)- and (E)-Crotylboranes. *Journal of the American Chemical Society* **1986**, *108* (19), 5919–5923. https://doi.org/10.1021/ja00279a042.

(42) Balieu, S.; Hallett, G. E.; Burns, M.; Bootwicha, T.; Studley, J.; Aggarwal, V. K. Toward Ideality: The Synthesis of (+)-Kalkitoxin and (+)-Hydroxyphthioceranic Acid by Assembly-Line Synthesis. *Journal of the American Chemical Society* **2015**, *137* (13), 4398–4403. https://doi.org/10.1021/ja512875g.

(43) Thomas, S. P.; French, R. M.; Jheengut, V.; Aggarwal, V. K. Homologation and Alkylation of Boronic Esters and Boranes by 1,2-Metallate Rearrangement of Boron Ate Complexes. *The Chemical Record* **2009**, *9* (1), 24–39. https://doi.org/10.1002/tcr.20168.

(44) Burns, M.; Essafi, S.; Bame, J. R.; Bull, S. P.; Webster, M. P.; Balieu, S.; Dale, J. W.; Butts, C. P.; Harvey, J. N.; Aggarwal, V. K. Assembly-Line Synthesis of Organic Molecules with Tailored Shapes. *Nature* **2014**, *513* (7517), 183–188. https://doi.org/10.1038/nature13711.

(45) Fujii, S.; Chang, S. Y.; Burke, M. D. Total Synthesis of Synechoxanthin through Iterative Cross-Coupling**. https://doi.org/10.1002/anie.201102688.

(46) Woerly, E. M.; Cherney, A. H.; Davis, E. K.; Burke, M. D. Stereoretentive Suzuki-Miyaura Coupling of Haloallenes Enables Fully Stereocontrolled Access to (-)-Peridinin. https://doi.org/10.1021/ja102721p.

(47) Lee, S. J.; Gray, K. C.; Paek, J. S.; Burke, M. D. Simple, Efficient, and Modular Syntheses of Polyene Natural Products via Iterative Cross-Coupling. *J. AM. CHEM. SOC* **2008**, *130*, 466–468. https://doi.org/10.1021/ja078129x.

(48) Gillis, E. P.; Burke, M. D. A Simple and Modular Strategy for Small Molecule Synthesis: Iterative Suzuki-Miyaura Coupling of B-Protected Haloboronic Acid Building Blocks. **2007**. https://doi.org/10.1021/ja0716204.

(49) Gray, K. C.; Palacios, D. S.; Dailey, I.; Endo, M. M.; Uno, B. E.; Wilcock, B. C.; Burke, M. D.; Meinwald, J. Amphotericin Primarily Kills Yeast by Simply Binding Ergosterol. https://doi.org/10.1073/pnas.1117280109/-/DCSupplemental.

(50) Jenke-Kodama, H.; Sandmann, A.; Müller, R.; Dittmann, E. Evolutionary Implications of Bacterial Polyketide Synthases. *Molecular Biology and Evolution* **2005**, *22* (10), 2027–2039. https://doi.org/10.1093/molbev/msi193.

(51) Ridley, C. P.; Ho, Y. L.; Khosla, C. Evolution of Polyketide Synthases in Bacteria. *Proceedings of the National Academy of Sciences of the United States of America* **2008**, *105* (12), 4595–4600. https://doi.org/10.1073/pnas.0710107105.

(52) Smith, S.; Tsai, S. C. The Type I Fatty Acid and Polyketide Synthases: A Tale of Two Megasynthases. *Natural Product Reports*. The Royal Society of Chemistry September 26, 2007, pp 1041–1072. https://doi.org/10.1039/b603600g.

(53) Vogt, T. Phenylpropanoid Biosynthesis. *Molecular Plant*. Oxford University Press 2010, pp 2–20. https://doi.org/10.1093/mp/ssp106.

(54)   Yu, D.; Xu, F.; Zeng, J.; Zhan, J. Type III Polyketide Synthases in Natural Product Biosynthesis. *IUBMB Life* **2012**, *64* (4), 285–295. https://doi.org/10.1002/iub.1005.

(55)   Lim, Y.; Go, M.; Yew, W. Exploiting the Biosynthetic Potential of Type III Polyketide Synthases. *Molecules* **2016**, *21* (6), 806. https://doi.org/10.3390/molecules21060806.

(56)   Driggers, E. M.; Hale, S. P.; Lee, J.; Terrett, N. K. The Exploration of Macrocycles for Drug Discovery - An Underexploited Structural Class. *Nature Reviews Drug Discovery*. Nature Publishing Group July 2008, pp 608–624. https://doi.org/10.1038/nrd2590.

(57)   Woerly, E. M.; Roy, J.; Burke, M. D. Synthesis of Most Polyene Natural Product Motifs Using Just 12 Building Blocks and One Coupling Reaction. **2014**. https://doi.org/10.1038/NCHEM.1947.

(58)   Merrifield, R. B. Solid Phase Peptide Synthesis. I. The Synthesis of a Tetrapeptide. *Journal of the American Chemical Society* **1963**, *85* (14), 2149–2154. https://doi.org/10.1021/ja00897a025.

(59)   Caruthers, M. H. Gene Synthesis Machines: DNA Chemistry and Its Uses. *Science* **1985**, *230* (4723), 281–285. https://doi.org/10.1126/science.3863253.

(60)   Plante, O. J.; Palmacci, E. R.; Seeberger, P. H. Automated Solid-Phase Synthesis of Oligosaccharides. *Science* **2001**, *291* (5508), 1523–1527. https://doi.org/10.1126/science.1057324.

(61)   Hahm, H. S.; Schlegel, M. K.; Hurevich, M.; Eller, S.; Schuhmacher, F.; Hofmann, J.; Pagel, K.; Seeberger, P. H. Automated Glycan Assembly Using the Glyconeer 2.1 Synthesizer. *Proceedings of the National Academy of Sciences of the United States of America* **2017**, *114* (17), E3385–E3389. https://doi.org/10.1073/pnas.1700141114.

(62)   Joseph, A. A.; Pardo-Vargas, A.; Seeberger, P. H. Total Synthesis of Polysaccharides by Automated Glycan Assembly. *Journal of the American Chemical Society* **2020**, *142* (19), 8561–8564. https://doi.org/10.1021/jacs.0c00751.

(63)   Li, J.; Ballmer, S. G.; Gillis, E. P.; Fujii, S.; Schmidt, M. J.; Palazzolo, A. M. E.; Lehmann, J. W.; Morehouse, G. F.; Burke, M. D. Synthesis of Many Different Types of Organic Small Molecules Using One Automated Process. *Science* **2015**, *347* (6227), 1221–1226. https://doi.org/10.1126/science.aaa5414.

HUMAN GUIDED ALGORITHMIC APPROACH TO IDENTIFYING IMPACTFUL UNSOLVED METHODOLOGIES IN NATURAL PRODUCT CHEMICAL SPACE

ABSTRACT

Organic chemistry methods development has proceeded largely through an ad hoc approach driven by custom synthesis for individual targets. We propose to instead utilize a human guided algorithm to analyze a building block approach to natural products and identify key methodologies. Additionally, the stereochemical make up around each coupling can be used to help guide the creation of a substrate table. Herein we report the use of an algorithm to systematically fragment all linear natural product, conduct an optimization to choose the smallest set of blocks required to cover >75% of natural product chemical space, and establish a list of impactful couplings. A data driven substrate scope can be prospectively identified for each coupling to guide methodology development to hopefully create a maximally generalized solution (**Figure 2-1**). Nathan Russell of the Peng group was responsible for all code writing, while intellectual development was a collaboration between me, Russell, and Andrea Palazzolo Ray.
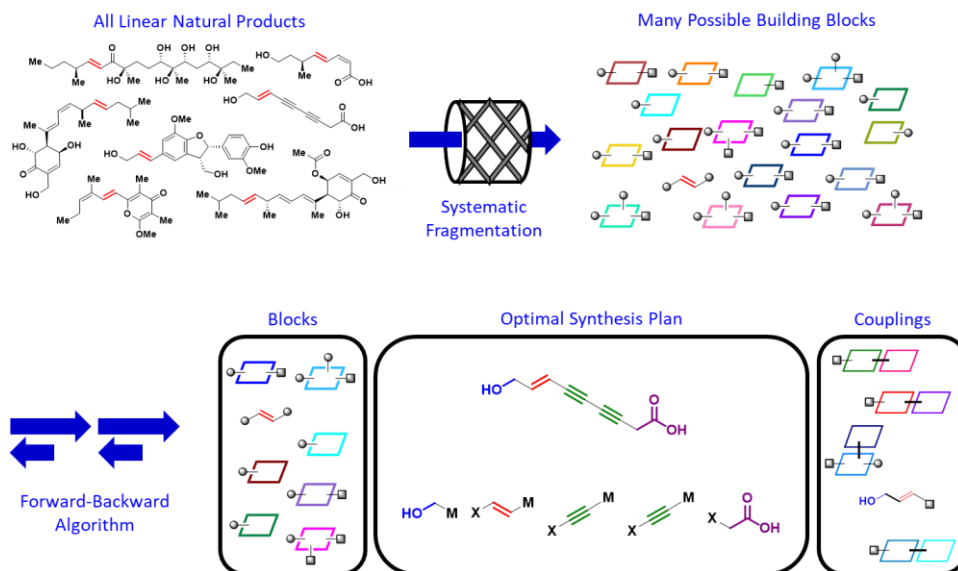
Figure 2-1 Overview of the computational process for identifying impactful methodologies

2-1 BUILDING A STEREOCHEMICALLY DEFINED DATABASE

To undertake such a project, we began by building a database of stereochemically defined small molecule natural products. The Dictionary of Natural Products (DNP) is the current gold standard for natural product databases, but the stereochemical information cannot be extracted from the entries. Many stereochemically encoded databases exist but are not limited to only natural products. To rectify this problem, we constructed a new database called the Natural Productome Database (NPDB). For each entry in the DNP, we collected a nonstereochemically defined IUPAC International Chemical Identifier (InChI) string, a unique character string identifier for a molecule. The simplified molecular-input line-entry system (SMILES) strings from stereochemically encoded databases PubChem and Supernatural II and were also collected. As it is possible to write multiple SMILES strings for a single molecule, these SMILES were canonicalized to ensure that identical molecules would have identical SMILES strings. These SMILES were then stripped of
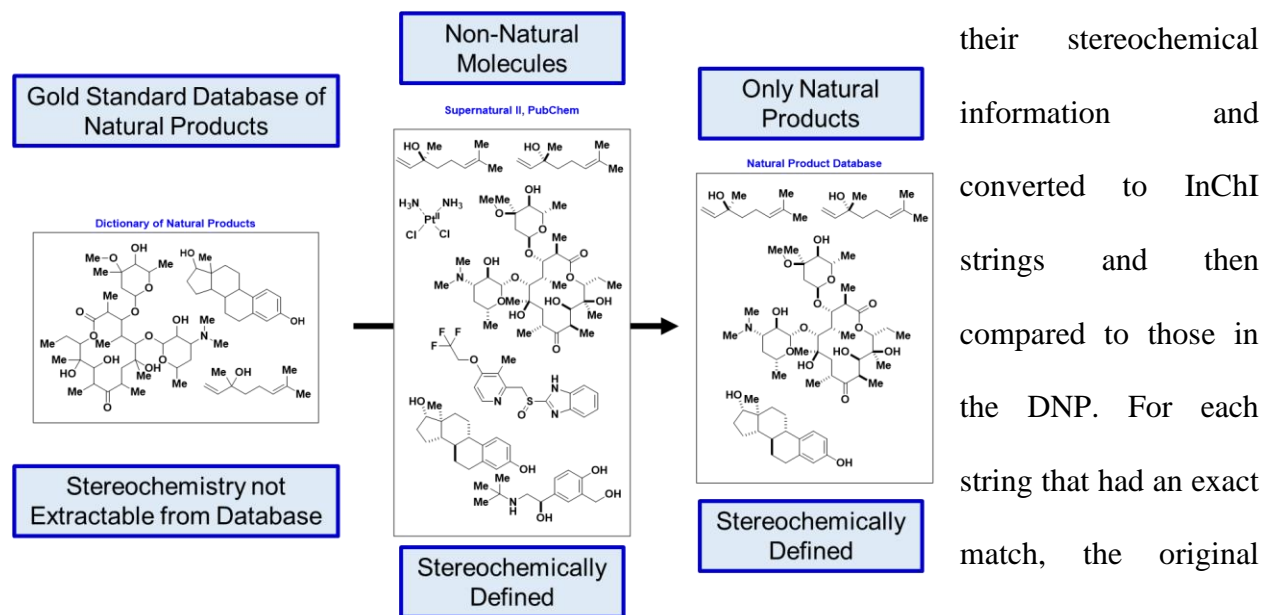
Figure 2-2 Construction of the stereochemically defined Natural Productome Database

their stereochemical information and converted to InChI strings and then compared to those in the DNP. For each string that had an exact match, the original canonical SMILES was deposited in the NPDB.

In this way we ensured all entries in our database have the same two-dimensional connectivity as

a natural product in the DNP. While we cannot guarantee that our database contains every natural stereoisomer or only natural stereoisomers, we feel it gives us a good representation of known natural products. The NPDB has 282,487 entries and covers 75% of the DNP (**Figure 2-2**).

The NPDB was then bifurcated into linear and cyclic (**Figure 2-3**). Linear natural products
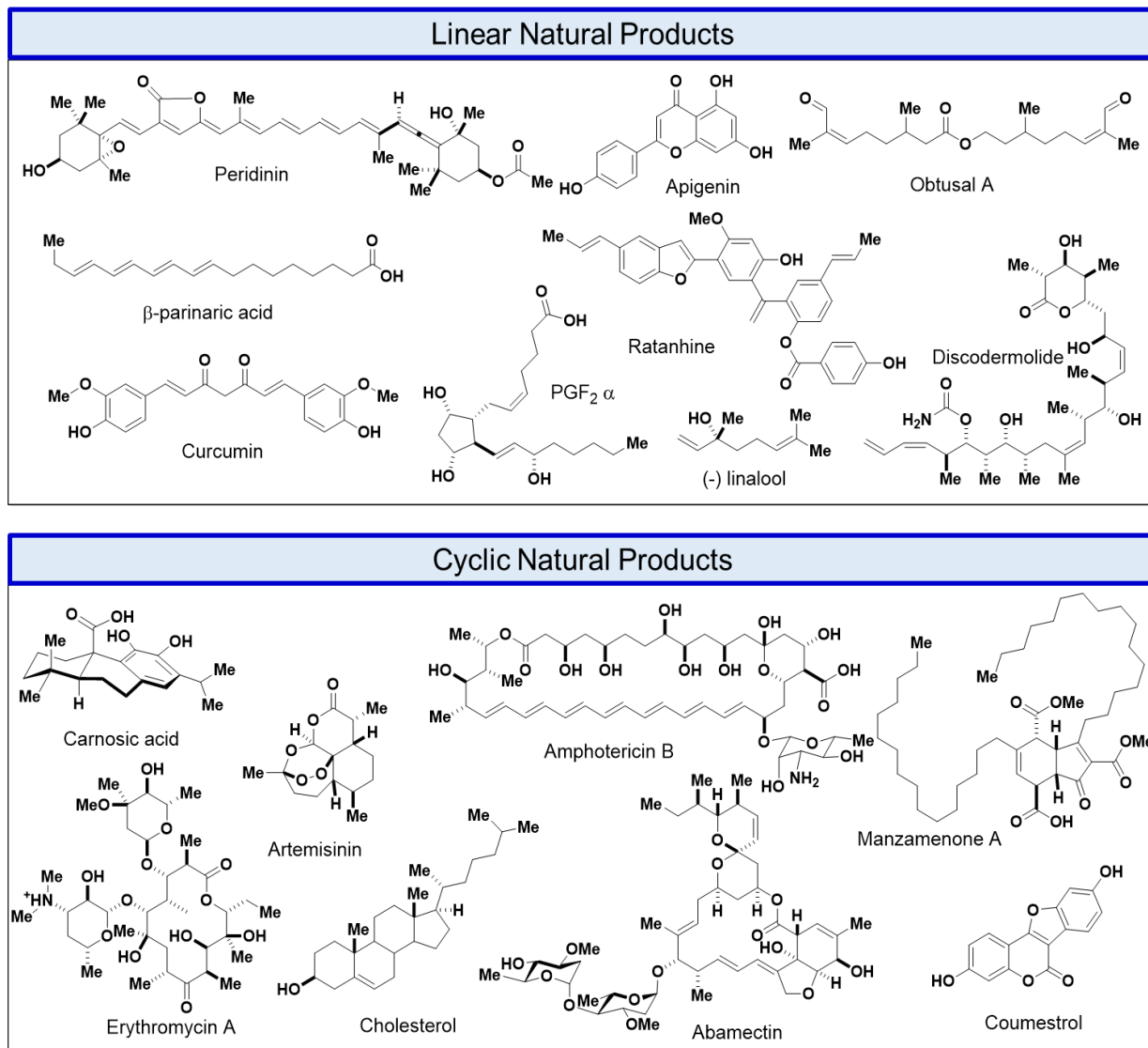
Figure 2-3 Bifurcation of NPDB into linear and cyclic natural products

are all molecules that can be synthesized through iterative assembly of building blocks, although those blocks may include rings ≤8 atoms or fused bicycles. Cyclic natural products are molecules that post assembly of a linear precursor require a cyclization event and possibly oxidation state

19

modifications. Cyclic natural products include both macrocyclic and polycyclic compounds. While we know that such transformations are possible in nature, there is not currently enough biosynthetic understanding or chemical cyclization methodology to undertake a systematic deconstruction of these cyclic natural products back to their linear precursors. For this reason, we decided to work with only the linear natural products, recognizing the future challenge of connecting cyclic natural products to their linear precursors. We also limited ourselves to linear products that had ≤14 breakable bonds due to computations cost of larger molecules. With our set of linear natural products in hand, we turned our attention to their systematic deconstruction.

2-2 DEFINING GUIDING PRINCIPLES OF OUR ALGORITHM

Driven by the hypothesis that only a few types of bond-forming reactions would be sufficient for building block assembly, we chose to limit our potential reactions to cross-couplings, heteroatom acylations, and glycosylations (**Figure 2-4**). Heteroatom acylations and glycosylations have already proven amenable to generalized automated conditions, and the rapidly expanding
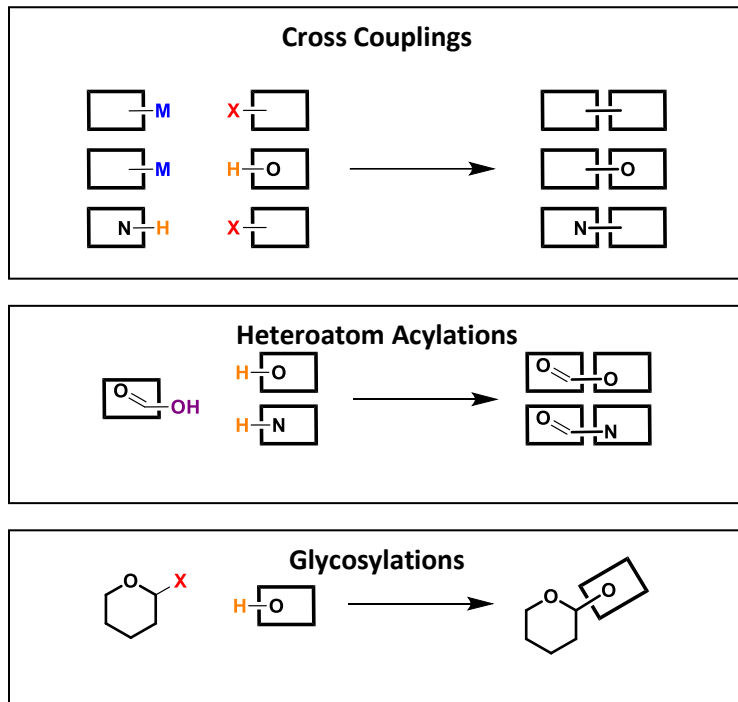
Figure 2-4 Allowed reaction types

scope of cross-coupling reactions suggests their potential to do the same. Within the field of cross-coupling, we believe the combination of Suzuki-Miyara, Buckwald-Hartwig, and Chan-Lam

couplings is best suited to cover all of the required C-C and C-N/O space. The numerous ligands for boron provide great flexibility for a broadly applicable iterative synthetic platform as reaction attenuating protecting groups such as 1,8-naphthalenediaminatoboryl (Bdan) and MIDA, provide multiple options for protection and deprotection conditions, while the large number of reactive boronic acid/ester options and the relative ease of switching between different boron ligands enables more options for coupling condition development. All such reaction types can employ non-toxic and shelf-stable building blocks, be highly efficient and stereospecific, and proceed under mild reaction conditions with high levels of functional group tolerance. Thus, in theory, the functional groups, oxidation states, and stereochemistry required for natural product assembly can be pre-installed into building blocks. Importantly, the fragmentation was not restricted to known couplings within these
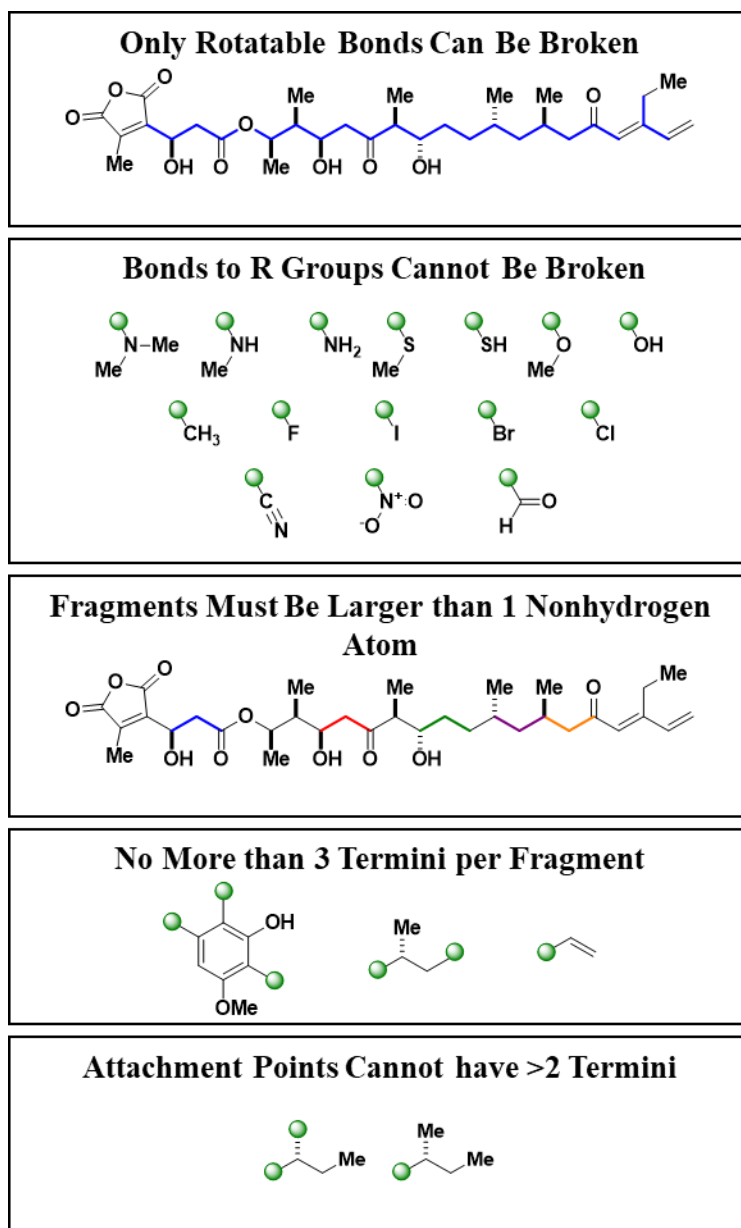
Figure 2-5 Rules to guide fragmentation

reaction types, thus allowing the analysis to prospectively identify couplings with maximized potential impact for generalized natural product synthesis regardless of current feasibility.

2-3 DEVELOPMENT OF RULES FOR FRAGMENTATION

With these choices consciously made upfront, we began to create rules to guide the fragmentation of the linear natural products. In accordance with our choice of reaction types, breakable bonds—bonds the algorithm was allowed to consider—were limited to single rotatable bonds. We also identified a set of R groups, where the bond to said group was defined as unbreakable. This allowed us to not only prevent the need to repeatedly install extremely common and small functional groups, but to also track the frequency of said functional groups to later help guide methodology development (**Figure 2-5**). A few specific instances of bonds were also defined as unbreakable to capitalize on the existing sugar chemistry, specifically the C—O bond adjacent to a glycosidic bond, and the C—C bond between C5 and C6 of a hexose, or to prevent unrealistic reactivity expectations such as peroxide bonds or alpha to an epoxide (**Figure 2-6**).
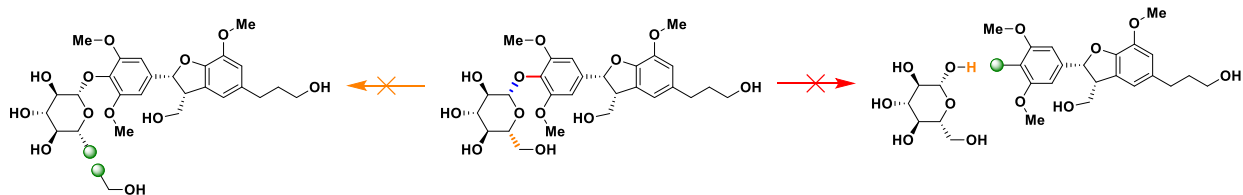
Figure 2-6 Some examples of bonds defined as unbreakable

As we began to break bonds, we needed ways to categorize and discuss the resulting pieces. Attachment points were defined as the nonhydrogen atom to which a new bond would form, and termini were defined as the functional group used to perform the reaction. Our choices for bond forming reactions required four terminus types: metal (M), (pseudo)halide (X), hydrogen (H), and hydroxyl (OH). Cross coupling can utilize M—X, M—H, or X—H pairings, while heteroatom acylations use H-OH and glycosylations use X—H (**Figure 2-7**). For us it was also important to be able to define a metric to measure how useful a block or set of blocks could be for natural

product synthesis. We settled on coverage of natural product chemical space for a block being the number of nonhydrogen atoms in the block times the number of times that block appears in natural products. Considering total percentage of non-hydrogen atoms covered also gave us a consistent way to compare the utility of different sets of blocks.

In addition to defining what bonds could be broken, we also placed limitations on the kinds of fragments that could be formed. For tractability reasons, we required that all fragments must consist of two or more nonhydrogen atoms. Fragments were allowed to have up to three termini, as
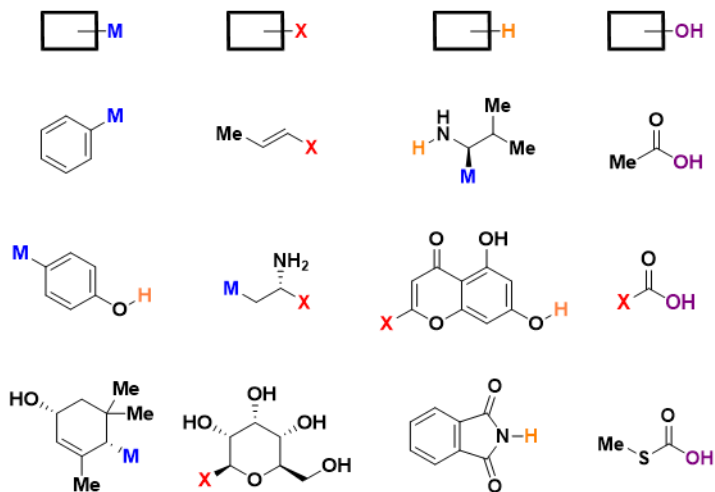
Figure 2-7 Termini and example blocks

the existence of trifunctional blocks was integral to handling branched natural products, but selective couplings among three termini still felt chemically possible. Finally, attachment points were limited to two termini, as 1,1-disubstituted couplings are both an important deconstruction motif and such reactivity is precedented (**Figure 2-5**).

With this set of rules in hand we were able to begin fragmentation. First all breakable bonds in a natural product are identified. Then a tree diagram is constructed where each breakable bond is represented as a node, and edges are placed between nodes that are directly connected to each other without another node in between (**Figure 2-8**). For example, nodes 8 and 9 share an edge because there are directly connected to each, but nodes 7 and 9 do not share an edge as node 8 is between them. This tree diagram is utilized to prevent the formation of multifunctionals of four or higher from occurring. For any node with a degree ≥4, all other nodes that share an edge with it
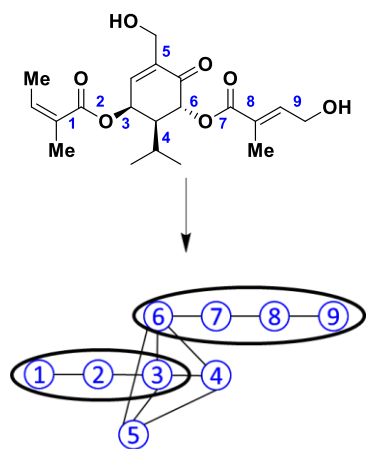
IF 1/2/3, 4, and 6/7/8/9 are broken THEN 5 cannot be broken

IF 1/2/3, 5, and 6/7/8/9 are broken THEN 4 cannot be broken

IF 1/2/3, 4, and 5 are broken   THEN 6, 7, 8, and 9 cannot be broken

IF 4, 5, and 6/7/8/9 are broken   THEN 1, 2, and 3 cannot be broken

Figure 2-8 Tree diagram to prevent creation of multifunctional fragments

are identified and assigned to separate categories. The nodes that do not share an edge are then classified into the category that contains the node between them and the original node. Looking at node 3 as an example, nodes 2,4,5, and 6 become category heads, and nodes 1 and 2 are placed in category 3, while nodes 7,8, and 9 are placed in category 6. Once these categories have been filled, a series of IF, THEN statements can be constructed that prevent simultaneous breakage of bonds in more than three of the categories, preventing the formation of multifunctionals. Similar IF, THEN statements are also created for atoms that have three or more breakable bonds, to prevent more than two termini on an attachment point, and for atoms where all bonds to nonhydrogen atoms are breakable, as breaking all bonds would create a single nonhydrogen atom fragment.

Taking any and all IF, THEN statements generated for a molecule into consideration, the maximum number of simultaneously breakable bonds is calculated and called k. To generate all possible fragments that are contained in a natural product scales with 2^k and to run an optimization for maximal percent coverage of natural product chemical space for a set as large as ours would require prohibitively large time and data storage space. For this reason, we moved away from a complete enumeration of fragmentations to focus on a targeted generation of fragmentations that

would encompass the blocks most likely to be selected in the optimization. Intuitively we realized the inverse correlation between size and frequency of a fragment, and knew we needed to focus on the fragmentations that gave us access to the smaller but highly redundant fragments. Knowing that breaking k bonds for each natural product would give us the most redundant fragments, a small test set was used to investigate breaking how many bonds less than k continued to give us blocks likely to be selected. The test revealed that enumerating fragmentations for k and k-1 bonds for each natural product gave us the best results for computational time (**Figure 2-9**).
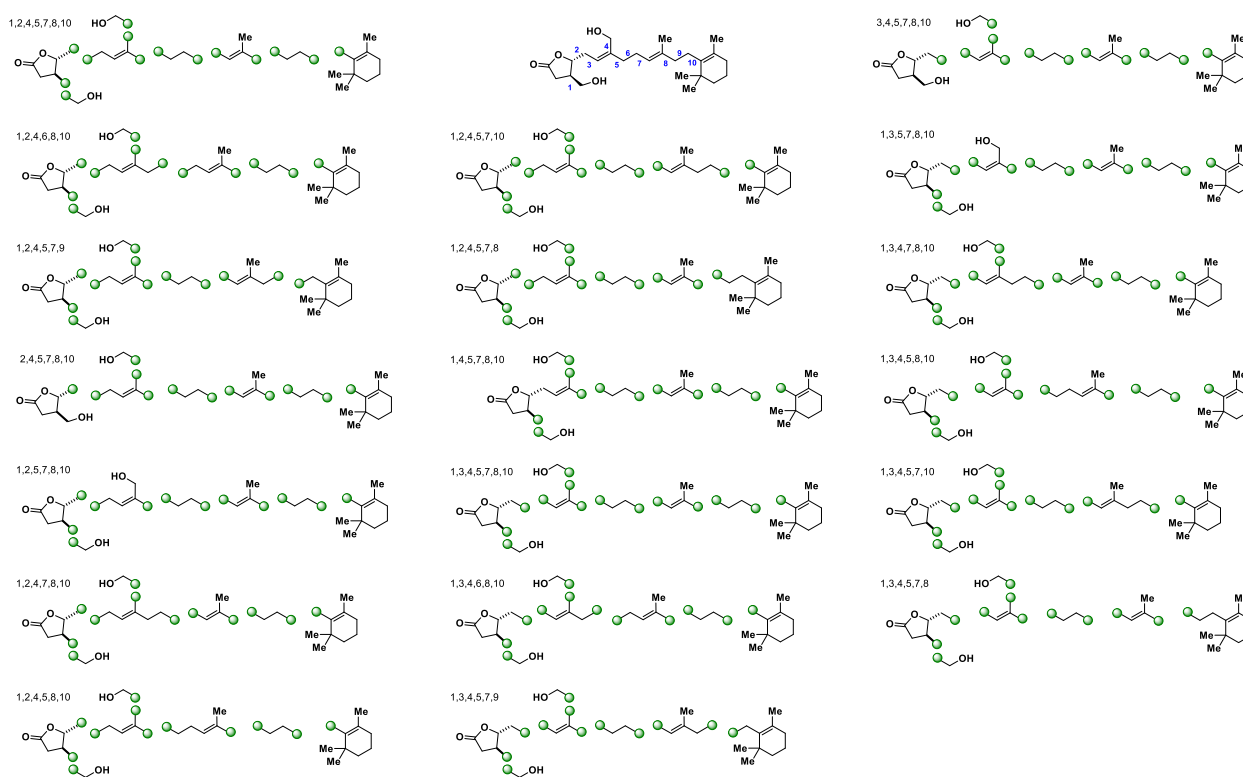
Figure 2-9 All valid fragmentations at *k* and *k-1* where *k* equals 7

2-4 CONVERTING FRAGMENTS INTO BLOCKS

As molecules are fragmented all attachment points are assigned a terminus. The vast majority of attachment points are assigned a placeholder terminus that will later be converted to X

or M. In some cases, like glycosylations and heteroatom acylations, the termini can be assigned immediately as there is only one choice for these reactions. Likewise, for oxygen and nitrogen atoms there is only one applicable terminus regardless of the reaction type,
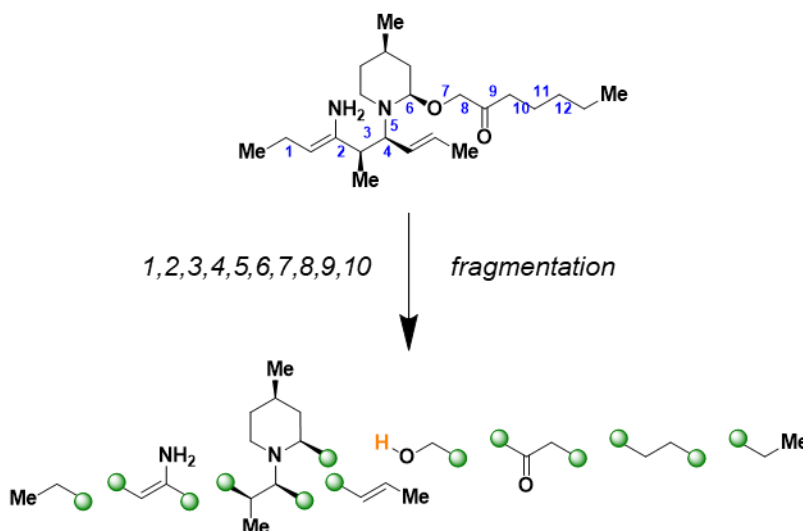
Figure 2-10 Installation of final termini for any unambiguous cases and of placeholder termini (represented by the green ball) everywhere else.

and so H is automatically assigned (**Figure 2-10**). To handle sulfur and phosphorus, a search of Scifinder was conducted to understand the types of chemistry available to these two atoms.[1–14] Based on oxidation state and what it is attached to, some termini can be placed immediately while others are given a special placeholder terminus that can later be converted to X or OH (**Figure 2-11**). While only current chemistry was taken into consideration for sulfur and phosphorus at this time, the flexible nature of termini assignment would allow for easy incorporation of any new methodological developments.

Post fragmentation, blockization is conducted by converting all place holder termini on all fragmentations. A last-in first-out (LIFO) stack recursion is utilized to carry out these conversions. The algorithm locates one mono-functional fragment as a starting point, preferring those with placeholder terminus over one assigned during fragmentation. From here all possible blockizations are generated. For each placeholder terminus encountered the string is cloned and the X and M termini are each placed on one of the clones (or OH and X in the case of sulfur and phosphorus) and both of these strings are placed back in the stack. The last string is then removed and if the

26
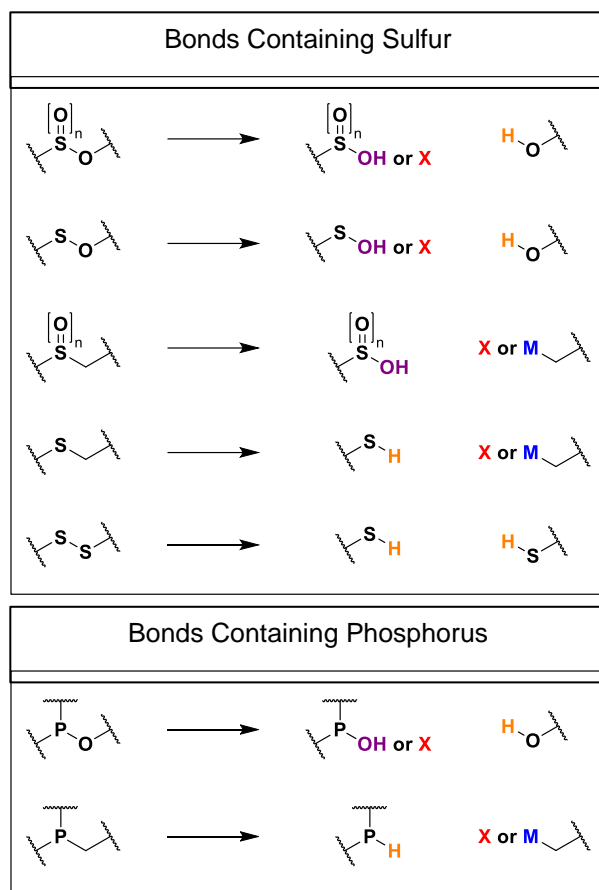
Figure 2-11 Termini for sulfur and phosphorus

next fragment's terminus was not preassigned, the coupling partner of the assigned monofunctional is used. So, for the M monofunctional the next fragment is assigned an X and for the X monofunctional the next fragment is assigned an M. The algorithm is prevented from creating blocks with two of the same termini, so the other end of the bifunctional fragment is then assigned without the need for cloning. The blockization continues down the chain, cloning whenever necessary, until it is finished (**Figure 2-12**). Then, following the LIFO principles this process repeats until the stack is empty. If at any point there is no valid termini to assign, the blockization is marked as invalid and discarded. Because the X and OH termini can be utilized in so many coupling types, the coupling partner of the terminus is stored to be used later in the synthetic planning step. This gives us the subclasses H^X, H^M, H^{OH}, H^H and OH^X, OH^M, OH^H.

2-5 DEFINING ORDER OF COUPLINGS TO CREATE A SYNTHETIC PLAN

The order of couplings is then determined in the synthetic planning step. All blockizations are first placed into one of two categories: linear or branched based on the absence or presence of any trifunctional blocks, respectively. For the linear examples synthetic planning is fairly straight forward. The algorithm identifies all monofunctional blocks—in this case two—and uses a LIFO

Figure 2-12 Blockization for a linear molecule

stack to check for a valid synthetic order. Preference is given to monofunctional M blocks as those are most likely to result in valid syntheses. The algorithm begins at the chosen monofunctional and checks if a valid coupling reaction can occur between these two blocks to create a new monofunctional block, which we dubbed a superblock. For a coupling to be valid the two active termini must be compatible and there must be another terminus not involved in the coupling through which turnover can occur, with M, H^X, H^{OH}, H^H, OH^X, and OH^H being the turnover permitting termini. The other option for valid couplings is for there to be no additional termini present indicating the final reaction. In the case of our MIDA based platform, turnover indicates the ability to purify the resulting superblock with a catch-and-release method before it is carried on to the deprotection to begin the next round of coupling. The turnover approved termini were

selected based on the desire to keep couplings flowing in one direction, which is also why bifunctional blocks with two of the same termini were prevented. While there are not currently protecting groups to satisfy these turnover requirements for the H and OH
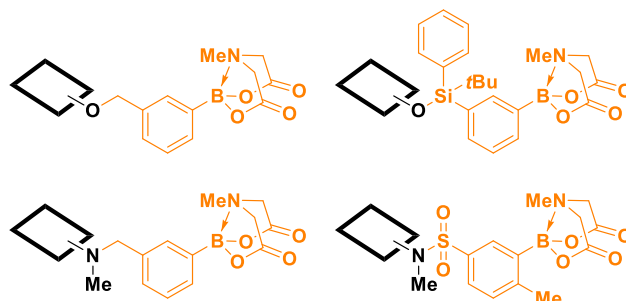
Figure 2-13 MIDA boronate containing protecting groups to allow for purification and turnover

termini, it is easy to envision how they could be achieved by appending a MIDA boronated onto an existing protecting group (**Figure 2-13**). Once the synthetic plan is complete or an invalid coupling is encountered, the blockization is stored or discarded respectively, and the algorithm moves on to the next in the stack until the stack is empty. While there are theoretically 0-2 synthetic
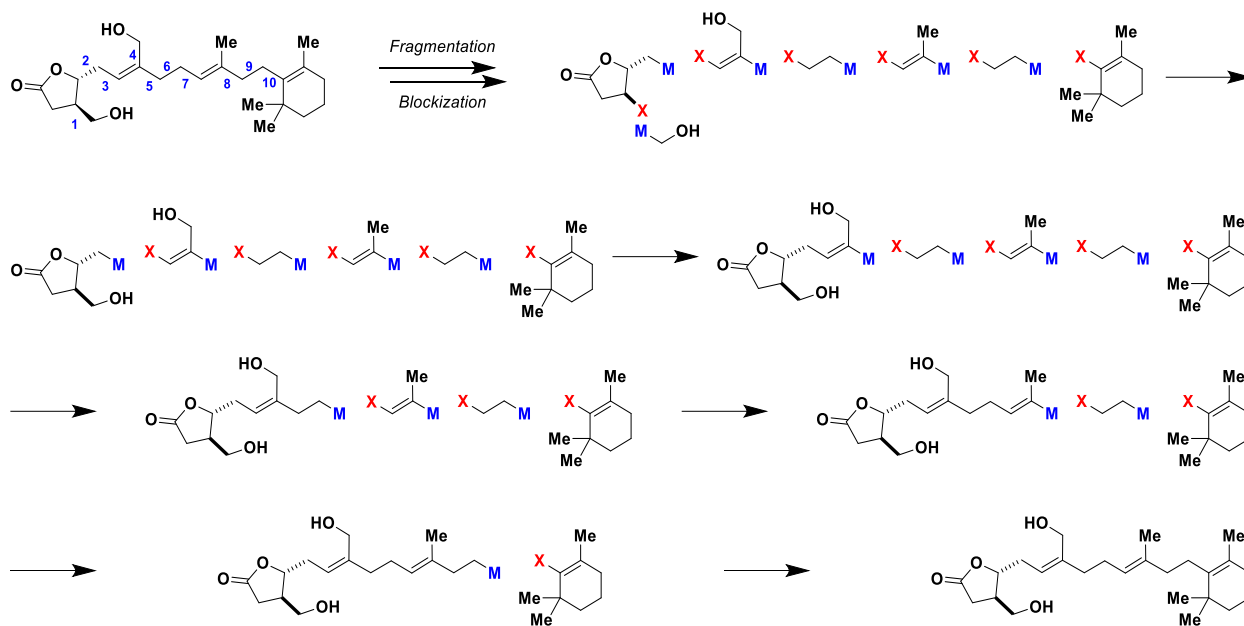
Figure 2-14 Synthetic planning determines order of couplings for given blockization

plans possible for every linear blockization in the vast majority of cases there will be only one, or occasionally zero, valid synthetic orderings (**Figure 2-14**).

In the case of trifunctionals, we run into the possibility of having duplicate termini on a superblock. To handles these cases, we believe an orthogonal protection strategy is simpler and

more favorable than trying to do selective couplings. For this reason, we introduced protected versions of each terminus, M^P, X^P, H^P, and OH^P. All subclasses of H and OH are combined when considering protection status as the terminus is not actually chemically different, and thus would have the same protecting group. We also introduced the deprotected metal classification, M^D, to designate the metal that is part of the coupling as separate from the M terminus of the next block. For these trifunctional cases we had to expand our list of requirements for valid couplings to include no more than one of any type of terminus, where protected (or deprotected) termini are considered a different type from their standard counterpart. Because multiple trifunctionals can exist in one molecule we also included the rule that there can be no more than 5 termini at time of coupling including the two in the active coupling, thus preventing the creation of a quadfunctional superblock. This is particularly important for synthetic plans with three or more trifunctionals.

Branching also complicates the ordering of a synthetic plan, so we utilized the terms "IN" and "OUT" to describe directionality around the trifunctionals. Imagine in a linear synthesis a bifunctional block of interest (A) in the middle of the chain. The superblock that has been created prior to reaching the block A is said to be coupling "IN" to A and the coupling that follows is said to be "OUT". In a valid synthetic plan all trifunctionals will ultimately end up with either 2 "IN"s and 1 "OUT" or 1 "IN" and 2 "OUT"s. To improve synthetic tractability and limit the amount of computational time required to process synthetic plans, we decided to discard all blockizations that contained a trifunctional without a M terminus, as this would assure the ability to turn over. Also, at this time the variety and orthogonality of protecting groups for boron are most well developed. If at a later time protecting group options of the other termini become abundant this requirement could be

"OUT"	"IN"	"EITHER"
M	X	H^{OH}
H^X	H^M	H^H
OH^X	OH^M	OH^H

Figure 2-15 Termini directionality

reconsidered. In general, for branched synthesis, we want to assemble all "IN" superblocks, couple them onto the trifunctional, and then proceed down all "OUT" branches. For some branches we can tell the directionality simply from the termini on the trifunctional. All X, H^M, and OH^M represent an "IN" branch while all M, H^X, and OH^X represent an "OUT" branch. This leaves H^H, H^{OH}, and OH^H as termini that could be attached to either "IN" or "OUT" branches depending on what is going on further down the branch (**Figure2-15).**
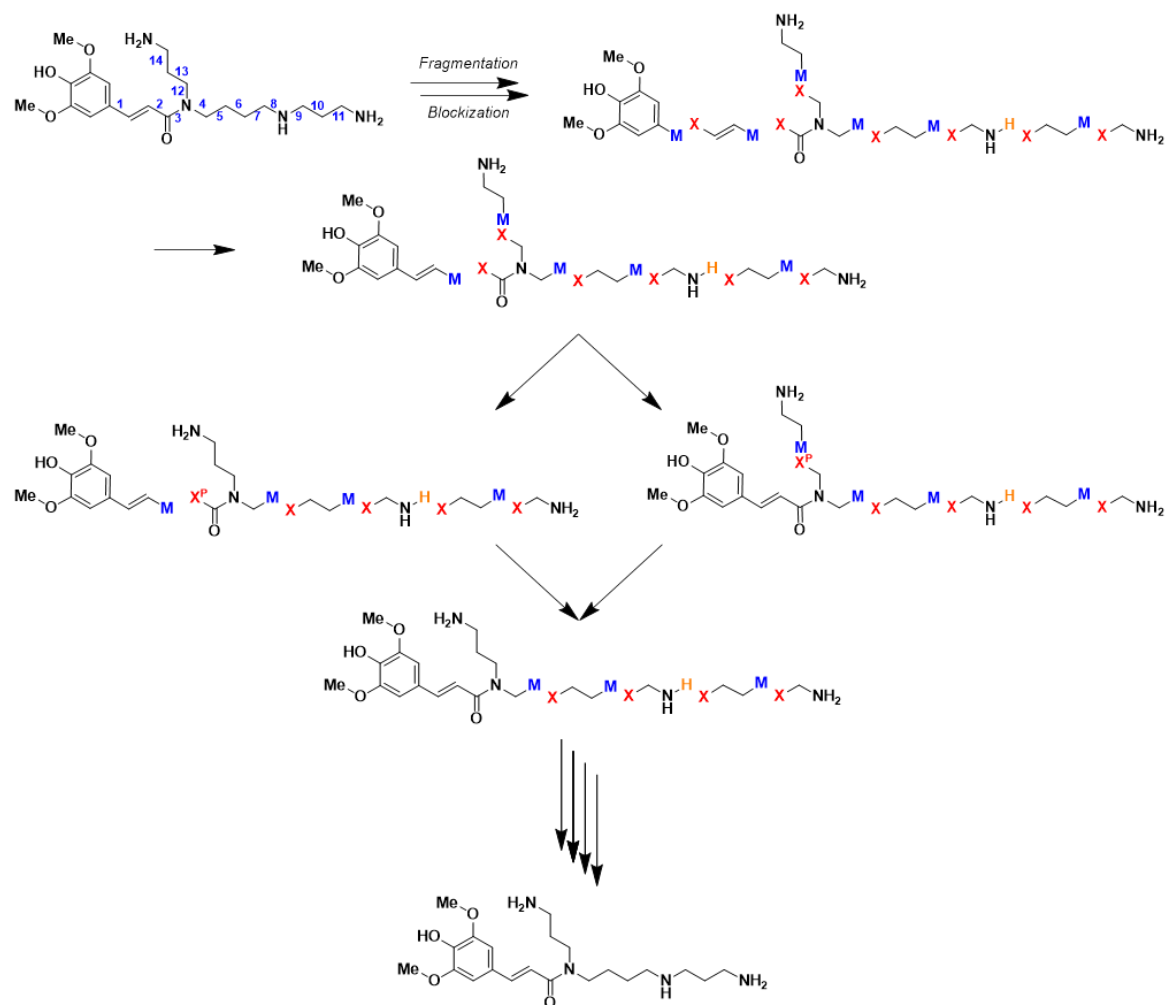
Figure 2-16 Example synthetic plan containing a 2 "IN" 1 "OUT" trifunctional where the X that is coupled second is converted to an X^P

To begin the synthesis, the algorithm once again identifies all monofunctionals as starting points and places them in the stack starting with a preference for M monofunctionals. Couplings

31

occurs down the chain checking for validity of coupling at each step, until a trifunctional is reached. The next monofunctional is them checked until they have either all been turned into superblocks or determined to not be a valid place to start. This creates exclusively "IN" superblocks. If a trifunctional has 2 completed "IN" superblocks, the synthetic plan is cloned with one of the superblocks being coupled in first and then the other (**Figure 2-16**). If the algorithm encounters a terminus of the same type as the one in the active coupling, it places the protection status to make sure all termini are of different types. Still following the LIFO stack recursion, the top synthetic plan is picked up and coupling is continued down the out chain until either the end of the synthesis is reached or another trifunctional is encountered.

The same cloning procedure is utilized for trifunctionals with 2 "OUT"s. The superblock is constructed and coupled "IN", and the plan is duplicated to give both possible orderings with protection status assigned as necessary. Coupling occurs down the first branch until either it is complete or a trifunctional is reached. The algorithm then returns to the trifunctional and couples down the second branch (**Figure 2-17**). If at any point an invalid coupling is encountered, that plan is thrown out and the next one is lifted from the stack. If no valid synthetic plan is found an error is raised and the algorithm moves onto the next blockization.

2-6 DEFINING THE CHEMICAL ENVIRONMENT AROUND A COUPLING

At this point we also chose to extract and store information about the immediate stereochemical environment around the coupling as well as the presence of distal functional groups. With this information we can understand what these kinds of couplings actually look like
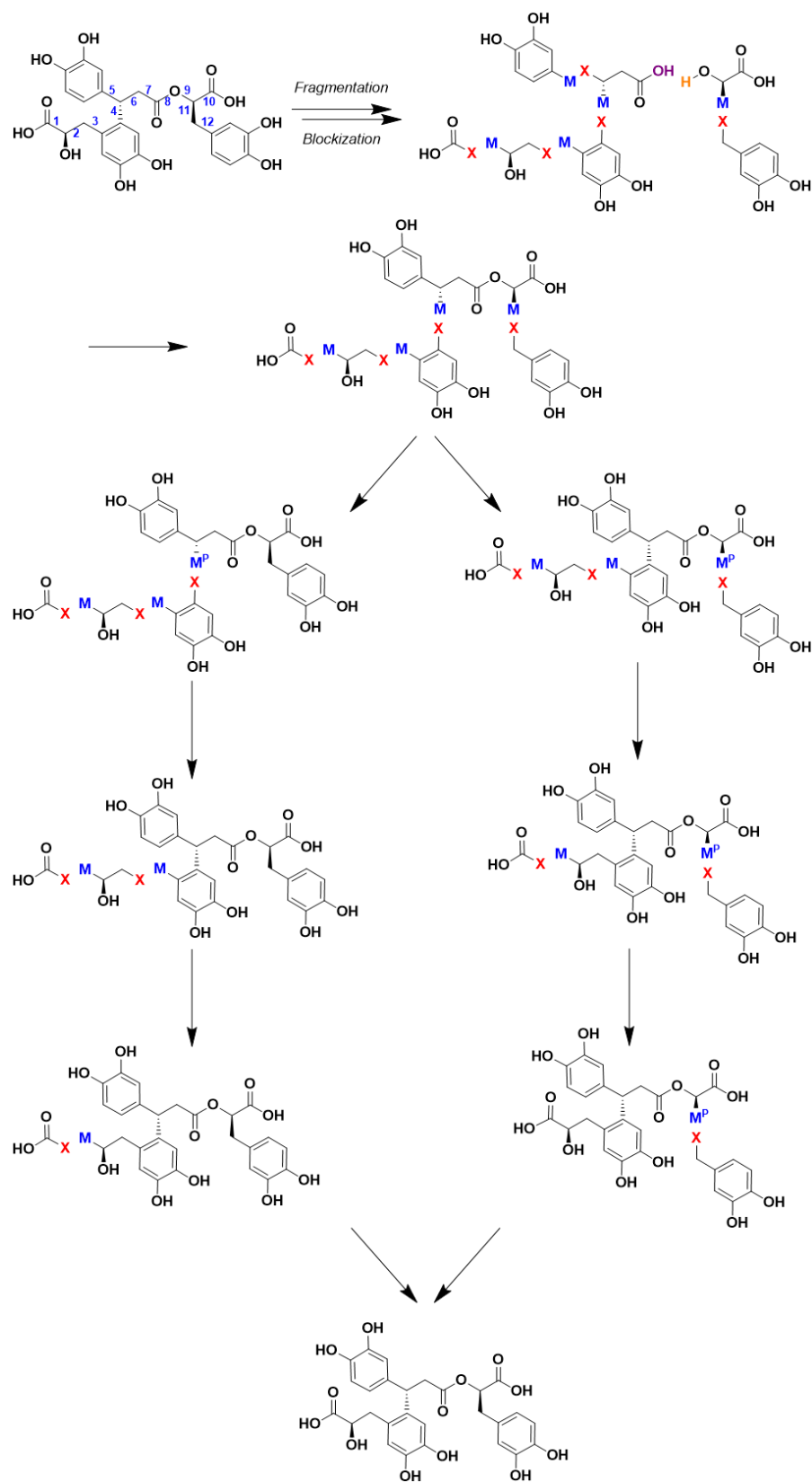
Figure 2-17 Example synthetic plan containing a 1 "IN" 2 "OUT" trifunctional

in natural products and begin to construct a data driven substrate table. This data can be used to help guide methodology development to be maximally effective and avoid the typical *ad hoc* construction of a substrate table fill out with other examples that happen to work under the conditions chosen from the optimization on the test reaction. We also choose to do this step before optimization on all valid synthetic plans rather than after optimization on only an optimal synthetic plan for each molecule. Even though it requires greater

compute time, we thought preemptively building in the ability to consider couplings in the optimization was a worth while trade off. Given our goal of finding a maximally efficient set of blocks to help illuminate new impactful methodologies, we chose not to place preferences on any particular coupling(s) in the optimization. However, this does allow for future changes to either prefer or limit any number of couplings as would be fitting for a different goal.

Coupling identities are created as the algorithm moves through a synthetic plan. At each coupling, a breadth first search is conducted on the blocks on each side of the coupling. We chose to use a breadth of two from the attachment point with the additional requirement that for any atom within this range that is part of a ring, the complete ring will be stored. We felt this ring completion requirement was important to accurately represent the chemistry as the steric and electronic conditions of the ring can be very different from a similar but open structure.

To carry out the coupling extraction, a clone of the synthetic plan where all manipulations are carried out is made, with the parent plan acting as a comparison to maintain stereochemistry. Moving sequentially down the synthetic plan, at each coupling all atoms within depth two plus ring completion are identified on the blocks on both sides of the coupling. The atoms outside of this depth are also scanned for R groups and other termini present, which are recorded as distal functional groups present at time of coupling. These external atoms are then deleted, and the remaining internal atoms are checked against the parent to make sure the deletion
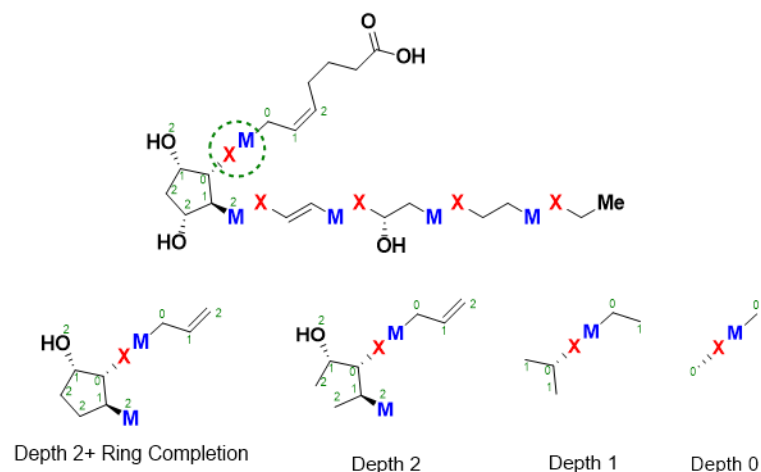
Figure 2-18 Depth 2+ring completion down to depth 0 for the highlighted coupling

of atoms did not accidentally remove any stereochemical information. A canonical SMILES of the extracted coupling is created and stored. This process is repeated at depth 2, 1, and 0 (**Figure 2-18**).

The algorithm returns to the parent synthetic plan and performs the coupling. This is carried out by first joining the two attachment points, deleting the termini, and finally imposing the stereochemistry of the parent on the newly created bond to accurately preserve stereochemistry (**Figure 2-19**). This process is then repeated on the next coupling. At the end, the final product is compared back to the parent natural product before it went through fragmentation to confirm a perfect match.
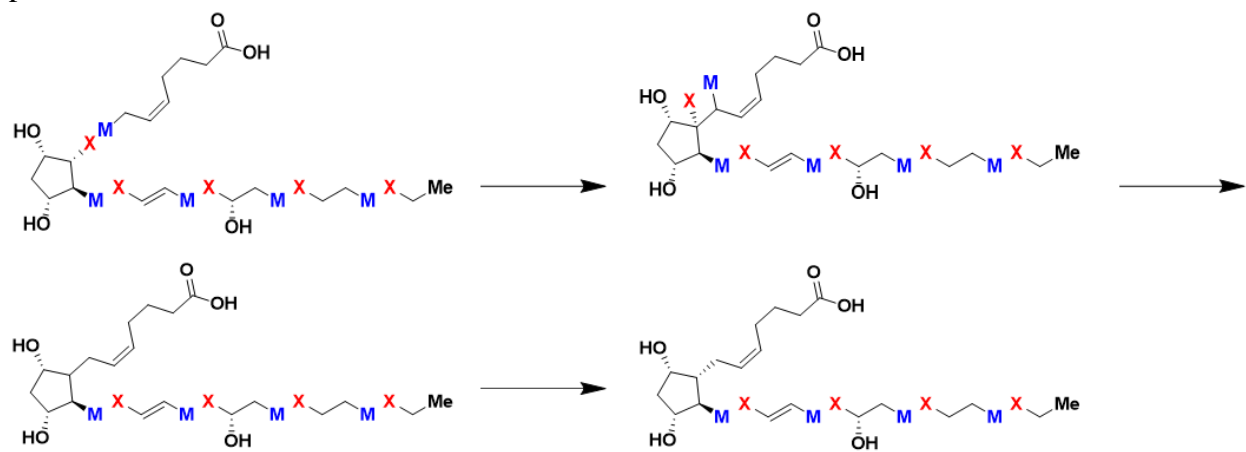
Figure 2-19 Algorithmic process for performing couplings during synthetic planning

2-7 OPTIMIZATION TO SELECT A SET OF BLOCKS

With this set of valid synthetic plans and their relevant coupling data, we could begin optimization. We chose to target a minimum number of blocks required to obtain 75% coverage of linear natural product chemical space. As our goal was to utilize data to reveal key unsolved methodological problems, we felt it was important to target a percent coverage that would represent most of natural product chemical space while remain obtainable. Knowing an

approximation would need to be utilized for computational cost reasons, we began by looking at a greedy approach, as the maximax set cover problem we are interested in is a submodular maximization. We ultimately developed a new heuristic approach which we call a forward-backward optimization. In this approach, blocks from all valid synthetic plans begin in an inactive set. Blocks in the inactive set are ranked according to their maximum potential to provide coverage (number of nonhydrogen atoms in block times number of times block appears). A best subset of
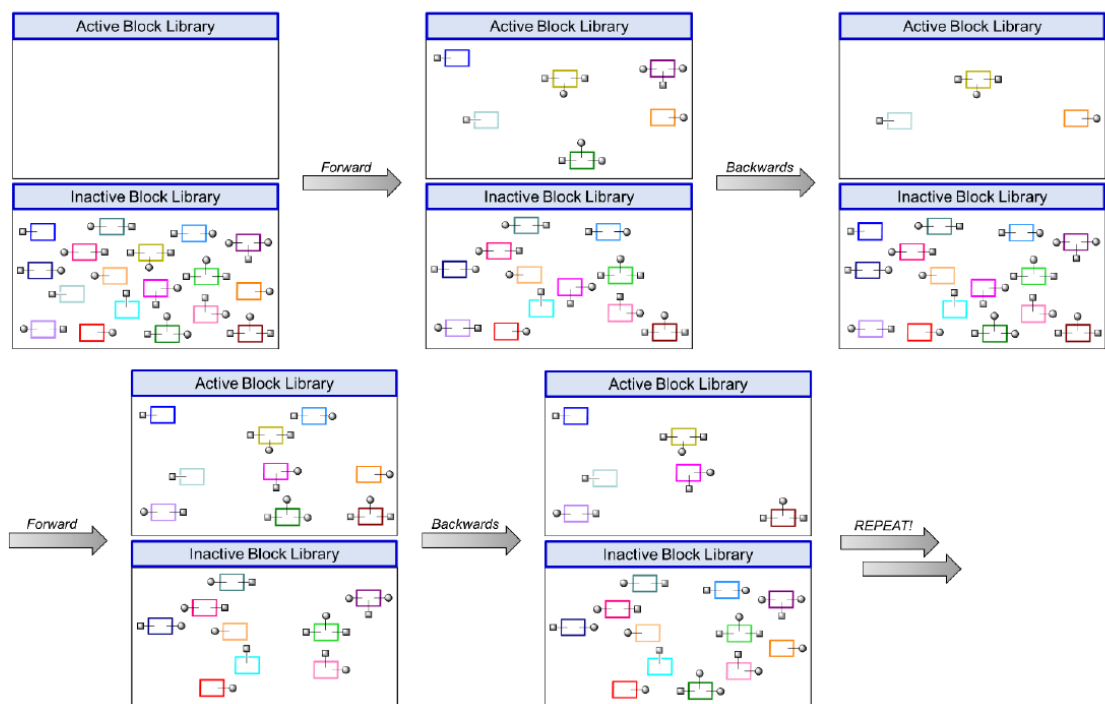
Figure 2-20 Representation of the Forward-Backward algorithm

N fragments is then added to the active set. All blocks in the active set are then ranked, and the small subset M that provide the least coverage are removed and placed back in the inactive set and this process is repeated (**Figure 2-20**). However due to the size of our starting set of inactive blocks being over 11 billion, creating such a rank ordering at every step would be ineffective.

Instead, a random sampling of 2-3 million blocks is taken, rank ordered, and the lowest frequency score is recorded. The algorithm continues to sample blocks and only if they are above the recorded minimum frequency are they added to the list. All others are set aside. Once this rank

36

ordered list of ~10 million has be completed, only the top 1 million plus a random sampling from the remaining 9 million are considered at each step of the optimization. The block frequencies following a zipf distribution allows us to feel confident that we are only excluding blocks from the long tail of the distribution that would be highly unlikely to ever be added to the active set.

At the time of calculation of frequency for each block, all natural products that contain that block are flagged. This way, when a block is added to the active set the algorithm only has to look at those natural products to calculated coverage. Additionally, the synthetic plan(s) with the highest coverage at each step are flagged and the natural product is only checked if different synthetic plan has the potential to surpass the current best with

Figure 2-21 *Top* Forward and Backward steps taken during optimization *Bottom* Complete steps taken reveals 1350 blocks needed to cover 75% of NP chemical space

addition of the block in question. This is determined by checking if any other synthetic plans are within X atoms of coverage away from the current best where X is the number of nonhydrogen atoms in the block. If the gap in coverage between the synthetic plans is larger than the block could possibly fill, then it cannot become the new best. This also applies when calculating coverage lost during the backwards step. Thus, as every step the active set to grow by (N-M) blocks. In this way, we counter the problem of a block's actual contribution to coverage changing based on what other

blocks exist in the set at that time. Ultimately this resulted in the removal of blocks from the active set that began to lose utility as other blocks were added. Furthermore, by not locking in one blockization beforehand, we avoided potentially getting caught in a local minimum where perhaps the second or third best synthetic plan for natural product in isolation, turns out to be the best synthetic plan when considered in conjunction with all molecules in the set.

As we move through the optimization the size of N changes because the increase in percent coverage for a set of blocks is much larger in the beginning than later on. Thus, once the curve begins to first level off around 40% a best fit line is applied to predict the number of blocks needed to gain 5% coverage. This prediction is used to calculate N and M and is redone after each step. Resulting in the step size increases over time (**Figure 2-21**). Carrying out this optimization procedure we concluded that 1350 blocks are required to cover 75% of linear natural product chemical space. A small selection of blocks can be seen in **Figure 2-22**, while the entire set can be found in the experimental section. The frequency of each block is determined by considering the highest coverage synthetic plan(s) flagged at the 75% step. Any block not in our set remains as part of the synthetic plan but is considered a specialty block—one that would have to be made independently in order to complete that particular natural product. If there is only one synthetic plan flagged, it is selected as the optimal synthetic plan, but in the case of multiple equivalently covered synthetic plans a tie breaker is applied.

The first tie breaker selects the synthetic plan(s) with the fewest number of couplings as a measure to increase synthetic tractability. Second, synthetic plans with the fewest number of specialty blocks are selected to minimize the total number of blocks outside the set that would have to be made. Finally, is there is still a tie, the algorithm determines the blocks that would be added in the next step of the forward backward. Pretending those blocks are part of the set the first
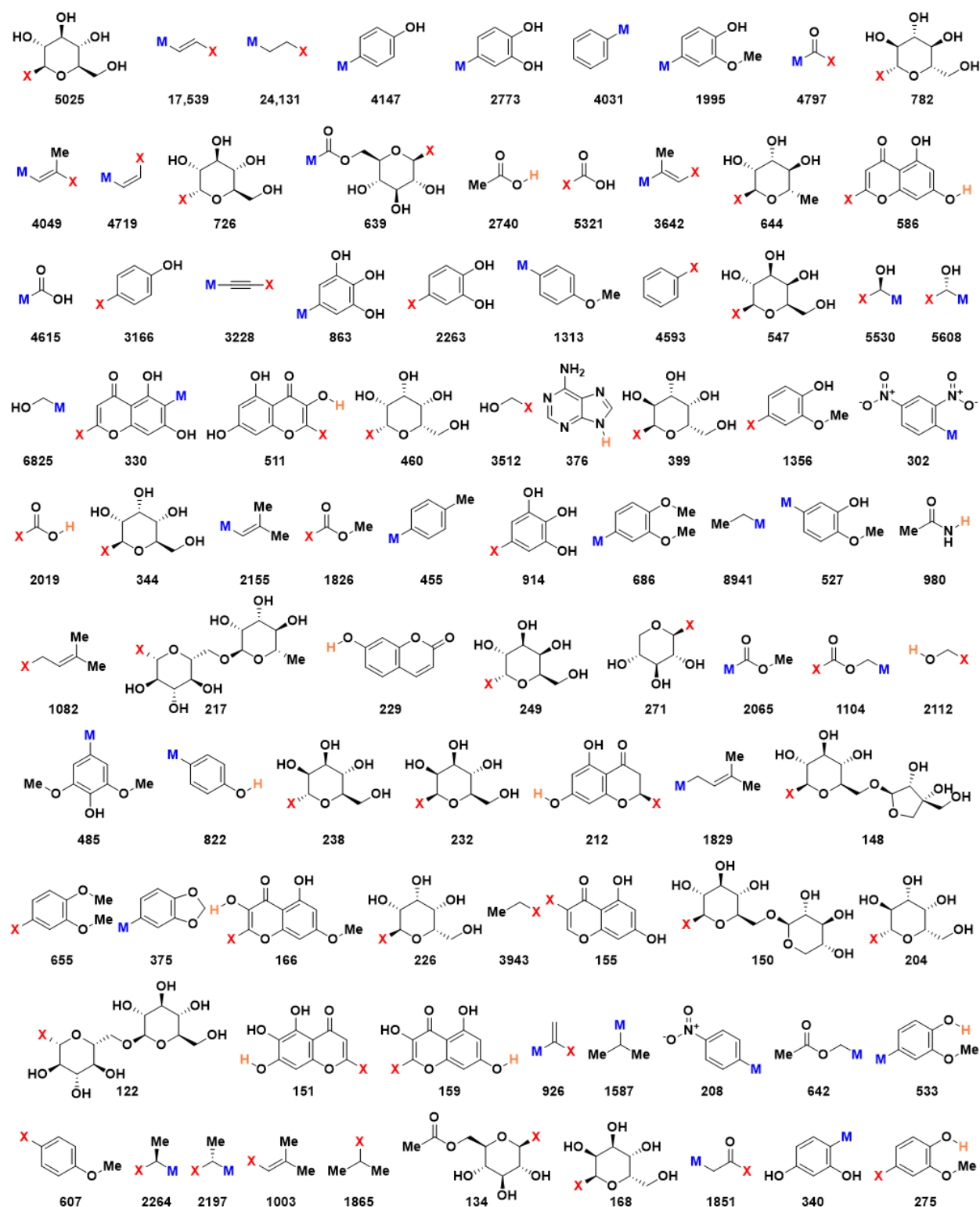
Figure 2-22 Example blocks from our set of 1350 with frequencies listed underneath

two tie breaking measures are again applied. Steps continue to be taken until the tie is broken. In

this way ties are broken with a priority to utilize the most useful specialty blocks. Such a preference
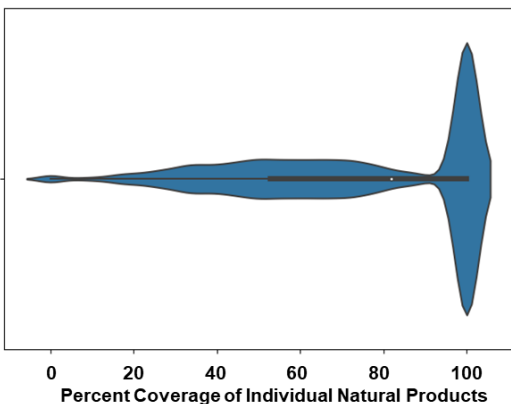
Figure 2-23 Coverage of individual natural products

could be included for the whole optimization, but we determined for our purposes it was not worth the additional cost.

This process ultimately results in the selection of a single optimal synthetic plan for each natural product. While we know the coverage is 75% across the whole set, we also wanted to see what coverage of individual natural products looked like. Excitingly we found that 44% of natural products were completely covered by the 1350 blocks in our set. In the violin plot in **Figure 2-23** the area under the curve indicates the number of natural products at each percent coverage, while the box and whisker plot inside it shows us that the mean coverage is 80% and the lower quantile is at 50%. We also wanted to know for the percent of a natural product not covered how many specialty blocks would be required to access the natural product. In addition to the 44% covered with zero special blocks, 53% are covered with only one specialty block (**Figure 2-24**). We feel that having 97% of natural products covered with one or less specialty blocks makes this solution very tractable.

Figure 2-24 Number Specialty Blocks required for linear natural product synthesis

Looking at the number of blocks per natural product (**Figure 2-25**), we can see that even though we only considered highly fragmented synthetic plans in the optimization the average number of blocks is still relatively low at 4.9. We also checked to see if there was a correlation
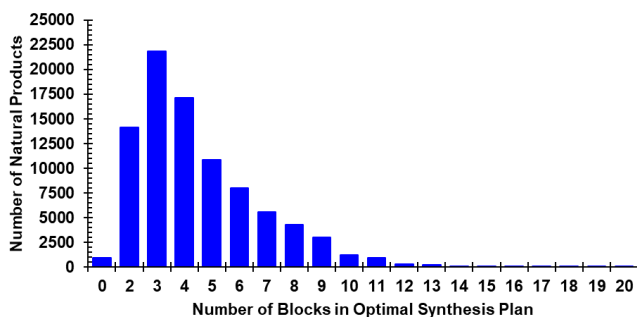
Figure 2-25 Distribution of number of blocks per natural product

between the percent coverage and size of the natural product. However, we see that there is a wide distribution of percent coverage at every size of natural product (**Figure 2-26**).

2-8 EXAMINING COUPLINGS AND DETERMINING SUBSTRATE SCOPES

Next, the coupling data extracted from all the optimal synthetic plans is collected and identical SMILES at each depth are clustered together. The number of SMILES strings in each cluster gives the frequency of that coupling. At this point we also introduced a bond classification clustering between depth 0 and 1, to more accurately represent the way chemists think about methodologies.
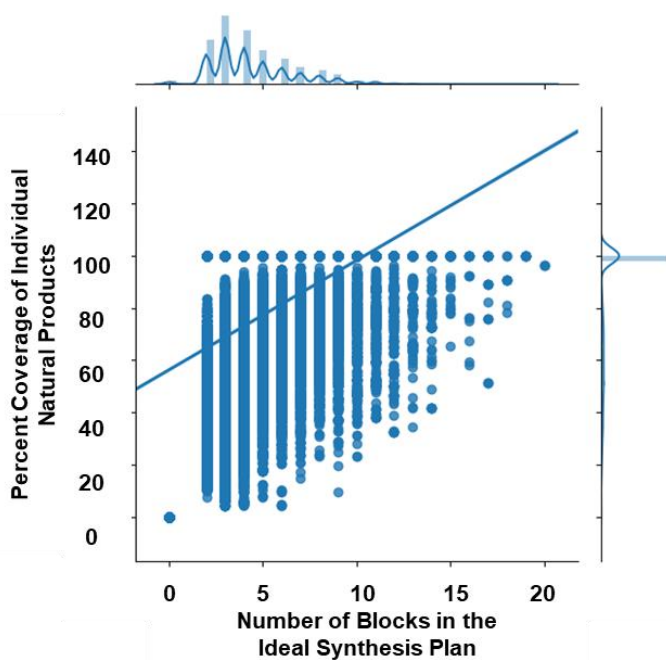
Figure 2-26 Percent coverage vs size of natural product

For example, we wanted to make sure that aryl rings with zero, one, or two ortho substituents were all grouped together even thought at depth 1 they have different SMILES. Ultimately, we ended up with bond classifications for sp^3 attachment points being congregated into primary, secondary, tertiary; those for sp^2 attachment points into aryl, vinyl, and acyl; and sp attachment points remaining as a single category.

We utilized a sunburst plot to show a rank ordering of the couplings at all depths (**Figure 2-27**). Looking at depth 0 reveals that C-M to C-X bonds represent the overwhelming majority of couplings that occur in natural products. Moving out to the bond classifications depth, we see a dramatic increase in the number of categories. To us the numbers for these categories represent the
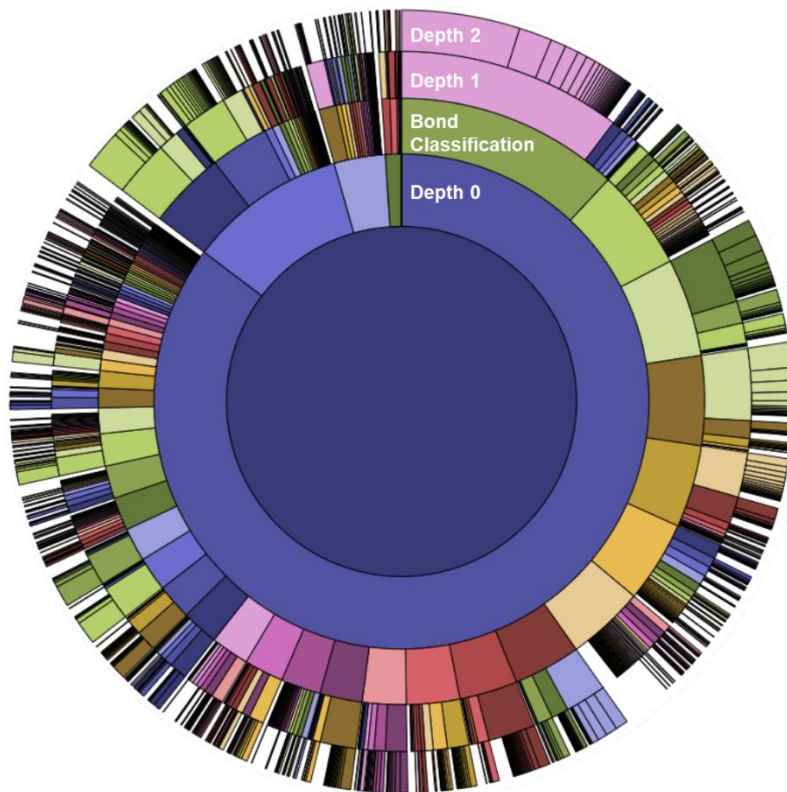
Figure 2-27 Sunburst diagram representing extracted coupling information

ultimate goal of identifying impactful unsolved methodology. Looking at the top 20 coupling categories, (**Figure 2-28**) we see a few methodologies that are well precedented, like the C9 aryl-aryl, but many more that have little to no precedence. Unsurprisingly, primary-primary couplings are the most common, with almost 37,000 examples. This top 20 list also highlights the significance of sp^3 couplings, with 14 of them containing one or more sp^3 coupling partners.

Moving into individual bond classifications on the sunburst reveals the information that can be used to construct a data driven substrate scope (**Figure 2-29**). The more categories at depth 1 and 2, the more diversity is represented within that coupling. Additionally, due to the immense amount of data involved, all categories containing less than 50 examples at any given depth were grouped together as miscellaneous and are represented by white space on the plot. Thus, more white space also represents a more diverse substrate scope. Comparing something like C1 primary-
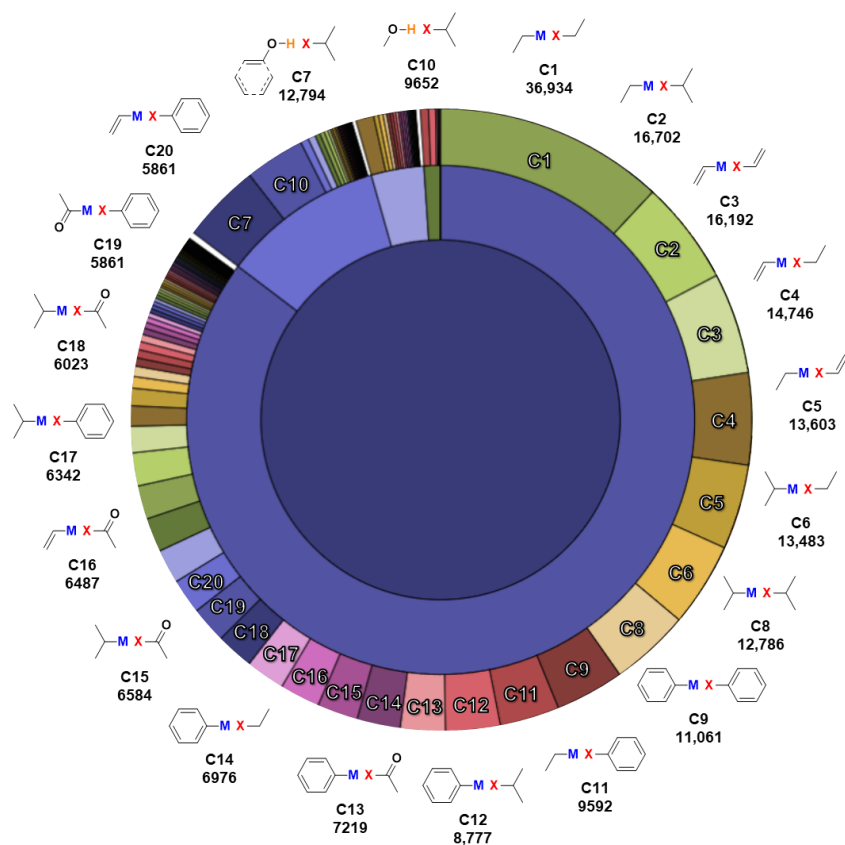
Figure 2-28 Top 20 couplings

primary to C9 secondary-secondary we can see just how much more diversity is contained within a secondary-secondary coupling, which makes sense.

We wanted to take our overarching goal of using data to identify impactful methodology and test it in the hood. In synthetic organic chemistry methodology development, typically once a target methodology has been identified a single set of test substrates are utilized to optimize conditions. Once conditions have been finalized, a substrate scope is built largely around trial and error of other similar substrates to see what also works. Demonstrating functional group tolerance is frequently important, but there is no standard for what functional groups should be tested.

Instead, we wanted to prospectively identify a substrate table based on the data for a particular coupling and optimize methodology across multiple sets of two substrates to arrive at generally applicable conditions. We personally chose to target the primary-vinyl coupling, the 5th most common coupling (**Figure 2-30**). Looking at the data for this coupling we can see that both cis and trans, as well a variety of methyl substitution patterns, are going to be important to consider when developing our conditions which is reported in Chapter 3.

Figure 2-29 Substrate scopes of top 20 couplings

2-9 FUTURE DIRECTIONS

Looking at our results, we noticed a few areas where further development could offer benefits. First, we were surprised to see that amide and ester bonds were not being utilized in

optimal synthetic plans as much as we would have expected, and that instead that breakage of the acyl bond on the other side was more prevalent than we desired. We attempted to increase the frequency of utilization of the heteroatom acylations by adding the neighboring acyl
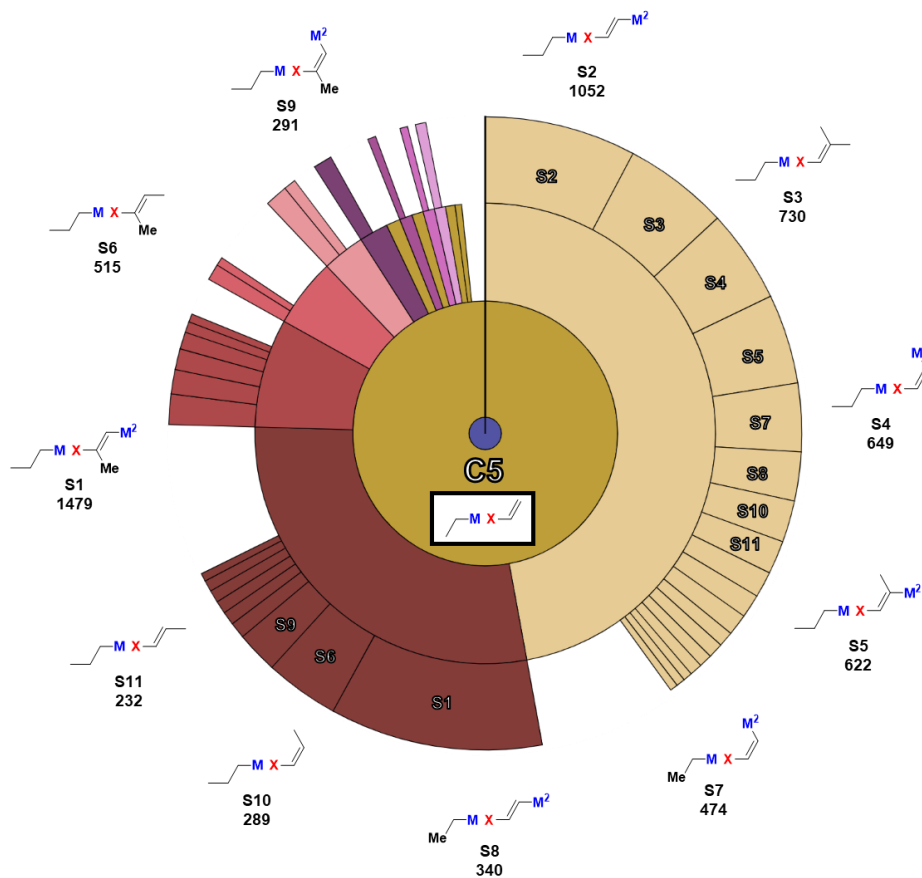
Figure 2-30 Substrate scopes of C5 primary vinyl

bond to the list of forbidden bonds. While we thought this would push the algorithm to break more amide and ester bonds, it instead most frequently encased the bonds on both sides of the carbonyl with in blocks and choose breakage points at other parts of the molecule. We had a significant reduction in the overall number of amide and ester couplings, so we removed this change.

Secondly looking to be able to include natural products with greater than 14 breakable bonds, we know it would be important to include the number of blocks per natural product as a factor during optimization. Both of these issues would benefit from a multi objective optimization strategy. To tackle such a strategy, we need to rethink the way we fragment molecules, as during optimization we need access to the larger blocks contained in fragmentations above the *k-1* limit that we have utilized here. As such, initial work has begun on implementation of a free tree

structure that would allow us to traverse useful paths of breakage from full molecule down to its most fragmented form, while abandoning branches that are unproductive before they are explored. This would give us access to the larger blocks at time of optimization while avoiding an exponential expansion of the number of fragmentations.

Then at time of optimization, instead of only considering number of blocks and percent coverage, we would also look at average number of blocks per natural product, and preferences for specific couplings. Knowing that we would still want to target 75% coverage, we could create a pareto front for 75% coverage based on number of blocks, average number of blocks per natural products, and a preference for the utilization of amide and ester bonds, and choose a point that we felt most met our needs.

2-10 SUMMARY AND CONCLUSIONS

We have successfully constructed an algorithm to fragment natural products, run an optimization on a large set of possible blocks, and ultimately reveal a set of blocks, proposed synthetic plans, and list of impactful methodologies for natural product synthesis. Within each coupling we can show the important structures and functional group tolerances to allow for a data driven and preemptive substrate table selection. We have also incorporated many points of flexibility where human input or preference can be implemented to tailor the results for a given objective. To that end, this algorithm works for any collection of molecules, and we believe many other classes of small molecules such as materials or pharmaceuticals could also benefit from this kind of overarching analysis. Data driven identification of important methodologies and work towards their solutions can only help advance the field of chemistry while the building block approach with focus on the possibility to automate can help expand the ability to make designer molecules to nonexperts and help advance related fields.

2-11 REFERENCES

(1)   Tian, R.; Mathey, F.-O. 7-Phosphanorbornenium Borohydrides: A Powerful Route to Functional Secondary Phosphine-Borane Complexes. *Organometallics* **2010**, *29*, 1873. https://doi.org/10.1021/om100053d.

(2)   Fu, T.; Qiao, H.; Peng, Z.; Hu, G.; Wu, X.; Gao, Y.; Zhao, Y. Palladium-Catalyzed Air-Based Oxidative Coupling of Arylboronic Acids with H-Phosphine Oxides Leading to Aryl Phosphine Oxides. *Organic and Biomolecular Chemistry* **2014**, *12* (18), 2895–2902. https://doi.org/10.1039/c3ob42470g.

(3)   Vijaikumar, S.; Pitchumani, K. Simple, Solvent Free Syntheses of Unsymmetrical Sulfides from Thiols and Alkyl Halides Using Hydrotalcite Clays. *Journal of Molecular Catalysis A: Chemical* **2004**, *217* (1–2), 117–120. https://doi.org/10.1016/J.MOLCATA.2004.03.002.

(4)   Pizova, H.; Bobal, P. An Optimized and Scalable Synthesis of Propylphosphonic Anhydride for General Use. *Tetrahedron Letters* **2015**, *56* (15), 2014–2017. https://doi.org/10.1016/j.tetlet.2015.02.126.

(5)   Kiyokawa, K.; Suzuki, I.; Yasuda, M.; Baba, A. Synthesis of Cyclopropane-Containing Phosphorus Compounds by Radical Coupling of Butenylindium with Iodo Phosphorus Compounds. *European Journal of Organic Chemistry* **2011**, *2011* (11), 2163–2171. https://doi.org/10.1002/ejoc.201001471.

(6)   Shih, H. W.; Chen, K. T.; Cheng, W. C. One-Pot Synthesis of Phosphate Diesters and Phosphonate Monoesters via a Combination of Microwave-CCl 3CN-Pyridine Coupling Conditions. *Tetrahedron Letters* **2012**, *53* (2), 243–246. https://doi.org/10.1016/j.tetlet.2011.11.032.

(7)   Deprez, P.; Mandine, E.; Gofflo, D.; Meunier, S.; Lesuisse, D. Small Ligands Interacting with the Phosphotyrosine Binding Pocket of the Src SH2 Protein. *Bioorganic and Medicinal Chemistry Letters* **2002**, *12* (9), 1295–1298. https://doi.org/10.1016/S0960-894X(02)00140-3.

(8)   Krouželka, J.; Linhart, I. Preparation of Arylmercapturic Acids by S-Arylation of N,N'-Diacetylcystine. *European Journal of Organic Chemistry* **2009**, *2009* (36), 6336–6340. https://doi.org/10.1002/ejoc.200900982.

(9)   Guo, F. J.; Sun, J.; Xu, Z. Q.; Kühn, F. E.; Zang, S. L.; Zhou, M. D. C-S Cross-Coupling of Aryl Halides with Alkyl Thiols Catalyzed by in-Situ Generated Nickel(II) N-Heterocyclic Carbene Complexes. *Catalysis Communications* **2017**, *96*, 11–14. https://doi.org/10.1016/j.catcom.2017.02.007.

(10)   Vijaikumar, S.; Pitchumani, K. Simple, Solvent Free Syntheses of Unsymmetrical Sulfides from Thiols and Alkyl Halides Using Hydrotalcite Clays. *Journal of Molecular Catalysis A: Chemical* **2004**, *217* (1–2), 117–120. https://doi.org/10.1016/j.molcata.2004.03.002.

(11)   Yoshimura, T.; Ohkubo, M.; Fujii, T.; Kita, H.; Wakai, Y.; Ono, S.; Morita, H.; Shimasaki, C.; Horn, E. Synthesis, Structure, and Thermolysis Mechanism of S-Alkoxythiazynes. *Bulletin of the Chemical Society of Japan* **1998**, *71* (7), 1629–1637. https://doi.org/10.1246/bcsj.71.1629.

(12)   Dherbassy, Q.; Djukic, J. P.; Wencel-Delord, J.; Colobert, F. Two Stereoinduction Events in One
         C−H Activation Step: A Route towards Terphenyl Ligands with Two Atropisomeric Axes.
         Angewandte Chemie - International Edition **2018**, *57* (17), 4668–4672.
         https://doi.org/10.1002/anie.201801130.

(13)   Kamble, R. B.; Chavan, S. S.; Suryavanshi, G. An Efficient Heterogeneous Copper Fluorapatite
         (CuFAP)-Catalysed Oxidative Synthesis of Diaryl Sulfone under Mild Ligand- and Base-Free
         Conditions. *New Journal of Chemistry* **2019**, *43* (3), 1632–1636.
         https://doi.org/10.1039/c8nj04845b.

(14)   Xie, F.; Ni, T.; Zhao, J.; Pang, L.; Li, R.; Cai, Z.; Ding, Z.; Wang, T.; Yu, S.; Jin, Y.; Zhang, D.; Jiang, Y.
         Design, Synthesis, and in Vitro Evaluation of Novel Antifungal Triazoles. *Bioorganic and Medicinal
         Chemistry Letters* **2017**, *27* (10), 2171–2173. https://doi.org/10.1016/j.bmcl.2017.03.062.

CHAPTER 2

EXPERIMENTAL SECTION

GENERAL MATERIALS AND METHODS

The code was developed using Python 3.7 using a combination of RDKIT and Openbabel are for molecular data manipulation. Cython 3.0.1 is utilized for speeding up in memory data manipulations. The parallel works per process with shard disk. The delopment of the code was carried out by Nathan Russell in Jian Pengs group.

While the code can be made freely available if requested, I did not participate in any of the code writing itself. I was heavily involved in development of the concepts and troubleshooting described in Chapter 2.

FINAL LIBRARY OF ACTIVE BLOCKS

All blocks in the set can be found in Appendix I. The set of blocks is rank ordered according to the number of times the block is used across all optimal synthesis plans. This frequency and rank are shown under each block.

CHAPTER 3

METHODS DEVELOPMENT FOR GENERALIZED APPILCATION TO A COMPUTATIONALLY PREDETERMINED SUBSTRATE SCOPE FOR PRIMARY CSP3 BORONATES AND VINYL HALIDES

ABSTRACT

Utilizing our human guided algorithm, we were successfully able to identify impactful couplings for natural products synthesis. Furthermore, we were able to use data to help illuminate their relevant substrate scopes. As an example, we undertook the challenge of developing methodology for the fifth most common coupling, primary alkyl organometallic to vinyl halide. By optimizing conditions on a set of substrates rather than a single example, we were able to rationally develop a new phosphine ligand to accomplish this coupling with good yields and high stereoselectivity.

This coupling methodology is amenable to modular and automatable synthesis. Hopefully with the similar development of further identified but unsolved methodologies can lead to the advancement of synthetic efforts toward natural products and natural product inspired small molecules.

3-1 LITERATURE PRECEDENT FOR UNACTIVATED PRIMARY-VINYL SUZUKI COUPLINGS

In a demonstration of this new concept of methodology development for predetermined targeted generality, we have undertaken the development of methodology identified as impactful but lacking a general solution—specifically the fifth most common coupling, primary alkyl organometallic to vinyl halide. As is most fitting with our platform we chose to target Suzuki methodology as a solution. Looking in the literature there are numerous examples of 9-BBN based primary-vinyl couplings[1–5], but unfortunately 9-BBN has several problems that prevent it from working within our constraints. While 9-BBN has successfully been used in iterative synthesis, the requirements of a terminal olefin and a hydroboration reaction would limit functional group tolerance and the types of blocks that could be made. The additional reactions required to create an iterative cycle make it less efficient and more difficult to automate, with the hydroboration reaction having the added complication of regioselectivity. Even though hydroboration generally has a very high regioselectivity, any
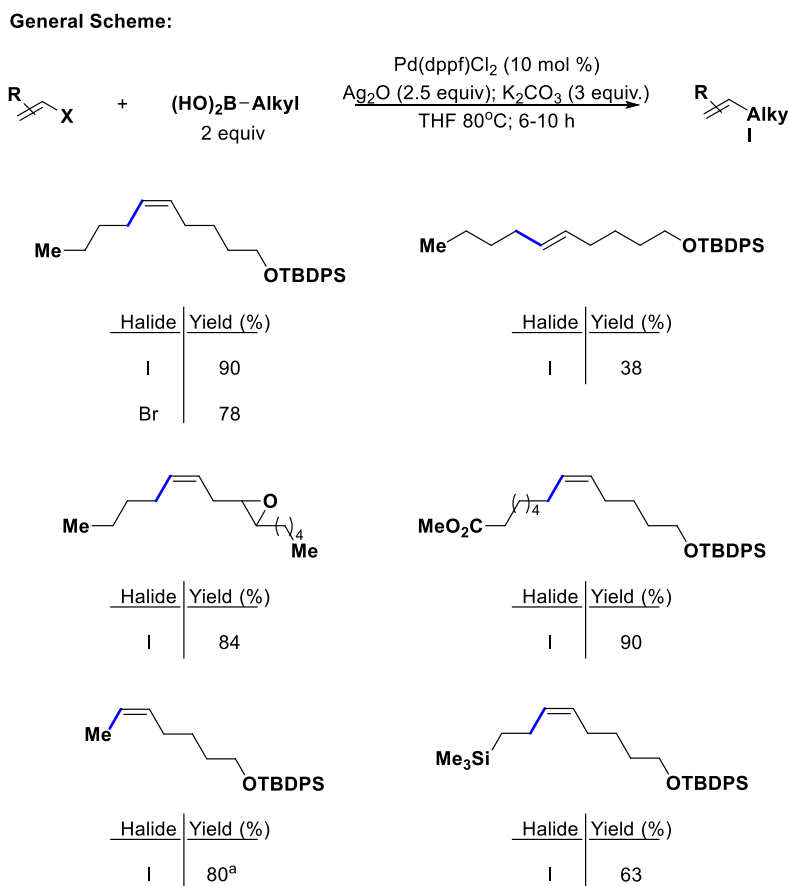
Figure 3-1 Silver mediated coupling of primary boronic acid to vinyl halides

51

stereoselectivity issue adds up over the course of multiple reactions creating difficult to separate product mixtures and reduction of yields.

General Scheme:
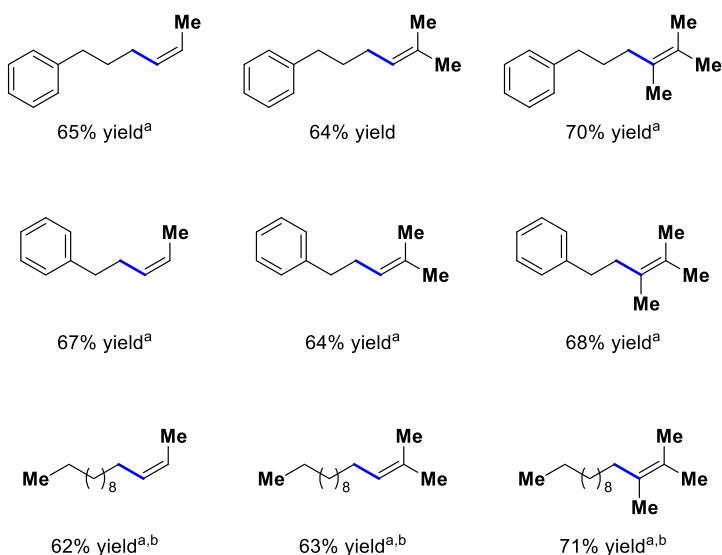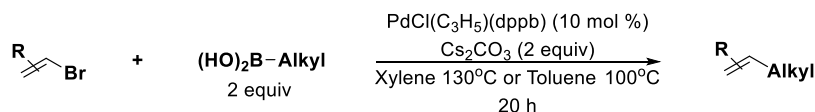
Figure 3-2 Aqueous biphasic coupling of primary boronate to vinyl halide

With this in mind, focus was turned to literature precedent for unactivated primary-vinyl couplings utilizing boronic acids, boronic esters, and trifluoroborate salts. In 2001, Falck reported on anhydrous silver oxide promoted couplings between primary boronic acids and Csp^2 halides (**Figure 3-1**). Both bromides and iodides showed good yields with the bidentate diphosphine ligand 1,1'-bis(diphenylphosphino)ferrocene (dppf), however the vast majority of examples were cis halides, with only one trans halide being shown to couple in a significantly lower yield.[6] Doucet has also published methodology using bidentate diphosphine ligands, specifically 1,3-bis(diphenylphosphino)propane (dppb), but in this case without a silver salt (**Figure 3-2**). Cis, symmetrically trisubstituted, and 1,1 disubstituted halides were all shown to couple in moderate yields, but there were no examples of trans halides.[7] The Molander group utilized dppf with trifluoroborates in an aqueous biphasic system to afford coupling with a variety of cis, tri-, and tetrasubstituted halides (**Figure 3-3**). Again, trans halides were noticeably absent from the substrate table.[8] In none of these reports, or the few papers that

have one off examples of unactivated primary vinyl couplings,[9,10] are E:Z ratios reported or discussed.

3-2 EXPLORING CONDITIONS FOR PRIMARY-VINYL SUZUKI COUPLING

Due to MIDA's incompatibility with aqueous biphasic conditions, and previous successes in our lab with silver mediated conditions,[11] conditions similar to those used by the Falck group were targeted. However, attempts by my former colleague Andrea Palazzolo Ray to utilize anhydrous conditions for primary boronic acids to vinyl halo-MIDA boronates proved unsuccessful. Significant decomposition issues were

General Scheme:

Substrate Scope:

halide	boronic acid	time	yield
		7.0 h	74
		3.0 h	93
		2.0 h	78
		5.0 h	82
		12.0 h	69
		3.0 h	54

Figure 3-3 Aqueous biphasic coupling of primary BF$_3$K salts to vinyl halide

encountered, and in a wide screen of ligands nothing gave better than 15% yield, while most gave trace to no product. At the time that I joined the lab, work on a second generation MIDA, specifically geared to withstand aqueous biphasic conditions, gave us the confidence to shift focus away from exclusively anhydrous conditions.

These advances on a second generation MIDA ligand were enabled by an in-depth study of what turned out to be the dual mechanism of MIDA deprotection. Depending on the conditions,

MIDA deprotection can occur after water attack of the dative N→B bond in mild base conditions, or hydroxide attack of the carbonyl in strong base conditions.[4] Given the desire to utilize this new MIDA ligand for aqueous biphasic conditions where the N→B bond is the site of deprotection,
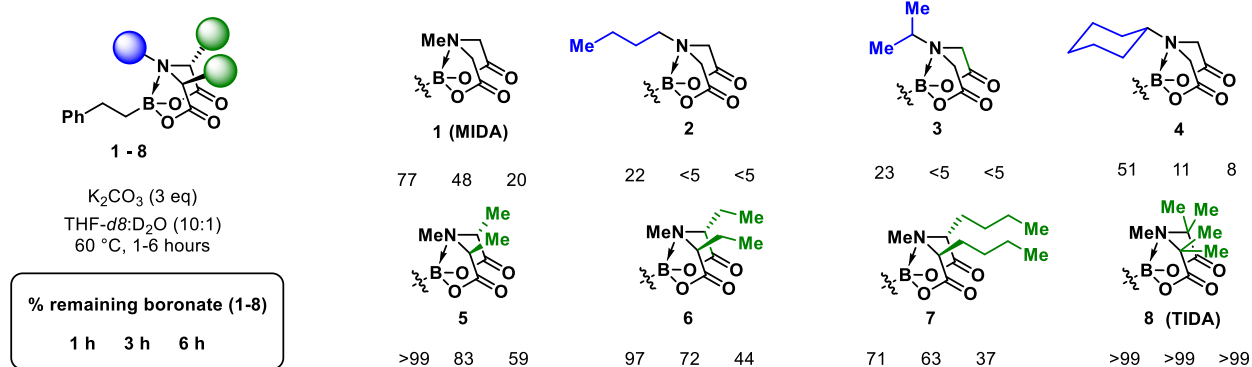
Figure 3-4 Development of second generation MIDA ligand

substitution of the nitrogen and carbon backbone of MIDA were explored to see if steric or electronic tuning of the MIDA cage could increase its hydrolytic stability (**Figure 3-4**). The tetramethylated variant of *N*-methyliminodiacetic acid (TIDA), was found to be exceptionally stable, hydrolyzing at least 50 times slower than MIDA. Study of x-ray crystal structures of TIDA boronates suggested a significant increase in the covalent character of the N—B bond due to charge redistribution, likely from hyperconjugation.

Now that we had an idea of the iterative platform that we wanted to utilize we could turn the data about the substrate scope
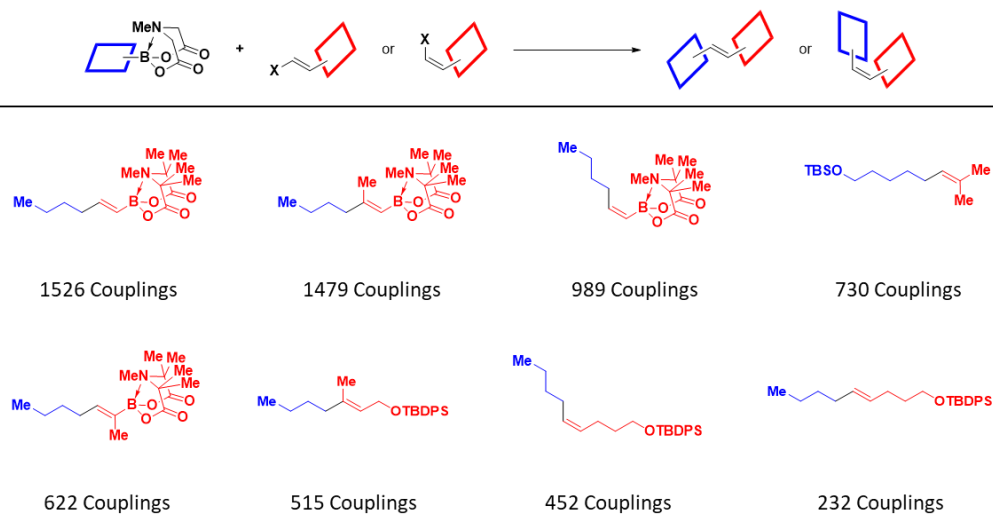
Figure 3-5 Finalized substrate scope

from the analysis into concrete examples. Looking at the top examples we first began by combining categories of terminal ethyl blocks with those of the blocks that extend beyond depth
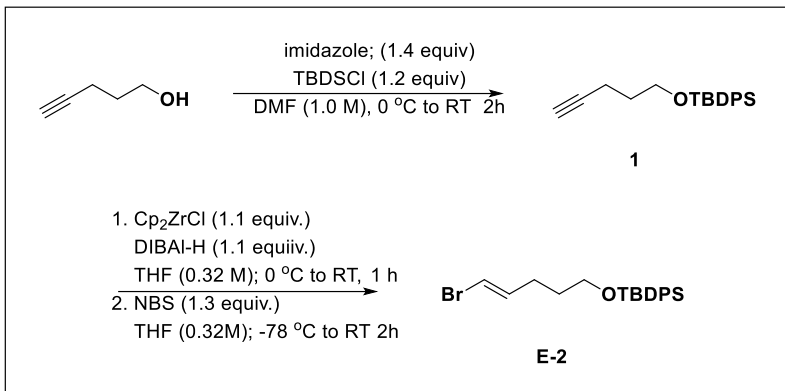
Figure 3-6 Synthesis of trans halide

two if they were coupling to identical halides. For example, S4 and S7 were combined as well as S2 and S8 (**Figure 2-31**). With this completed we discovered that ~50% of this substrate scope could be covered with 8 example couplings. Blocks where the next terminus was visible were created as bifunctional TIDA boronates. Blocks that did not contain a terminus within depth 2 were extended out and attached to a functional group that would allow for facile detection and purification, in this case a tert-butyldiphenylsilyl (TBDPS) protected oxygen. This gave us the target substrate scope in **Figure 3-5**.

Given our predetermined substrate scope we knew that it would be important to screen for conditions utilizing both E and Z halides. Because of the low yield for the singular trans halide example in the literature, we decided to first target trans olefin **E-2** for our initial ligand screen to make sure we found a starting point that could afforded the product for the trans. **E-2** was synthesized from 4-pentynol as shown in **Figure 3-6**. TBDPS protection of the free alcohol,
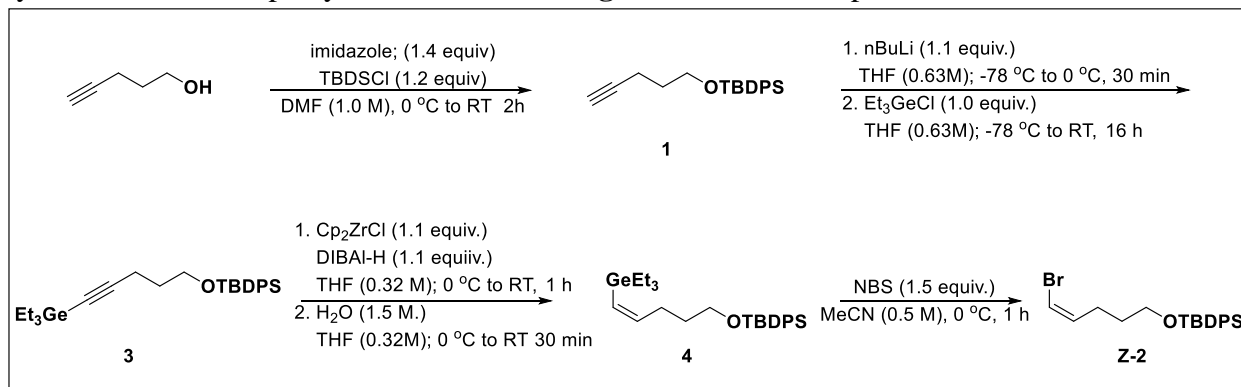
Figure 3-7 Synthesis of cis halide

followed by hydrozirconation and in situ bromodezirconation gave the desired product with excellent stereospecificity (99:1 E:Z). Across a wide screen of ligands including, trialkyl phosphines, triaryl phosphines, bidentate diphosphines, and buckwald ligands, overall triaryl phosphines performed the best. We decided to move forward with triaryl phosphines as the main ligand class of focus and begin to screen against both cis and trans substrates.

To make the cis equivalent of our halide, the same OTBDPS protected 4-pentynol was utilized. A triethyl germanium group was installed on the alkyne, before hydrozirconation and in situ hydrodezirconation was used to afford the cis germanium alkene. Stereospecific bromodegermination gave **Z-2** in excellent sterospecificity (3:97 E:Z) (**Figure 3-7**). Cis and trans products were independently synthesized utilizing a Negishi reaction and an HPLC method was developed to track E:Z ratios. It was at this point that we noticed something odd. When triphenylphosphine was used significant isomerization was observed for the E halide, while the Z halide showed complete retention of stereochemistry (**Figure 3-15** *entry 1*).

3-3 OLEFIN ISOMERIZATION ISSUES AND POTENTIAL MECHANISMS

While E:Z ratio has rarely been reported for primary-vinyl Suzuki couplings, studies by the Lipshutz group indicate that olefin isomerization is highly ligand dependent in Stille[12], Negishi[13], and Suzuki[14] couplings. While no mechanistic studies were done to investigate the means of isomerization, a mechanism with a zwitterionic-metal based carbene intermediate was proposed. Even

Figure 3-8 Proposed mechanism for Zwitterionic-metal carbene mediated isomerization
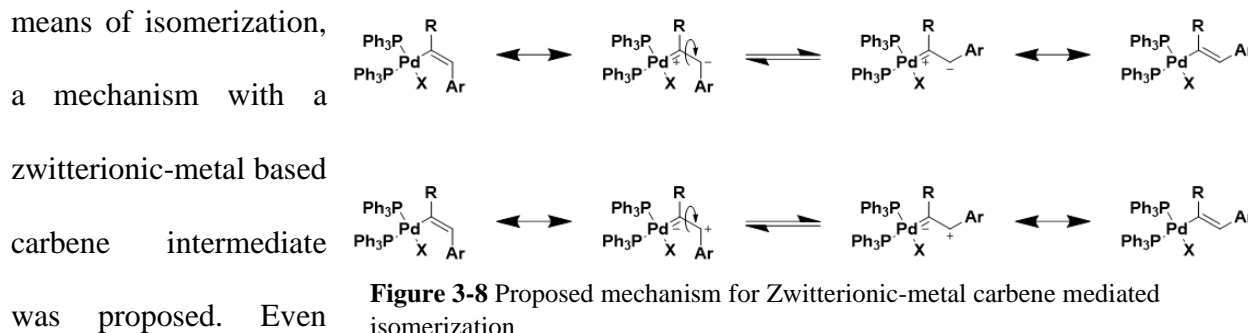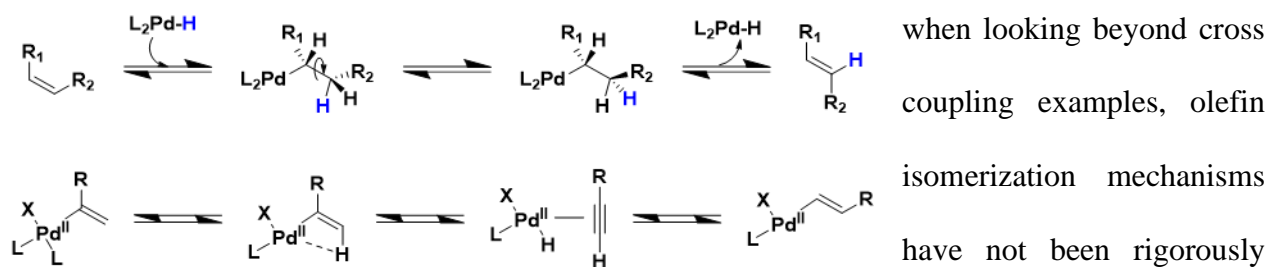
Figure 3-9 Proposed mechanism for palladium hydride mediated isomerization

when looking beyond cross coupling examples, olefin isomerization mechanisms have not been rigorously studied. Proposals have tended to fall into three main categories: zwitterionic-metal carbene mediated, palladium hydride mediated, and phosphine mediated. In addition to cross couplings, Zwitterionic-metal carbene intermediates have been proposed as the source of isomerization for carbopalladation,[15] carbonylation,[16] and migratory insertion.[17–19] While there is some NMR data that supports this
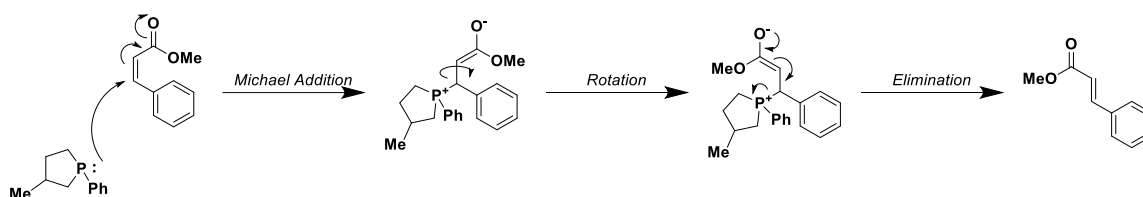
Figure 3-10 Proposed mechanism for phosphine mediated isomerization in the Wittig reaction

hypothesis,[15–17] overall the mechanism is not well understood (**Figure 3-8**). The Skyrdstrup group has proposed palladium hydride mediated isomerization for both cis to trans[20], and 1,1-disubstituted to trans olefins[21] (**Figure 3-9**). Phosphine mediation isomerization of the product has been proposed for the Wittig reaction,[22] (**Figure 3-10**) while indications of C-P reductive elimination from oxidative addition adducts being responsible for isomerization was reported by Ozawa and co-workers in 2009.[23] This report was of most interest to me, as it showed trans to cis isomerization as opposed to most of the other proposals which focused on cis to trans isomerization.

In a study of oxidative addition adducts of various E and Z styrenyl compounds, they observed an isomer dependent ability to undergo C-P reductive elimination and oxidative addition.

The E oxidative addition adduct **E-5** readily underwent C-P reductive elimination to afford **E-6**. Addition of free phosphine ligand increased conversion to **E-6**. On the other hand, the Z oxidative addition adduct **Z-5** was stable to reductive elimination, even when tested at increased time and temperatures. However
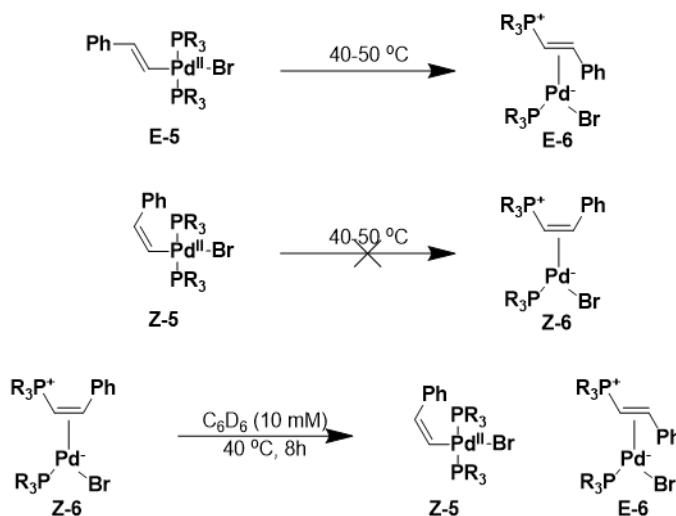
Figure 3-11 C-P reductive elimination studies

independent synthesis of **Z-6** revealed that it readily underwent oxidative addition to give a mixture of **Z-5** and **E-6**, implying a mechanism for isomerization between **Z-6** and **E-6** exists (**Figure 3-11**). These reactions were monitored by NMR, and x-ray crystal structures of all 4 compounds were obtained as confirmation. DFT calculations on optimized structures that were a good match for the crystal structures suggest that the C-P reductive elimination of **E-5** to **E-6** is exothermic while that of **Z-5** to **Z-6** is endothermic. [23]

3-4 LIGNAD DESIGN FOR MITIGATING ISOMERIZATION AND INCREASING YIELD FOR A COMPUTATIONALLY PREDETERMINED SUBSTRATE SCOPE

This led us to reason that perhaps differential ability of E and Z oxidative addition adducts to undergo C-P reductive elimination was responsible for the isomerization observed in our reaction. Post oxidative addition of the E halide, a reversible C-P reductive elimination and isomerization could afford intermediates **E-8** and **Z-8** respectively. An irreversible
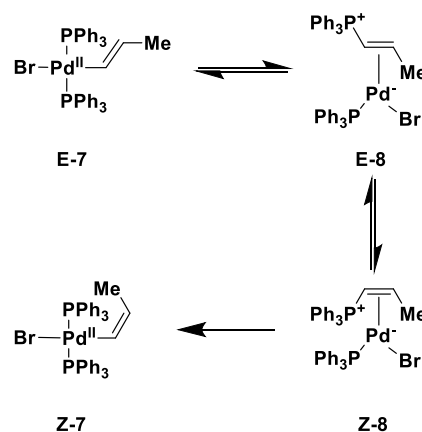
Figure 3-12 Possible mechanism for isomerization in our system
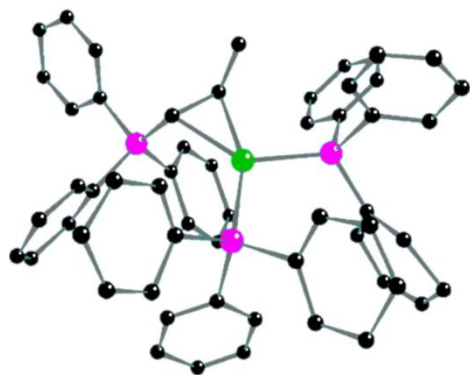
Figure 3-13 Crystal structure of C-P reductive elimination

C-P oxidative addition would then afford **Z-7**, which would become "trapped" as the Z-isomer and proceed through transmetallation and reductive elimination to give the ultimate Z product (**Figure 3-12**). However post oxidative addition of the Z halide, no C-P reductive elimination would occur, providing no mechanism for isomerization to occur. To see if this was a possibility, my colleague Daniel Blair was able to obtain a crystal structure of the reaction between (E)1-bromopro-1-ene and Pd(Ph$_3$)$_4$ which showed that C-P reductive elimination had occurred (**Figure 3-13**).

Knowing this was a possibility in our system, we began to consider how we could prevent this C-P reductive elimination. The Lipshutz group showed P(*o*-tol)$_3$ to be an effective ligand for mitigating isomerization in their studies of both Stille[12] and Suzuki[14] reactions. Also, P(*o*-tol)$_3$ is known to be
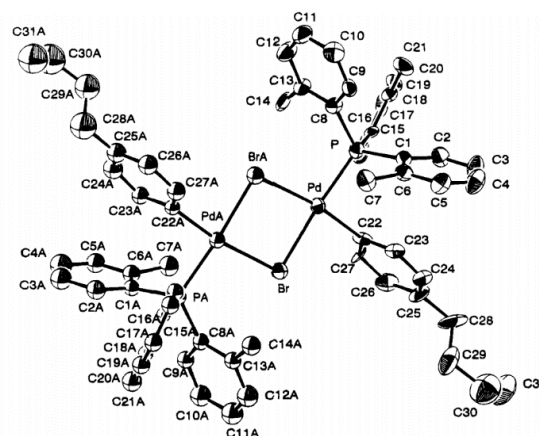
Figure 3-14 Crystal structure of P(*o*-tol)$_3$

monodentate from its crystal structure (**Figure 3-14**)[24] and given that the presence of excess ligand increased the amount of C-P reductive elimination in the Ozawa[23] report, we wondered if a monodentate ligand might decrease the amount of C-P reductive elimination

Upon coupling with P(*o*-tol)$_3$ we were gratified to find that not only was E:Z isomerization completely prevented, but also yield increased for both E and Z substrates (**Figure 3-15** *entry 2*). Encouraged by this increase in yield we wanted to explore modification of the ortho substituent. We speculated that this increase in yield could come from a promotion of reductive

	E-Halide			Z-Halide		
Ligand	Yield **E**	E:Z	DS	Yield **Z**	E:Z	DS
P(Ph)$_3$	6%	65:35	31%	31%	2:98	>99%
(o-Me-C$_6$H$_4$)$_3$P	57%	99:1	>99%	69%	2:98	>99%
(o-iPr-C$_6$H$_4$)$_3$P	74%	99:1	>99%	83%	3:97	>99%
(o-isobutyl-C$_6$H$_4$)$_3$P	14%	98:2	99%	--	--	--
(o-cyclopropyl-C$_6$H$_4$)$_3$P	48%	>99:1	>99%	63%	2:98	>99%
(o-cyclobutyl-C$_6$H$_4$)$_3$P	79%	97:3	96%	83%	3:97	99%
(o-cyclopentyl-C$_6$H$_4$)$_3$P	76%	99:1	>99%	79%	3:97	99%
(o-cyclohexyl-C$_6$H$_4$)$_3$P	59%	>99:1	>99%	--	--	--
(o-CH$_2$OMe-C$_6$H$_4$)$_3$P	54%	>99:1	>99%	57%	2:98	>99%
(o-CH$_2$CH$_2$OMe-C$_6$H$_4$)$_3$P	68%	99:1	>99%	75%	2:98	>99%
(o-CH$_2$Ph-C$_6$H$_4$)$_3$P	72%	99:1	>99%	76%	2:98	>99%

Figure 3-15 Ligand Optimization
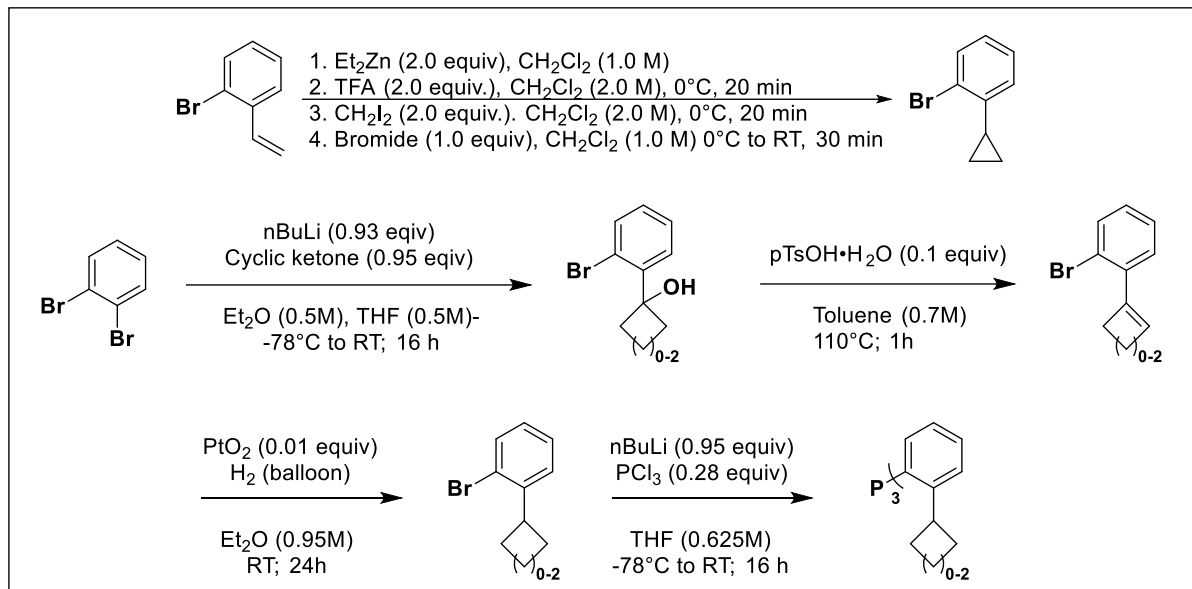
Figure 3-16 Synthetic routes to cyclo-ortho substituted ligands

elimination as phosphine ligands with large cone angle are known to promote reductive elimination.[25,26] Evidence from our own lab suggests that the interesting pinwheel structure of P(*o*-tol)$_3$ causes one ortho substituent to project above the plane of the square-planar transition state, and another below the plane. This helps block access to open coordination sites on the palladium which in the case of secondary couplings was shown to significantly increase branched to linear ratio by preventing β-hydride elimination.[11] In our case, we wondered if larger ortho substituents projecting out above and below the plane of the transition state could mimic the bidentate diphosphate ligands frequently used in literature[6–8], and promote reductive elimination.

Looking at an increase in size of the ortho substituent from H to Me to *i*Pr showed a steady climb in
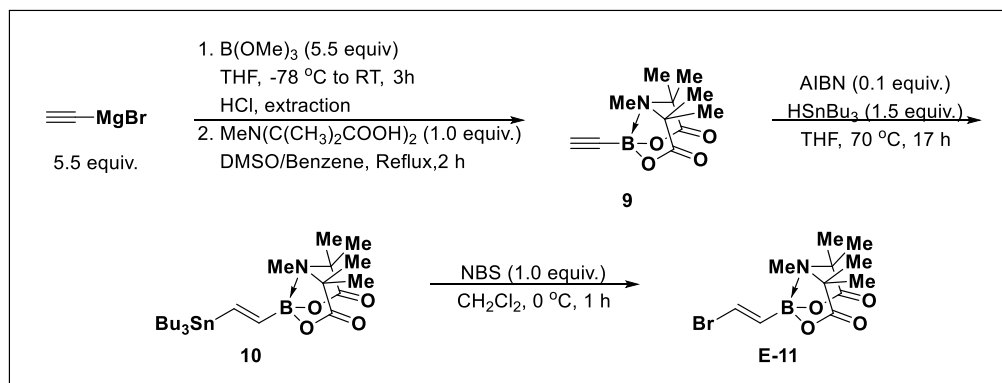
Figure 3-17 Synthetic route to trans TIDA

61

yield while adding a Me group to each side of the *i*Pr, crashed the yield down to 14%, suggesting an improvement in yield for increased size up to a point (**Figure 3-15** *entries 1-4*). Wondering if these branched substituents could be tied back into rings, we'd first have to find a way to access these ortho substituted aryl bromides. The cyclopropyl variant was created from 1bromo-2-vinylbenzene with a Simmons-Smith reaction. The cyclobutyl, -pentyl, and -hexyl were all access from the same route beginning with the correctly sized cyclic ketone and 1,2 dibromobenzene. Deoxygenation followed by reduction lead to the desired aryl halides, which were complexed to PCl$_3$ (**Figure 3-16**).

Tying the *i*Pr back to form the cyclopentyl resulted in a drop in yield but using the larger cyclobutyl and cyclopentyl rings showed comparable and high yields. Once again, a size of ligand was reached with the cyclohexyl that caused the yield to drop (**Figure 3-15** *entries 5-8*). Finally, we wanted to see if substituents containing functional groups other than pure alkyl chains or rings would have any affect. Testing CH$_2$OH, CH$_2$CH$_2$OH, and

Ligand	Yield **E**	E/Z	DS
P (o-Me)	38%	>99:1	>99%
P (CHMe$_2$)	40%	>99:1	>99%
P (cyclopentyl)	64%	>99:1	>99%
P (CH$_2$Ph)	40%	>99:1	>99%

Pd:Ligand Ratio	Yield **E**	E/Z	DS
1:2	75%	>99:1	>99%
1:1	60%	>99:1	>99%

Base	Yield **E**	E:Z	DS
K$_2$CO$_3$	69%	>99:1	>99%
Cs$_2$CO$_3$	48%	>99:1	>99%
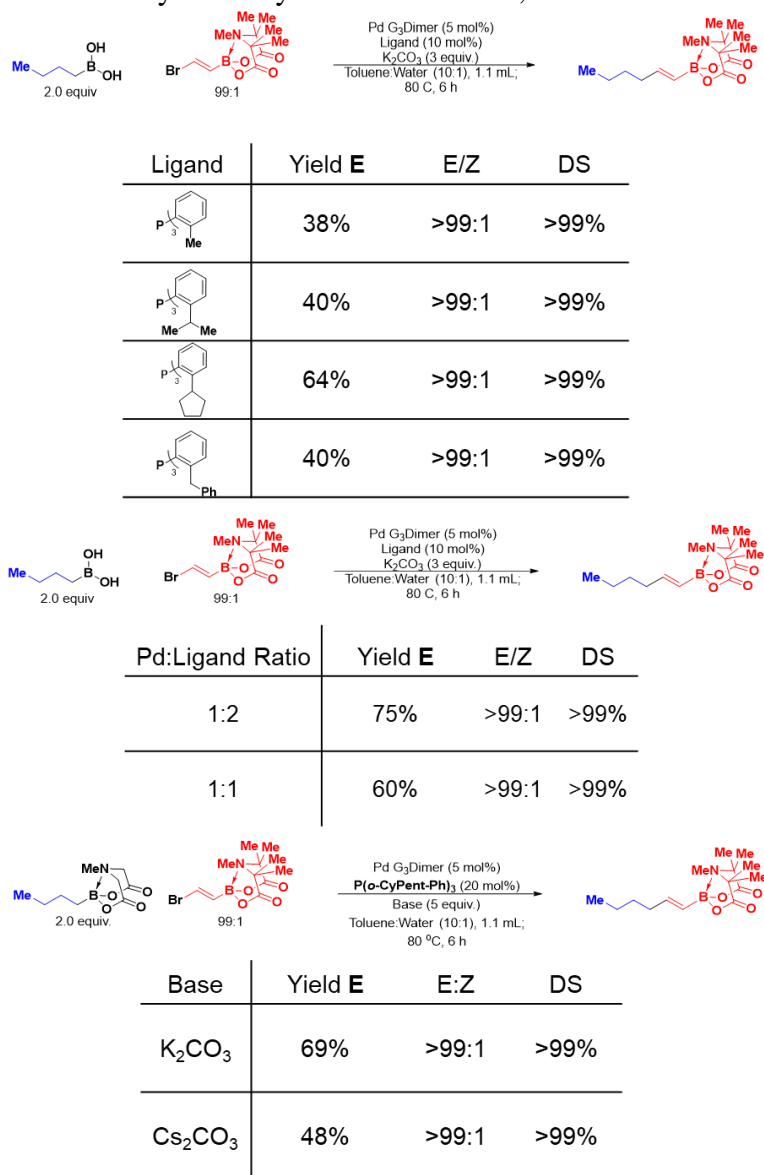
Figure 3-18 Ligand screen with E-11 and condition optimization

iPhos as ortho substituents, all performed reasonably well with iPhos performing the best (**Figure 3-15** *entries 9-11*). We wanted to select a small panel of ligands to test with a bifunctional TIDA boronate block. Our best four ligands across cis and trans were *i*Pr, cyclobutyl, cyclopentyl, and iPhos. We ended up excluding cyclobutyl as it was so similar to cyclopentyl but harder to access and replacing it with P(*o*-tol)$_3$.

To gain access to trans-bromo-TIDA, alkynyl MgBr was converted to the boronic ester and then complex with TIDA. Hydrostanylation to the trans olefin followed by stereospecific bromodestanylation afforded **E-11** (**Figure 3-17**). Testing our small four ligand panel showed the cyclopentyl ligand as the clear best choice. Optimization of reaction conditions to allow for slow-release MIDA coupling without causing decomposition of TIDA, gave us a second set of conditions (**Figure 3-18**). With our two sets of conditions in had we began to make the required blocks to fill out our predetermined substrate scope.

3-5 SYNTHESIS AND COUPLINGS FOR PREDETERMINED SUBSTRATE SCOPE

The cis TIDA boronate **Z-11** was also accessed from the alkynyl TIDA boronate **9**. Hydroboration followed by invertive bromodeborylation afforded the desired product. The 1-methyl **15** was synthesized from a route similar to **E-11** but starting from 1-propynylmagnesium-bromides. **E-17** was accessed from the conversion and complexation of 1-propenyl MgBr to the TIDA boronate. The alkene was then brominated, and subsequent elimination gave the desired product. Boryldebromination of **E-17** followed by invertive bromodeborylation furnished **Z-17**. The last substrate was synthesized from crotyl alcohol. An alkene bromination and selective elimination gave intermediate **20**, and an TBDPS protection yielded **21** (**Figure 3-19**).

With all required building blocks in hand, we proceeded to fill out our substrate table (**Figure 3-20**). We were pleased to see that stereoretention remained near perfect. We did however, run into two motifs that caused problems: 1-methyl double bonds and the cis TIDA boronate. Neither of these types of halides showed reactivity under our conditions, possibly do to issues of steric congestion. While not ideal, we felt it was important to investigate other methodologies that could be used to fill in the gaps still
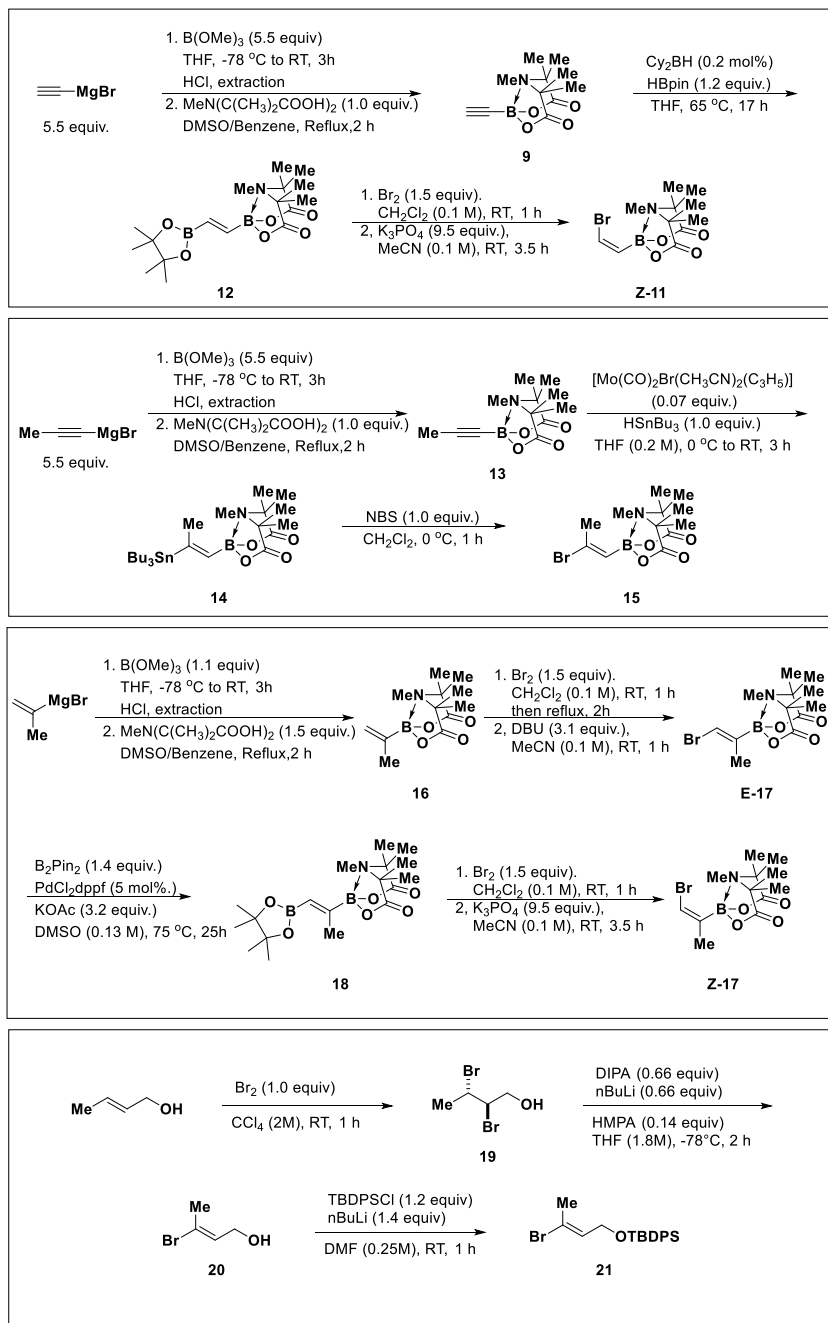
Figure 3-19 Synthetic routes to remaining substrates

present. We were able to achieve coupling with **Z-11** in moderate yield and adequate selectivity with a Negishi reaction. Additionally, we found that photoredox conditions with BF$_3$K salts gave access to the 1-methyl substrates in yields comparable to our main conditions and good selectivities **(Figure 3-21).** Even though more than one set of conditions was ultimately needed to

cover our predetermined substrate scope, selection of conditions is easily predictable based on specific motifs of the double bonds which makes it overall a highly impactful solution.
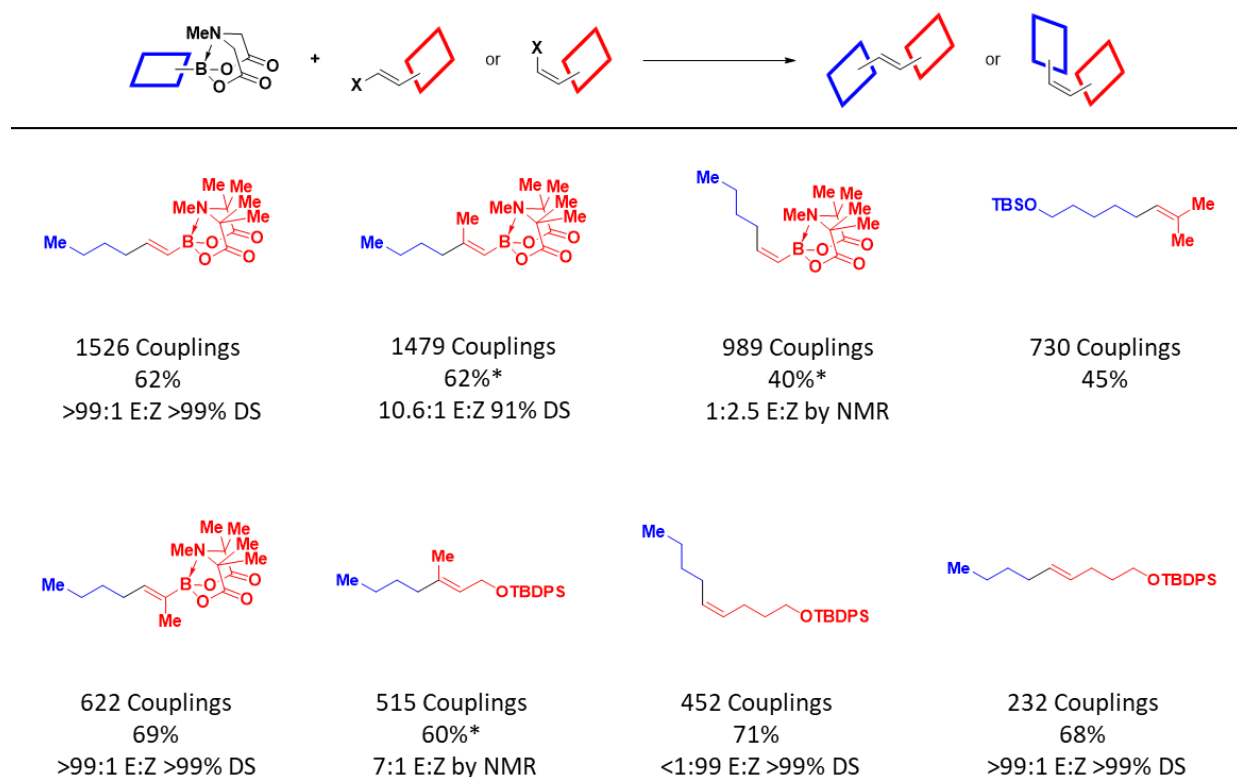
Figure 3-20 Substrate scope

3-6 SUMMARY AND CONCLUSIONS

We were able to take a computationally derived substrate scope and develop conditions that facilitate access to these important motifs in a way that is commensurate with a wider vison of utilizing modular and automated platforms to advance organic synthesis. When issues of isomerization were encountered, we were able to search the literature for possible mechanisms and use that to guide our ligand development. Future directions include testing functional group tolerance of these conditions as well as expanding this approach to methodology development to additional top priority couplings identified by our human guided algorithm.
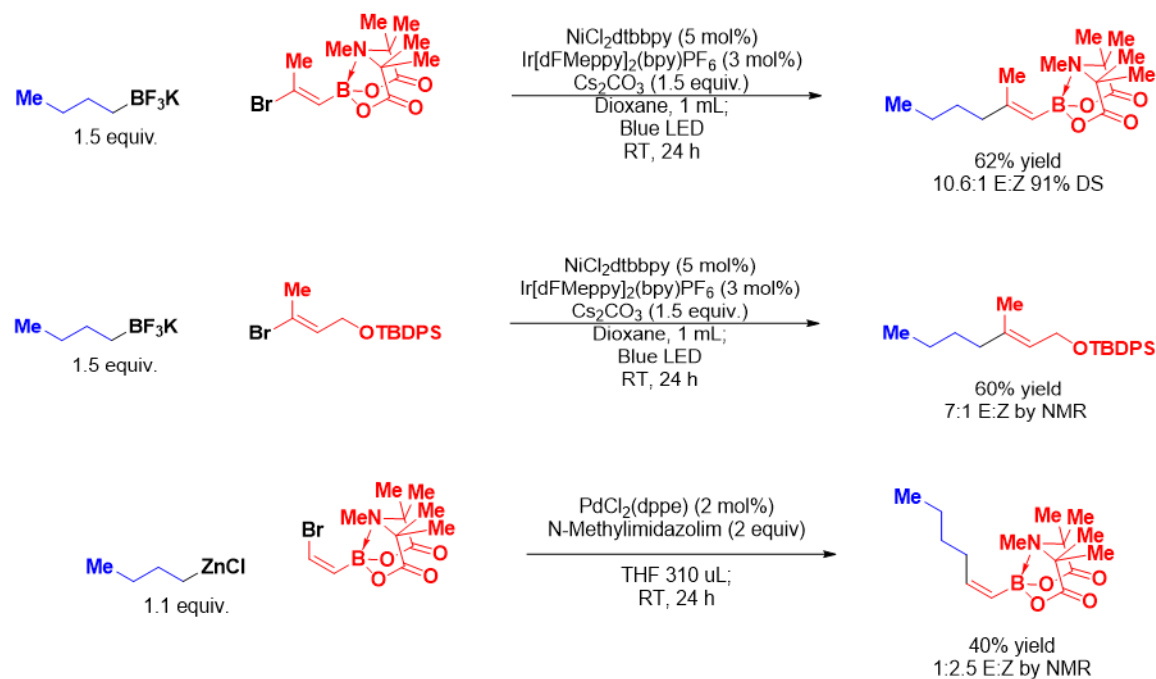
Figure 3-21 Specialized conditions

3-7 REFERENCES

(1)   Gersbach, P.; Jantsch, A.; Feyen, F.; Scherr, N.; Dangy, J. P.; Pluschke, G.; Altmann, K. H. A Ring-Closing Metathesis (RCM)-Based Approach to Mycolactonesa A/B. *Chemistry - A European Journal* **2011**, *17* (46), 13017–13031. https://doi.org/10.1002/chem.201101799.

(2)   Jana, R.; Pathak, T. P.; Sigman, M. S. Advances in Transition Metal (Pd,Ni,Fe)-Catalyzed Cross-Coupling Reactions Using Alkyl-Organometallics as Reaction Partners. *Chemical Reviews*. American Chemical Society March 9, 2011, pp 1417–1492. https://doi.org/10.1021/cr100327p.

(3)   Soderquist, J. A.; Matos, K.; Rane, A.; Ramos, J. Alkynylboranes in the Suzuki-Miyaura Coupling. *Tetrahedron Letters* **1995**, *36* (14), 2401–2402. https://doi.org/10.1016/0040-4039(95)00322-4.

(4)   Gonzalez, J. A.; Maduka Ogba, O.; Morehouse, G. F.; Rosson, N.; Houk, K. N.; Leach, A. G.; H-Y Cheong, P.; Burke, M. D.; Lloyd-Jones, G. C. MIDA Boronates Are Hydrolysed Fast and Slow by Two Different Mechanisms. **2016**. https://doi.org/10.1038/NCHEM.2571.

(5)   Fürstner, A.; Seidel, G. Palladium-Catalyzed Arylation of Polar Organometallics Mediated by 9-Methoxy-9-Borabicyclo[3.3.1]Nonane: Suzuki Reactions of Extended Scope. *Tetrahedron* **1995**, *51* (41), 11165–11176. https://doi.org/10.1016/0040-4020(95)00677-Z.

(6)   Zou, G.; Reddy, Y. K.; Falck, J. R. Ag(I)-Promoted Suzuki-Miyaura Cross-Couplings of n-Alkylboronic Acids. *Tetrahedron Letters* **2001**, *42* (41), 7213–7215. https://doi.org/10.1016/S0040-4039(01)01536-2.

(7)   Fall, Y.; Doucet, H.; Santelli, M. Palladium-Catalysed Suzuki Cross-Coupling of Primary Alkylboronic Acids with Alkenyl Halides. **2008**, No. April, 503–509. https://doi.org/10.1002/aoc.1432.

(8)   Molander, G. A.; Ham, J.; Seapy, D. G. Palladium-Catalyzed Cross-Coupling Reaction of Alkenyl Bromides with Potassium Alkyltrifluoroborates. *Tetrahedron* **2007**, *63* (3), 768–775. https://doi.org/10.1016/j.tet.2006.10.088.

(9)   Xu, T.; Hu, X. Copper-Catalyzed 1,2-Addition of a -Carbonyl Iodides to Alkynes**. **2015**, No. entry 2, 1307–1311. https://doi.org/10.1002/anie.201410279.

(10)   Muthusamy, G.; Pansare, S. V. Modular Synthesis of Allyl Vinyl Ethers for the Enantioselective Construction of Functionalized Quaternary Stereocenters †. *RSC Advances* **2016**, *6*, 104556–104559. https://doi.org/10.1039/C6RA24284G.

(11)   Lehmann, J. W.; Crouch, I. T.; Blair, D. J.; Trobe, M.; Wang, P.; Li, J.; Burke, M. D. Axial Shielding of Pd(II) Complexes Enables Perfect Stereoretention in Suzuki-Miyaura Cross-Coupling of Csp 3 Boronic Acids. https://doi.org/10.1038/s41467-019-09249-z.

(12)   Lu, G. P.; Voigtritter, K. R.; Cai, C.; Lipshutz, B. H. Ligand Effects on the Stereochemistry of Stille Couplings, as Manifested in Reactions of Z-Alkenyl Halides. *Chemical Communications* **2012**, *48* (69), 8661–8663. https://doi.org/10.1039/c2cc33294a.

(13)   Krasovskiy, A.; Lipshutz, B. H. Ligand Effects on Negishi Couplings of Alkenyl Halides. *Organic Letters* **2011**, *13* (15), 3818–3821. https://doi.org/10.1021/ol2010165.

(14)   Lu, G. P.; Voigtritter, K. R.; Cai, C.; Lipshutz, B. H. Ligand Effects on the Stereochemical Outcome of Suzuki-Miyaura Couplings. *Journal of Organic Chemistry* **2012**, *77* (8), 3700–3703. https://doi.org/10.1021/jo300437t.

(15)   Amatore, C.; Bensalem, S.; Ghalem, S.; Jutand, A. Mechanism of the Carbopalladation of Alkynes by Aryl-Palladium Complexes. *Journal of Organometallic Chemistry* **2004**, *689* (24 SPEC. ISS.), 4642–4646. https://doi.org/10.1016/j.jorganchem.2004.05.032.

(16)   Zargarian, D.; Alper, H. Palladium-Catalyzed Hydrocarboxylation of Alkynes with Formic Acid. *Organometallics* **1993**, *12* (3), 712–724. https://doi.org/10.1021/om00027a022.

(17)   Huggins, J. M.; Bergman, R. G. Mechanism, Regiochemistry, and Stereochemistry of the Insertion Reaction of Alkynes with Methyl(2,4-Pentanedionato)(Triphenylphosphine)Nickel. A Cis Insertion That Leads to Trans Kinetic Products. *Journal of the American Chemical Society* **1981**, *103* (11), 3002–3011. https://doi.org/10.1021/ja00401a016.

(18)   Blackmore, T.; Bruce, M. I.; Stone, F. G. A. Cyclopentadienylruthenium Phosphine Complexes. Part II. Reactions between Hydridobis(Triphenylphosphine)(π-Cyclopentadienyl)Ruthenium and Acetylenes. *Journal of the Chemical Society, Dalton Transactions* **1974**, No. 1, 106–112. https://doi.org/10.1039/DT9740000106.

(19)   Yang, Y.; Wang, L.; Zhang, J.; Jin, Y.; Zhu, G. An Unprecedented Pd-Catalyzed Trans-Addition of Boronic Acids to Ynamides. *Chemical Communications* **2014**, *50* (18), 2347–2349. https://doi.org/10.1039/c3cc49069f.

(20)   Gauthier, D.; Lindhardt, A. T.; Olsen, E. P. K.; Overgaard, J.; Skrydstrup, T. In Situ Generated Bulky Palladium Hydride Complexes as Catalysts for the Efficient Isomerization of Olefins. Selective Transformation of Terminal Alkenes to 2-Alkenes. https://doi.org/10.1021/ja9108424.

(21)   Hansen, A. L.; Ebran, J.-P.; Gøgsig, T. M.; Skrydstrup, T. Investigations on the Suzuki-Miyaura and Negishi Couplings with Alkenyl Phosphates: Application to the Synthesis of 1,1-Disubstituted Alkenes. **2007**. https://doi.org/10.1021/jo070912k.

(22)   O'Brien, C. J.; Nixon, Z. S.; Holohan, A. J.; Kunkel, S. R.; Tellez, J. L.; Doonan, B. J.; Coyle, E. E.; Lavigne, F.; Kang, L. J.; Przeworski, K. C. Part I: The Development of the Catalytic Wittig Reaction. *Chemistry - A European Journal* **2013**, *19* (45), 15281–15289. https://doi.org/10.1002/chem.201301444.

(23)   Wakioka, M.; Nakajima, Y.; Ozawa, F. Mechanism of C-P Reductive Elimination from Trans-[Pd(CH=CHPh)Br(PMePh2)2]. *Organometallics* **2009**, *28* (8), 2527–2534. https://doi.org/10.1021/om801207k.

(24)   Paul, F.; Patt, J.; Hartwig, J. F. Structural Characterization and Simple Synthesis of {Pd[P(o-Tol)3]2}, Dimeric Palladium(II) Complexes Obtained by Oxidative Addition of Aryl Bromides, and Corresponding Monometallic Amine Complexes. *Organometallics* **1995**, *14* (6), 3030–3039. https://doi.org/10.1021/om00006a053.

(25)   Hartwig, J. F. Electronic Effects on Reductive Elimination to Form Carbon-Carbon and Carbon-Heteroatom Bonds from Palladium(Ll) Complexes. *Inorganic Chemistry*. American Chemical Society March 19, 2007, pp 1936–1947. https://doi.org/10.1021/ic061926w.

(26)   Tolman, C. A. Steric Effects of Phosphorus Ligands in Organometallic Chemistry and Homogeneous Catalysis. *Chemical Reviews* **1977**, *77* (3), 313–348. https://doi.org/10.1021/cr60307a002.

(27)   Kim, Y. J.; Yoon, Y.; Lee, H. Y. An Asymmetric Total Synthesis of (+)-Pentalenene. *Tetrahedron* **2013**, *69* (36), 7810–7816. https://doi.org/10.1016/j.tet.2013.05.095.

(28)   Lisboa, M. P.; Jeong-Im, J. H.; Jones, D. M.; Dudley, G. B. Toward a New Palmerolide Assembly Strategy: Synthesis of C16-C24 Synthesis of Palmerolide C16-C24. https://doi.org/10.1055/s-0031-1290675.

CHAPTER 3

EXPERIMENTAL SECTION

TABLE OF CONTENTS

1. GENERAL MATERIALS AND METHODS

Commercial reagents were purchased from Sigma-Aldrich, EMD Millipore, Fisher Scientific, Alfa Aesar, Frontier Scientific, Oakwood Products, or Strem and were used without further purification unless otherwise noted. Unless otherwise noted, building block syntheses were carried out in oven- or flame-dried glassware under a dry inert atmosphere. Unless otherwise noted: Celite™ refers to Celite™ 545 filter aid (not acid washed); Darco® refers to activated carbon, Darco® G-60, -100 mesh, powder; and K_2CO_3 was anhydrous and was freshly and finely ground in a 120 °C mortar and pestle. Solvents were purified via passage through packed columns as described by Pangborn and coworkers (*35*) (THF, Et_2O, CH_3CN, CH_2Cl_2: dry neutral alumina; hexanes, benzene, toluene: dry neutral alumina and Q5 reactant; DMSO, DMF: activated molecular sieves. Water was deionized.

Thin layer chromatography (TLC) was performed using the indicated eluent on E. Merck silica gel 60 F254 plates (0.25 mm). Compounds were visualized by exposure to a UV lamp (λ = 254 and/or 366 nm) and/or a basic solution of $KMnO_4$ followed by brief heating with a Varitemp® heat gun. Flash chromatography was performed as described by Still and coworkers (*36*) using EM Merck silica gel 60 (230-400 mesh). ^{1}H NMR spectra were recorded at room temperature on one of the following instruments: Varian Unity 500, Varian VXR 500, Varian Unity Inova 500NB, or Carver B500 with broad-band CryoProbe. Chemical shifts (δ) are reported in parts per million (ppm) downfield from tetramethylsilane and referenced to residual protium in the NMR solvent ($CDCl_3$, δ = 7.26; $(CD_3)_2CO$, δ = 2.05, center line; CD_2Cl_2, δ = 5.32, center line; $(CD_3)_2SO$, δ = 2.50, center line). Data are reported as follows: chemical shift, multiplicity (s = singlet, d = doublet, t = triplet, q = quartet, quint = quintet, sept = septet, m = multiplet, br = broad, app = apparent, dd = doublet of doublets, dt = doublet of triplets, dq = doublet of quartets), coupling constant (*J*) in

Hertz (Hz), and integration. ^{13}C NMR spectra were recorded at room temperature on one of the following instruments: Varian Unity 500, Varian VXR 500, or Carver B500. Chemical shifts (δ) are reported in ppm downfield from tetramethylsilane and referenced to carbon resonances in the NMR solvent (CDCl$_3$, $\delta = 77.16$, center line; (CD$_3$)$_2$CO, $\delta = 29.84$, center line; CD$_2$Cl$_2$, $\delta = 53.84$; (CD$_3$)$_2$SO, $\delta = 39.52$, center line). Carbons bearing boron substituents are sometimes not observed due to quadrupolar relaxation. High resolution mass spectra (HRMS) were performed by Furong Sun and Elizabeth Eves at the University of Illinois School of Chemical Sciences Mass Spectrometry Laboratory.

2. COMPUTATIONALLY DETERMINED SUBSTRATE SCOPE

General Procedure for TIDA containing couplings

To oven dried 7 mL vials equipped with stir bars as added TIDA containing bifunctional vinyl bromides (0.1 mmol; 1.0 equiv) and MIDA boronate (2.0 equiv). Vials were then brought into the glovebox and were charged with reagents in the following order: catalyst (5 mol% of Pd dimer; 10 mol% Pd), ligand (20 mol%), and base (5 equiv). Finally, the vials were sealed with PFTE lined septa caps and brought out of the glovebox. After sealing the vial with electrical tape, the vials were charged with 1.1 mL of 10:1 Toluene:H$_2$O placed in a 80 °C aluminum heating block (on the outside of a circular heating block stirring at 540 RPM) for 6 hours. After the completion of the reaction, vials were removed from the aluminum heating block and allowed to cool to room temperature at which point they were filtered through celite (~0.5 mL in a 3 mL syringe). The vial was rinsed with EtOAc (3 x 1 mL). The resulting solution concentrated in vacuo using a high vac (3 h) at which point a crude NMR was taken in CDCl$_3$ (0.5 mL). After the crude NMR, the NMR tube was transferred back to a 7 mL vial rinsing with CH$_2$Cl$_2$ (2 x 0.5 mL). To the resulting 1.5

mL was added celite. The resulting suspension was concentrated in vacuo and was loaded onto a

10 g regular phase MPLC column and purified by MPLC.

Cartridge	SNAP Ultra 10g	Detection Mode	Lambda-all
Flowrate	36 ml/min	Baseline Correction	On
Solvent A	n-Hexane	UV1 (Monitor)	254 nm (Red)
Solvent B	Acetone	UV2 (Monitor)	210 nm (Black)
		Lambda-all (Collect)	(Brown)
Rack Type	16x150 mm	Collect All	On
Max Fraction Volume	20 ml	Start Threshold	20 mAU
Dispense Order	S		

Gradient

	Solvents Mix		Length (CV)	
Equil.	A/B	5%	3.0	flowrate 36 ml/min
1	A/B	5%	2.0	
2	A/B	5% - 20%	8.5	
3	A/B	20%	4.5	
4	A/B	20% - 40%	8.0	
5	A/B	40%	1.2	

Crude product purified by MPLC method (62% yield). ^{1}H NMR (500 MHz, Acetone-d_6) δ 7.33

(d, J = 4.4 Hz, 4H), 7.27 (dq, J = 8.8, 4.2 Hz, 1H), 4.49 (s, 2H), 4.20 (d, J = 16.7 Hz, 2H), 3.96 (d,

J = 16.7 Hz, 2H), 3.20 (s, 2H), 3.19 (s, 3H), 2.80 (d, J = 17.3 Hz, 1H); ^{13}C NMR (126 MHz,

Acetone) δ 206.11, 206.05, 205.93, 168.84, 129.07, 128.39, 128.17, 62.92, 46.20, 30.30, 30.15,

29.99, 29.84, 29.69, 29.53, 29.38; ^{11}B NMR (161 MHz, Acetone) δ 10.90; HRMS (ES+) calculated

for $C_{13}H_{17}O_5NB$ [M+H]$^{+}$ m/z 278.1200, found 278.1195

Crude product purified by MPLC method (69% yield) 1H NMR (500 MHz, CDCl3) δ 5.98 (t, J = 6.9 Hz, 1H), 2.55 (s, 3H), 2.11 (q, J = 7.0 Hz, 2H), 1.74 (s, 6H), 1.64 (s, 3H), 1.63 (s, 6H), 1.40 – 1.28 (m, 4H), 0.90 (t, J = 7.1 Hz, 3H). 13C NMR (126 MHz, CDCl3) δ 174.90, 142.83, 37.03, 31.28, 28.62, 22.72, 15.10, 14.14. 11B NMR (161 MHz, CDCl3) δ 9.00. HRMS (ES+) calculated for $C_{16}H_{28}O_4NB$ [M+H]$^+$ *m/z* 310.2190, found 310.2201

General Procedure for non-TIDA containing couplings

To oven dried 7 mL vials equipped with stir bars was added vinyl bromides (0.1 mmol; 1.0 equiv) and MIDA boronate (2.0 equiv). Vials were then brought into the glovebox and were charged with reagents in the following order: catalyst (5 mol% of Pd dimer; 10 mol% Pd), ligand (10 mol%), and base (7 equiv). Finally, the vials were sealed with PFTE lined septa caps and brought out of the glovebox. After sealing the vial with electrical tape, the vials were charged with 300 uL 20:1 Dioxane:H_2O placed in a 100 °C aluminum heating block (on the outside of a circular heating block stirring at 540 RPM) for 14 hours. After the completion of the reaction, vials were removed from the aluminum heating block and allowed to cool to room temperature at which point they were filtered through celite (~0.5 mL in a 3 mL syringe). The vial was rinsed with EtOAc (3 x 1 mL). The resulting solution concentrated in vacuo using a high vac (3 h) at which point a crude NMR was taken in CDCl3 (0.5 mL). After the crude NMR, the NMR tube was transferred back to a 7 mL vial rinsing with CH_2Cl_2 (2 x 0.5 mL) and concentrated *in vacuo*. The resulting solution was taken up in MeCN and wet loaded onto a 10g reverse phase MPLC column and purified by

MPLC.

	Solvents Mix		Length (CV)	
Cartridge	SNAP Ultra C18 12g		Detection Mode	Lambda-all
Flowrate	36 ml/min		Baseline Correction	On
Solvent A	Water		UV1 (Monitor)	254 nm (Red)
Solvent B	Acetonitrile		UV2 (Monitor)	214 nm (Black)
			Lambda-all (Collect)	(Brown)
Rack Type	16x150 mm		Start Threshold	25 mAU
Max Fraction Volume	20 ml			
Dispense Order	S			
Initial Waste	20 CV			

Gradient

	Solvents Mix		Length (CV)	
Equil.	A/B	65%	3.0	flowrate 36 ml/min
1	A/B	65%	2.5	
2	A/B	65% - 95%	28.5	
3	A/B	95%	22.0	
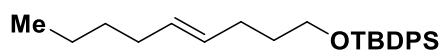
Crude product purified by MPLC method (68% yield). ^{1}H NMR (500 MHz, Acetone-d_6) δ 7.33 (d, $J = 4.4$ Hz, 4H), 7.27 (dq, $J = 8.8$, 4.2 Hz, 1H), 4.49 (s, 2H), 4.20 (d, $J = 16.7$ Hz, 2H), 3.96 (d, $J = 16.7$ Hz, 2H), 3.20 (s, 2H), 3.19 (s, 3H), 2.80 (d, $J = 17.3$ Hz, 1H); ^{13}C NMR (126 MHz, Acetone) δ 206.11, 206.05, 205.93, 168.84, 129.07, 128.39, 128.17, 62.92, 46.20, 30.30, 30.15, 29.99, 29.84, 29.69, 29.53, 29.38; ^{11}B NMR (161 MHz, Acetone) δ 10.90; HRMS (ES+) calculated for $C_{13}H_{17}O_5NB$ [M+H]$^{+}$ m/z 278.1200, found 278.1195
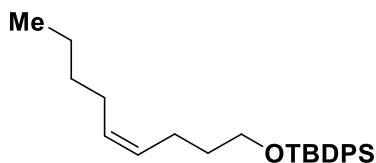
Crude product purified by MPLC method (71% yield). ^{1}H NMR (500 MHz, Acetone-d_6) δ 7.33 (d, $J = 4.4$ Hz, 4H), 7.27 (dq, $J = 8.8$, 4.2 Hz, 1H), 4.49 (s, 2H), 4.20 (d, $J = 16.7$ Hz, 2H), 3.96

(d, J = 16.7 Hz, 2H), 3.20 (s, 2H), 3.19 (s, 3H), 2.80 (d, J = 17.3 Hz, 1H); ^{13}C NMR (126 MHz, Acetone) δ 206.11, 206.05, 205.93, 168.84, 129.07, 128.39, 128.17, 62.92, 46.20, 30.30, 30.15, 29.99, 29.84, 29.69, 29.53, 29.38; ^{11}B NMR (161 MHz, Acetone) δ 10.90; HRMS (ES+) calculated for $C_{13}H_{17}O_5NB$ [M+H]$^+$ m/z 278.1200, found 278.1195.
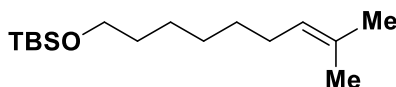
Crude product purified by silica column eluted with hexanes (45% yield) 1H NMR (500 MHz, CDCl3) δ 5.11 (dddd, J = 8.4, 7.2, 2.5, 1.3 Hz, 1H), 3.60 (t, J = 6.6 Hz, 2H), 1.96 (d, J = 6.8 Hz, 2H), 1.68 (s, 3H), 1.60 (s, 3H), 1.51 (p, J = 6.8 Hz, 2H), 1.36 – 1.26 (m, 7H), 0.89 (d, J = 1.0 Hz, 9H), 0.05 (s, 6H). ^{13}C NMR (126 MHz, CDCl$_3$) δ 131.20, 124.88, 63.34, 32.89, 29.89, 29.72, 29.13, 27.99, 26.00, 25.75, 25.73, 18.40, 17.66, -5.24. HRMS (ES+) calculated for $C_{16}H_{35}OSI$ [M+H]$^+$ m/z 271.2457, found 271.2465.

Procedures for couplings requiring special conditions

Photo redox conditions

To oven dried 7 mL vials equipped with stir bars was added NiCl2·dme (0.01 mmol; 10 mol%) and 4,4'di-tert-butyl-2,2'-bipyridine (0.01 mmol; 10 mol%) before being removed from glovebox. THF was added and vials were heated briefly with heat gun until full dissolution of reactions was achieved and obvious color change was observed. THF was removed under vacuo, vials were taken back into glovebox and the following reagents were added: vinyl bromide (0.1 mmol 1 equiv.), BF$_3$K salt (0.15 mmol 1.5 equiv.), Iridium catalyst (Ir[dFCH3ppy](bpy)PF$_6$) (0.03 mmol; 3 mol%), base (0.15 mmol; 1.5 equiv.), and dioxane (1 mL). Vials were capped,

removed from glovebox, and degassed in hood for 10 min, and sealed with parafilm. Vials were

irradiated with light source, and 6" fan was used during the illumination period to maintain a

constant temperature. After the completion of the reaction, vials were removed from light sourse

and were filtered through celite (~0.5 mL in a 3 mL syringe). The vials were rinsed with EtOAc

(3 x 1 mL). The resulting solution concentrated in vacuo using a high vac (3 h) at which point a

crude NMR was taken in CDCl$_3$ (0.5 mL). After the crude NMR, the NMR tube was transferred

back to a 7 mL vial rinsing with CH$_2$Cl$_2$ (2 x 0.5 mL) and concentrated *in vacuo*. The resulting

solution was taken up in MeCN and wet loaded onto a 10g reverse phase MPLC column and
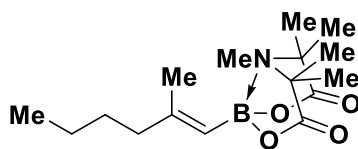
purified by MPLC.

Crude product purified by MPLC method (62% yield) ^{1}H NMR (500 MHz, CDCl$_3$) δ 5.02 (q, *J*

= 1.2 Hz, 1H), 2.55 (s, 3H), 2.05 (t, *J* = 7.6 Hz, 2H), 1.78 (s, 3H), 1.71 (s, 6H), 1.57 (s, 6H), 1.39

(tt, *J* = 8.4, 7.1 Hz, 2H), 1.28 (dt, *J* = 15.2, 7.4 Hz, 2H), 0.88 (t, *J* = 7.3 Hz, 3H). ^{13}C NMR (126

MHz, CDCl$_3$) δ 174.47, 174.39, 154.23, 154.07, 43.01, 36.20, 36.12, 34.80, 30.77, 30.17, 29.71,

27.17, 22.88, 22.43, 19.53, 14.12, 14.02. ^{11}B NMR (161 MHz, CDCl$_3$) δ 8.74.
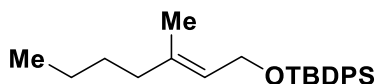
Crude product purified by MPLC method (60% yield). 1H NMR (500 MHz, CDCl3) δ 7.74 –

7.67 (m, 4H), 7.46 – 7.36 (m, 6H), 5.41 – 5.35 (m, 1H), 4.23 (d, J = 6.4 Hz, 2H), 1.97 (t, J = 7.5

Hz, 2H), 1.46 – 1.42 (m, 4H), 1.40 – 1.25 (m, 7H), 1.08 – 1.04 (m, 9H), 0.91 (t, J = 7.2 Hz, 3H).
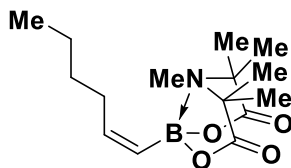
Crude product purified by MPLC method (60% yield). NMR contains both cis and trans isomers. Integrations set for trans at 1 and cis at 3 1H NMR (500 MHz, CDCl3) δ 6.23 (d, J = 17.5 Hz, 1H), 6.15 (dt, J = 14.5, 7.5 Hz, 3H), 5.39 (dt, J = 17.4, 1.6 Hz, 1H), 5.28 (dt, J = 14.0, 1.7 Hz, 4H), 2.57 (s, 11H), 2.51 (s, 3H), 2.21 (qd, J = 7.2, 1.7 Hz, 8H), 2.14 – 2.08 (m, 2H), 1.72 (s, 27H), 1.40 – 1.28 (m, 20H), 1.25 (s, 9H), 0.88 (q, J = 7.0 Hz, 16H). 13C NMR (126 MHz, CDCl3) δ 174.51, 174.29, 148.21, 147.44, 36.59, 36.20, 35.30, 31.83, 30.90, 30.69, 30.17, 29.71, 29.37, 22.70, 22.38, 22.31, 14.13, 14.05, 13.95, 1.02. 11B NMR (161 MHz, CDCl3) δ 8.69.

3. SYNTHESIS OF BUILDING BLOCKS
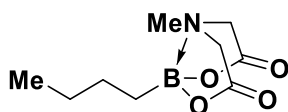
SI-1

Prep adapted from Balmer *et al.*[2] A 1 L round bottom flask equipped with a stirbar was charged with nbutyl boronic acid (25.0g; 245.24 mmol; 1.0 equiv), MIDA (46.3 g; 294.29 mmol; 1.2 equiv.), benzene (236 mL; 1.04 M) and DMSO (12.3 mL; 19.9 M). The round bottom was then fitted with a dean stark trap and reflux condenser. Reaction was heated to reflux for 6 h, then removed from heat and allowed to stir for an additional 45 min. Acetone (15 mL) was added followed by Et₂O (4 x 40 mL) swirling after each addition. Solution was filtered through medium

frit, and washed with Et₂O (100 mL). Solid was collected and dried *in vacuo* to yield a white solid 51.2 g 98% yield. (51.2 g 98% yield). ^{1}H NMR (500 MHz, Acetone-d_6) δ 4.16 (d, J = 16.9 Hz, 2H), 4.00 (d, J = 16.9 Hz, 2H), 3.08 (s, 3H), 1.34 (ddt, J = 7.6, 4.5, 2.4 Hz, 4H), 0.90 – 0.87 (m, 3H), 0.65 – 0.60 (m, 2H); ^{13}C NMR (126 MHz, Acetone) δ 206.12, 168.84, 62.64, 46.20, 30.30, 30.15, 29.99, 29.84, 29.69, 29.53, 29.38, 27.26, 26.60, 14.28; HRMS (ES+) calculated for $C_9H_{16}NO_4B$ [M+H]$^+$ *m/z* 214.1251, found 214.1246.

9
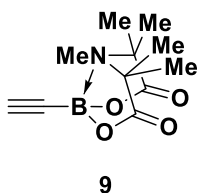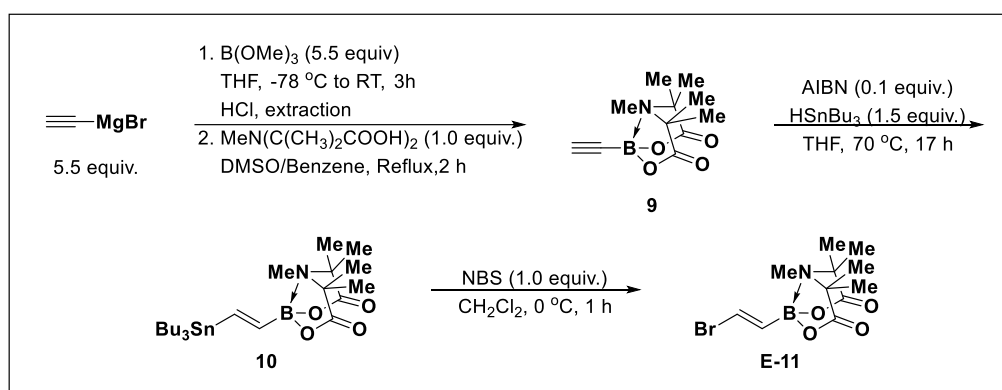
Prep adapted from Lee, *et al.*[1] To an oven dried 250 mL round bottom flask equipped with a magnetic stir bar and placed under nitrogen was added THF (112 mL; 0.667 M to grignard, 0.133 to TIDA) and trimethylborate 9.20 mL; 8.57 g; 82.50 mmol; 5.5 equiv.). the resulting solution was cooled to -78 °C. Following equilibration, ethynyl magnesium bromide (150 mL; 0.5 M in THF; 75 mmol; 5.0 equiv.) was added dropwise over 20 minutes. The reaction vessel was removed from the bath and allowed to warm to ambient temperature over 3 hours resulting in a opaque white

slurry. After 3 hours, the reaction was cooled to 0 °C (15 minutes) and quenched with the addition of 1N HCl (50 mL; 10.0 equiv.). The resulting mixture was transferred to a sep. funnel rinsing with Et$_2$O. Layers separated and the aqueous later was back extracted with Et$_2$O (1 x 50 mL). Combined organics washed with brine (2 x 50 mL), dried over MgSO$_4$, filtered into a flask containing 62 mL benzene. The resulting solution was concentrated in vacuo without heating the bath until the solvent in the collection flask started to bump or no more solvent was collecting on the dry ice trap. To the resulting solution was added 6.2 mL DMSO, TIDA (3.05 mg; 15 mmol; 1.0 equiv.), and a stirbar. The 1L recovery flask was fitted with dean-stark trap, and a reflux condensor and heated to reflux with stirring (set bath to 105 C to get benzene collecting in the dean-stark). Covered the apparatus in foil to assist in heating. The dean-stark trap was filled with benzene at the start of the reaction. After 30 minutes, the trap was regularly emptied. As the reaction got more concentrated it transitioned from a opaque solution to a deep orange, clear solution. After 2.5 hours, the reaction mixture was transferred to a round bottom flask and concentrated in vacuo to afford a DMSO slurry. Slurry was transferred to a separatory funnel rinsing with EtOAc. Layers separated, aqueous layer was back-extracted with EtOAc (2 x 100 mL). Combined organics were concentrated and washed with brine (5 x 100 mL), dried over MgSO$_4$ with DARCO, filtered and concentrated *in vacuo* to afford a white solid. Solid triterated with Et$_2$O (~300 mL). The first triteration afforded pure product a white powder (1.833g; 51% yield). Rf = 0.36 in EtOAc, visualized via KMnO$_4$; ^{1}H NMR (500 MHz, Chloroform-d) δ 2.71 (s, 3H), 2.37 (s, 1H), 1.64 (s, 12H), 1.48 (s, 3H); ^{13}C NMR (126 MHz, CDCl$_3$) δ 173.65, 37.36; ^{11}B NMR (161 MHz, CDCl$_3$) δ 3.91; HRMS (ES+) calculated for C$_{11}$H$_{17}$NO$_4$B [M+H]$^+$ *m/z* 238.1251, found 238.1242.

10

Prep adapted from Woerly, *et al.*[4] To an oven dried 25 mL schlenk flask equipped with a magnetic stir bar was charged with TIDA boronate **117-1** (1.69 g; 7.12 mmol; 1.0 equiv.) and AIBN (117 mg; 0.712 mmol; 0.1 equiv.) and placed under nitrogen. To the flask was added THF (36 mL; 0.2 M) followed by HSnBu$_3$ (2.88 mL; 10.7 mmol; 1.5 equiv.). The solution was lowered into a 70 °C oil bath to bring the reaction mixture to an internal temperature of 65 °C and allowed to stir at that temperature. After 47 h, the reaction mixutre was allowed to cool to room temperature and was transferred to a separatory funnel rinsing with EtOAc and DI H$_2$O. Layers separated and organic layer was washed with 1N HCl (50 mL), saturated NaHCO$_3$ (50 mL), and brine (50 mL). The solution was dried over MgSO$_4$, filtered, and concentrated *in vacuo* to afford a pale yellow oil that solidified over time on high vac. The crude material was purified by flash chromatography (5 x 15 cm SiO$_2$ column; 13 x 100 mm fractions; loaded as a solution in 4:1 Hexanes:EtOAc) eluting with 4:1 Hexanes:EtOAc (500 mL) 1:1 Hexanes:EtOAc (1 L). Fractions 18-51 were concentrated *in vacuo* to afford product as a white solid after drying on high vac (Rf = 0.85 in EtOAc, visualized via KMnO$_4$, 354.6 mg; 71% yield). ^{1}H NMR (500 MHz, Chloroform-*d*) δ 7.17 (d, *J* = 21.7 Hz, 1H), 6.33 (d, *J* = 21.7 Hz, 1H), 2.55 (s, 3H), 1.75 (s, 6H), 1.62 (s, 6H), 1.54 – 1.46 (m, 6H), 1.31 (app. h, *J* = 7.3 Hz, 6H), 0.94 – 0.88 (m, 15H); ^{13}C NMR (126 MHz, CDCl$_3$) δ 174.66, 150.25, 36.69, 29.35, 27.44, 13.89, 9.60; ^{11}B NMR (161 MHz, CDCl$_3$) δ 6.91. HRMS (ES+) calculated for C$_{32}$H$_{45}$BNO$_4$Sn [M+H]$^+$ *m/z* 530.2464, found 530.2476.

E-11

Prep adapted from Woerly, *et al.*[4] To an oven dried 250 mL round bottom equipped with a magnetic stir bar sealed with a septa cap, and placed under nitrogen was added vinyl stannane **117-2** (3.25 g; 6.15 mmol; 1.0 equiv.) as a solution in DCM (20 mL + 50 mL; 0.089 M). The resulting solution was cooled to 0 °C in an ice bath. After equilibration NBS (1.16 g; 6.15 mmol; 1.0 equiv.) was added portionwize over 2 minutes at 0 °C. The resulting solution was stirred for that temperature for 1 h. After 1 h the reaction mixture was quenched with saturated Na_2SO_3 (50 mL) at 0 °C under nitrogen. The reaction mixture was transferred to a separatory funnel rinsing with water and DCM (25 mL each). Layers were separated and aqueous layer was back-extracted with CH_2Cl_2 (2 x 50 mL). Combined organics washed with brine (3 x 50 mL), dried over $MgSO_4$ with DARCO, filtered over celite, and concentrated in vacuo to afford crude material. Crude material was triterated with Et_2O resulting in a white solid (1.669g; 85% yield). Rf = 0.38 in EtOAc, visualized via $KMnO_4$; ^{1}H NMR (500 MHz, Chloroform-*d*) δ 6.79 (d, *J* = 14.7 Hz, 1H), 6.30 (d, *J* = 14.7 Hz, 1H), 2.54 (s, 3H), 1.73 (s, 6H), 1.60 (s, 6H); ^{13}C NMR (126 MHz, $CDCl_3$) δ 173.84, 119.79, 36.78; ^{11}B NMR (161 MHz, $CDCl_3$) δ 8.20; HRMS (ES+) calculated for $C_{11}H_{18}BNO_4Br$ [M+H]$^+$ m/z 318.0512, found 318.0511.

12
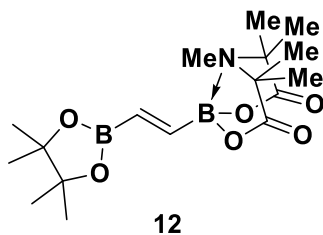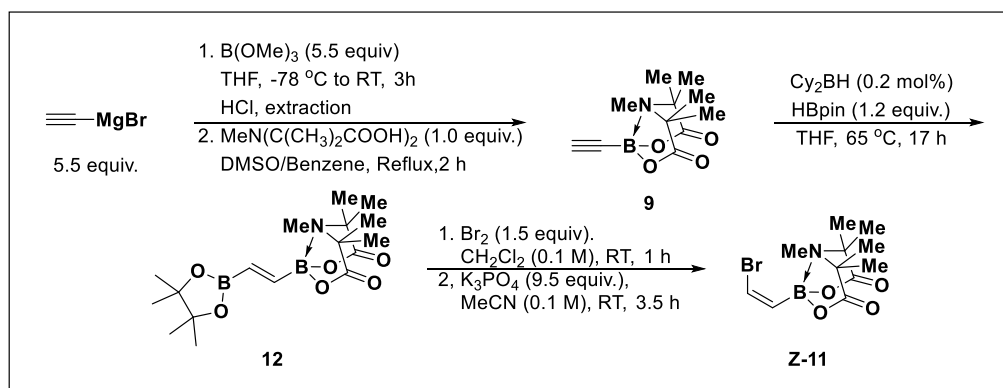
Prep adapted from Struble, *et al.*[5] To a oven dried 40 mL vial equipped with a magnetic stir bar and charged with TIDA boronate **117-1** (768 mg; 3.24 mmol; 1.0 equiv.) The vial was taken into the glovebox where solid dicyclohexylborane (115.41 mg; 0.65 mmol; 20 mol%) was added. The vial was capped with a PFTE lined septa cal, removed from the glovebox, and placed under nitrogen. To the vial was added THF (6.5 mL; 0.5 M). and neat pinacolborane (564 µL; 497 mg; 3.89 mmol; 1.2 equiv.). The resulting solution was placed in an aluminum heating block preheated to 85 °C and allowed to stir for 17 h. The reaction vessel was removed from the heating block and allowed to cool to ambient temperature at which point it was concentrated in vacuo. The resulting solid was purified by flash chromatography (4.5 x 9 cm SiO_2 column; 16 x 150 mm fractions; loading on celite as an EtOAc slurry) eluting with 2:1 Hexanes:EtOAc (450 mL) 1:2 Hexanes:EtOAc (600 mL) to EtOAc (500 mL). Fractions 42-56 were concentrated *in vacuo* to afford product as a white solid after drying on high vac (Rf = 0.31 in EtOAc, visualized via $KMnO_4$, 771.9 mg; 65 % yield). ^{1}H NMR (500 MHz, Chloroform-*d*) δ 6.76 (d, *J* = 20.7 Hz, 1H), 6.36 (d, *J* = 20.7 Hz, 1H), 2.53 (s, 3H), 1.72 (s, 6H), 1.57 (s, 6H), 1.26 (s, 12H); ^{13}C NMR (126

MHz, CDCl₃) δ 174.33, 83.50, 36.81, 24.97; ^{11}B NMR (161 MHz, CDCl₃) δ 30.22, 8.01; HRMS (ES+) calculated for $C_{17}H_{30}B_2NO_6$ [M+H]$^+$ m/z 366.2259, found 366.2270.
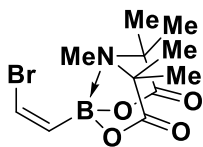
Z-11

Prep adapted from Woerly, *et al.*[6] To an oven dried 40 mL vial equipped with a magnetic stir bar was added TIDA boronate **117-3** (771 mg; 2.11 mmol; 1.0 equiv.). Reaction vial was placed under nitrogen and charged with CH_2Cl_2 (21 mL; 0.1 M). To the resulting solution was added neat Br₂ (0.165 mL; 3.17 mmol; 1.5 equiv). The resulting solution was stirred at room temperature for 1 h at which point it was concentrated in vacuo to afford crude material as a yellow solid. Solid was azeotroped with CH_2Cl_2 to remove residual bromine (3 x 20 mL). To the resulting solid was added K_3PO_4 (4.26 g; 20.06 mmol; 9.5 equiv.) and MeCN (21 mL; 0.1 M). The resulting suspension was stirred at room temperature for 3.5 h. After 3.5 h the resulting suspension was poured into 50 mL EtOAc and 50 mL sat NHCO₃. The mixture was shaken and the aqueous layer removed. The organic layer was washed with sat NHCO₃ (30 mL). The combined aqueous layers were back extracted with EtOAc (2 x 50 mL). The combined organic layers were dried over MgSO₄, filtered, and concentrated in vacuo to afford a pale yellow solid. The resulting solid was triterated with Et₂O (~100 mL) and was collected by vacuum filtration rinsing with Et₂O (15 mL) to yield TIDA boronate (Z)-Br-1 as a colorless solid (393 mg; 59% yield). Rf = 0.38 in EtOAc, visualized via KMnO₄; ^{1}H NMR (500 MHz, Chloroform-*d*) δ 6.95 (d, *J* = 9.3 Hz, 1H), 6.25 (d, *J* = 9.4 Hz, 1H), 2.68 (s, 3H), 1.81 – 1.67 (m, 6H), 1.59 (s, 6H); ^{13}C NMR (126 MHz, CDCl₃) δ 173.90,

121.84, 36.41; z^{11}B NMR (161 MHz, CDCl$_3$) δ 8.04; HRMS (ES+) calculated for C$_{11}$H$_{18}$BBrNO$_4$ [M+H]$^+$ m/z 318.0512, found 318.0518.

13
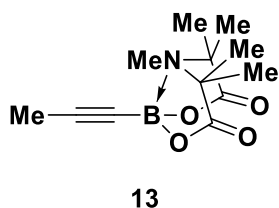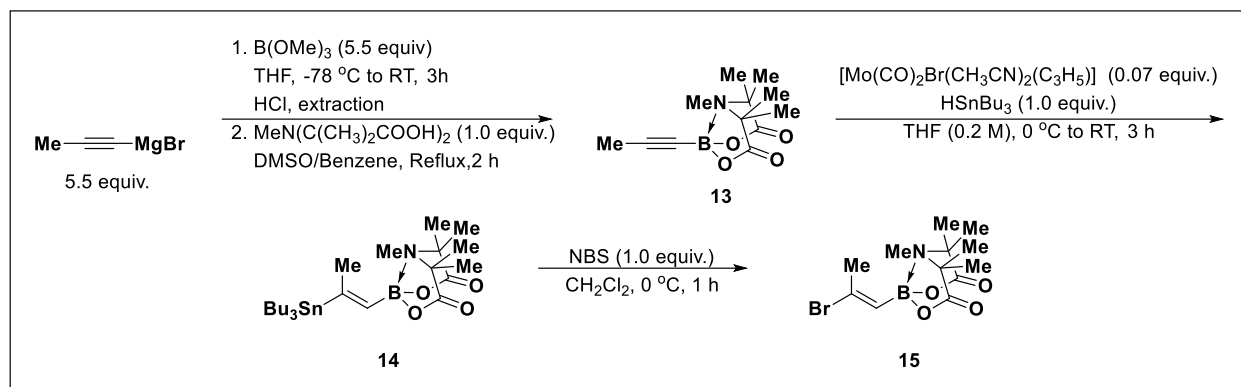
Prep adapted from Woerly, *et al.*[4] To an oven dried 500 mL round bottom flask equipped with a magnetic stir bar with an addition funnel and placed under nitrogen was added THF (112 mL; 0.667 M to grignard, 0.133 to TIDA) and trimethylborate 9.20 mL; 8.57 g; 82.50 mmol; 5.5 equiv.). the resulting solution was cooled to -78 °C. Following equilibration, ethynyl magnesium bromide (150 mL; 0.5 M in THF; 75 mmol; 5.0 equiv.) was added dropwise over 20 minutes. The reaction vessel was removed from the bath and allowed to warm to ambient temperature over 3 hours resulting in an opaque white slurry. After 3 hours, the reaction was cooled to 0 °C (15 minutes) and quenched with the addition of 1N HCl (50 mL; 10.0 equiv.). The resulting mixture was transferred to a sep. funnel rinsing with Et$_2$O. Layers separated and the aqueous later was back extracted with Et$_2$O (1 x 50 mL). Combined organics washed with brine (2 x 50 mL), dried over MgSO$_4$, filtered into a flask containing 185 mL benzene. The resulting solution was concentrated

in vacuo without heating the bath until the solvent in the collection flask started to bump or no more solvent was collecting on the dry ice trap. To the resulting solution was added 30 mL DMSO, TIDA (3.05 mg; 15 mmol; 1.0 equiv.), and a stirbar. The 1L recovery flask was fitted with dean-stark trap, and a reflux condensor and heated to reflux with stirring (set bath to 105 C to get benzene collecting in the dean-stark). Covered the apparatus in foil to assist in heating. The dean-stark trap was filled with benzene at the start of the reaction. After 30 minutes, the trap was regularly emptied. As the reaction got more concentrated it transitioned from a opaque solution to a deep orange, clear solution. After 2.5 hours, the reaction mixture was transferred to a round bottom flask and concentrated in vacuo to afford a DMSO slurry. Slurry was transferred to a separatory funnel rinsing with EtOAc. Layers separated, aqueous layer was back-extracted with EtOAc (2 x 50 mL). Combined organics were concentrated and washed with DI water (2 x 75 mL), brine (3 x 75 mL), dried over MgSO$_4$ with DARCO, filtered and concentrated *in vacuo* to afford a white solid. Solid triterated with Et$_2$O (~300 mL) to afford pure product a white powder (1.174g; 31% yield). Rf = 0.39 in EtOAc, visualized via KzMnO$_4$; ^{1}H NMR (500 MHz, Chloroform-*d*) δ 2.73 (s, 3H), 1.87 (s, 3H), 1.70 (s, 13H); ^{13}C NMR (126 MHz, CDCl$_3$) δ 173.89, 37.37, 4.69; ^{11}B NMR (161 MHz, CDCl$_3$) δ 4.22; HRMS (ES+) calculated for C$_{12}$H$_{19}$BNO$_4$ [M+H]$^+$ m/z 252.1407, found 252.1408.

14
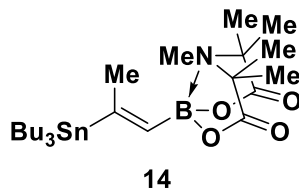
Prep adapted from Woerly, et al.[4] To an oven dried 40 mL vial equipped with a stirbar was added TIDA Boronate **SI-6** (499 mg; 1.99 mmol; 1.0 equiv). Vial was taken into the glovebox and charged with THF (10 mL; 0.2 M). To the resulting suspension was added Mo cat. (50.0 mg; 0.14

mmol; 0.07 equiv.) affording a bright yellow/orange solution. The vial was sealed with a PFTE lined septa cap, removed from the glovebox and cooled to 0 °C in an ice bath. After equilibration (10 min) tributyltin hydride (0.6 mL; 609 mg; 2.09 mmol; 1.05 equiv.) was added dropwise over 5 minutes to give a deep red to brown solution at which point a second portion of the Mo cat (50.7 mg; 0.14 mmol; 0.07 equiv) in 0.5 mL THF was added in one portion followed by an additional equivalent of tributyltin hydride (600 µL; 609 mg; 2.09 mmol; 1.05 equiv.) added dropwise over 5 minutes. After completion of the addition and five additional minutes of stirring, the ice bath was removed and the dark brown solution was allowed to warm to room temperature with stirring over 2 hours at which point it was transferred to a round bottom and concentrated *in vacuo* to afford a deep orange oil. The crude material was loaded onto celite as a DCM slurry and was purified by flash chromatography (4.5 x 8 cm SiO_2 column; 16 x 150 mm fractions) eluting with 2:1 Hexanes:EtOAc (500 mL) to 1:2 Hexanes:EtOAc (500 mL). Fractions 23-28 (Rf = 0.65 in 2:1 Hexanes:EtOAc; visualized with $KMnO_4$) were concentrated *in vacuo* to afford product as a clear colorless oil that upon leaving on high vac overnight afforded a white solid (718 mg; 67% yield). ^{1}H NMR (500 MHz, Chloroform-*d*) δ 5.64 (q, *J* = 1.8 Hz, 1H), 2.59 (s, 3H), 2.10 (d, *J* = 1.8 Hz, 3H), 1.72 (s, 6H), 1.59 (s, 6H), 1.52 – 1.42 (m, 6fH), 1.29 (app. h, *J* = 7.3 Hz, 6H), 0.87 (app. t, *J* = 7.6 Hz, 15H); ^{13}C NMR (126 MHz, CDCl3) δ 174.52, 163.07, 36.28, 29.39, 27.54, 24.37, 13.89, 9.51; ^{11}B NMR (161 MHz, $CDCl_3$) δ 7.41; HRMS (ES+) calculated for $C_{24}H_{47}BNO_4Sn$ [M+H]+ m/z 544.2620, found 544.2616.

15
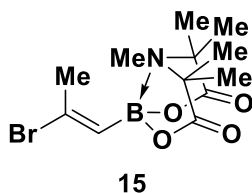
Prep adapted from Woerly, *et al.*[4] To an oven dried 40 mL vial preconcentrated with vinyl stannane

SI-7 (781.6 mg; 1.44 mmol; 1.0 equiv.), equipped with a magnetic stir bar, sealed with a PFTE

lined septa cap, and placed under nitrogen was added DCM (16.5 mL; 0.089 M). The resulting

solution was cooled to 0 °C in an ice bath. After equilibration NBS (266 mg; 1.44 mmol; 1.0

equiv.) was added in one portion at 0 °C. The resulting solution was stirred for that temperature

for 2 h. After 2 h the reaction mixture was quenched with saturated Na_2SO_3 (20 mL) at 0 °C under

nitrogen. The reaction mixture was transferred to a separatory funnel rinsing with water and DCM

(5 mL each). Layers were separated and aqueous layer was back-extracted with CH_2Cl_2 (2 x 20

mL). Combined organics washed with brine (3 x 20 mL), dried over $MgSO_4$ with DARCO, filtered

over celite, and concentrated in vacuo to afford crude material which was triterated with Et_2O

resulting in a white solid (346 mg; 72% yield). Rf = 0.38 in EtOAc, visualized with $KMnO_4$; [1]H

NMR (500 MHz, Chloroform-*d*) δ 5.85 (q, *J* = 1.1 Hz, 1H), 2.58 (s, 3H), 2.46 (d, *J* = 1.1 Hz, 3H),

1.73 (s, 6H), 1.60 (s, 6H); ^{13}C NMR (126 MHz, CDCl3) δ 173.80, 135.31, 36.32, 27.86; ^{11}B NMR

(161 MHz, CDCl3) δ 7.97; HRMS (ES+) calculated for $C_{12}H_{20}BNO_4Br$ [M+H]$^+$ m/z 332.0669,

found 332.0668.

16

16
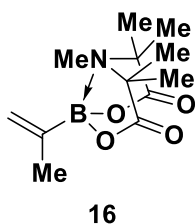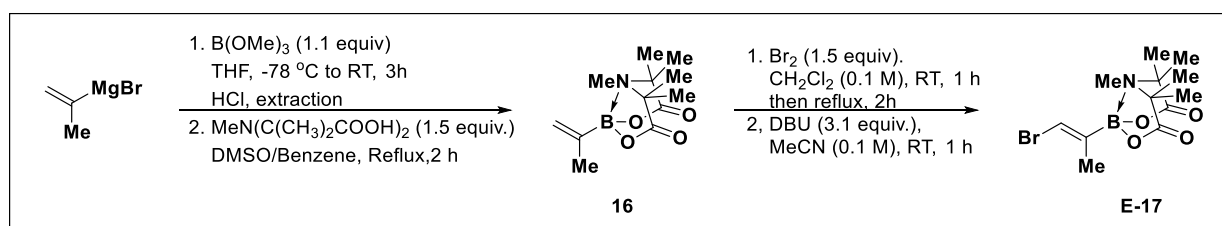
Prep adapted from Lee, *et al.*[1] To an oven dried 100 mL round bottom flask equipped with a magnetic stir bar and placed under nitrogen was added THF (SDS; 15 mL; 0.666 M) and trimethylborate (1.3 mL; 11mmol; 1.1 equiv) then placed in -78°C bath for 40 m. Isopropenyl magnesium bromide (0.5 M in THF; 20 mL; 10mmol; 1.0 equiv) was added dropwise over 11 minutes. The reaction vessel was removed from the bath and allowed to warm to room temperature over 2 hours resulting in an opaque white slurry. After 2 hours, the reaction was cooled to 0°C for 10 min and quenched with 1M HCl (20 mL). The resulting mixture was transferred to a separatory funnel rinsing with Et_2O (10 mL), aqueous layer extracted Et_2O (1 x 20 mL), dried over $MgSO_4$. Benzene (125mL) and DMSO (12.5mL) were added and ether was removed *in vacuo*. To the solution of boronic acid in DMSO/Benzene was added TIDA (3.0062 g; 15 mmol; 1.5 equiv). The round bottom flask was equipped with a dean-stark trap and a reflux condensor and heated to reflux. After 16 hours, the stir bar was removed and reaction mixture was concentrated *in vacuo* to afford a DMSO slurry. Slurry was transferred to a separatory funnel rinsing with DCM, aqueous layer was extracted with DCM (1 x 30mL), washed with brine (30mL), dried over $MgSO_4$, filtered, and concentrated *in vacuo*. Crude solid was triturated with Et_2O to afford product as white solid (1.5243g, 60% yield). R_f = 0.07 in 1:1 Hexanes:EtOAc, visualized via $KMnO_4$; ^{1}H NMR (500 MHz, Chloroform-*d*) δ 5.60 (s, 1H), 5.50 (s, 0H), 2.58 (s, 2H), 1.82 (s, 1H), 1.76 (s, 6H), 1.63 (s, 4H); ^{13}C NMR (126 MHz, $CDCl_3$) δ 174.52, 127.80, 77.26, 77.01, 76.75, 37.00, 22.14; ^{11}B NMR (161 MHz, $CDCl_3$) δ 8.82; HRMS (ES+) calculated for $C_{12}H_{21}O_4BN$ [M+H]$^+$ *m/z* 254.15637, found 254.15570

E-17
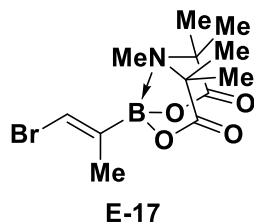
Prep adapted from Woerly *et al.*[7] An oven dried, stir bar equipped 150 mL round bottom flask was charged with **SI-10** TIDA boronate (1.4890g; 5.92mmol, 1.0 equiv) and backfilled. DCM (SDS, 56mL, 0.106 M) was added and flask was lowered into a 0∘C for 40 min. Br_2 (0.6mL; 11.85 mmol; 2.0 equiv) was added dropwise over 4 min. Icebath was then removed and reaction was allowed to stir and warm to room temperature. After 1.5 hour solution was concentrated *in vacuo*, azeotroped with DCM (3 x 25 mL) to afford a foamy pale yellow solid. A stir bar equipped 150 mL round bottom flask was backfilled and MeCN (SDS, 38mL, 0.128M) was added. DBU (2.6 mL, 17.78mmol; 3.0 equiv) was added over 3 min, causing yellow solution to become paler is color. Reaction was allowed to stir at 60°C for 1.5 hours and was then transferred to a separatory funnel with EtOAc (45 mL) 1M HCl (45 mL). Organic layer was washed with 3:2 $NaHSO_3$:Brine (20 mL), brine (20mL), dried over $MgSO_4$, and concentrated *in vacuo*. Crude solid was triterated with Et_2O to afford product as white solid (1.4595g, 75% yield). R_f =   0.19   in   1:2 Hexane:EtOAc, visualized with $KMnO_4$; ^{1}H NMR (500 MHz, Chloroform-*d*) δ 6.67 (s, 0H), 2.56 (s, 3H), 1.61 (s, 7H), 1.55 (s, 6H); ^{13}C NMR (126 MHz, $CDCl_3$) δ 173.93, 118.49, 77.26, 77.01, 76.75, 37.02, 19.28; ^{11}B NMR (161 MHz, $CDCl_3$) δ 8.46; HRMS (ES+) calculated for $C_{12}H_{20}O_4$-BNBr [M+H]$^+$ *m/z* 332.0669, found 332.0655.

18
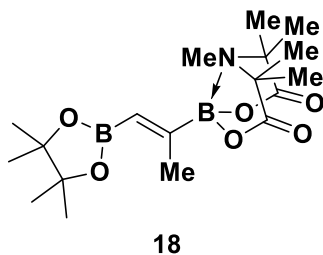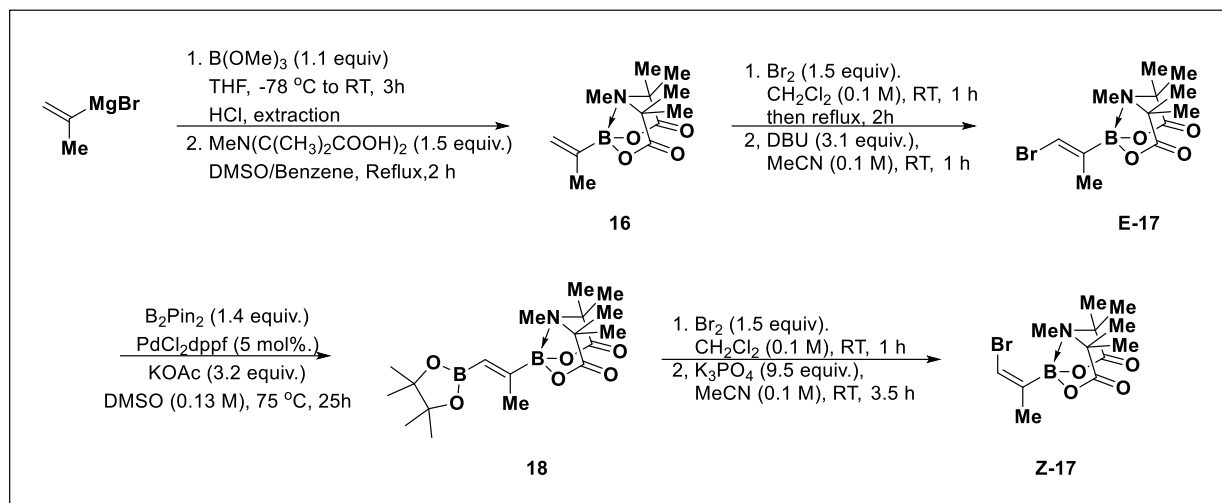
Prep adapted from Woerly *et al.*[7] To a 40mL vial containing bifunctional TIDA **SI-11** (0.657g; 1.98mmol; 1.0 equiv) and a stir bar, in a glovebox, was added B_2Pin_2 (0.7615g; 3.00mmol; 1.5 equiv), KOAc (0.6183g; 6.30mmol; 3.2 equiv), and $PdCl_2dppf \cdot CH_2Cl_2$ (85.3mg; 0.1mmol; 0.05 equiv). Vial was capped with septum cap, removed from glovebox, and placed under N_2. DMSO (SDA, 16mL, 0.125M) was added in one portion. Nitrogen inlet was then removed and reaction was stirred at 75°C for 25 h . Reaction was transferred to separatory funnel with EtOAc (75 mL) and H_2O (50mL). Aqueous layer was extracted with EtOAc (2 x 35 mL). Combined organic layers were washed with H2O (2 x 50 mL), dried over MgSO4, filtered, and concentrated in vacuo. Crude solid was then triterated with Et2O giving a brown solid (552.7mg 70% yield). Rf = 0.62 in 2:1 Hexanes:EtOAc; visualize with $KMnO_4$; ^{1}H NMR (500 MHz, Chloroform-*d*) δ 6.01 (s, 1H), 2.56 (s, 3H), 2.02 (s, 3H), 1.71 (s, 6H), 1.58 (s, 6H), 1.27 (s, 12H); ^{13}C NMR (126 MHz, CDCl$_3$) δ

174.44, 82.93, 77.27, 77.01, 76.76, 24.92, 20.38; ^{11}B NMR (161 MHz, CDCl$_3$) δ 30.02, 8.32; HRMS (ES+) calculated for Calculated for C$_{18}$H$_{31}$B$_2$NO$_6$ (M+H)$^+$ m/z 380.2416, found 380.2409

Z-17
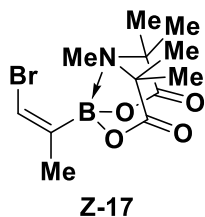
Prep adapted from Woerly *et al.*[7] A 40 mL vial containing the bisborylated block **SI-12** (618.5mg; 1.63mmol; 1.0 equiv) was backfilled and DCM (SDS; 16mL; 0.10M) was added. Br$_2$ (0.13mL; 2.45mmol; 1.5 equiv.) was added dropwise over 1 min. The reaction was allowed to stir at room temperature for 1 hour. Reaction was then concentrated, and azeotroped with DCM (3 x 15mL). Finely ground K$_3$PO$_4$ (3.5892g; 16.3 mmol; 10 equiv) was added and then vial was backfilled. MeCN (SDS; 16mL; 0.10M) was added and reaction was allowed to stir at room temperature. After 4.5 hours reaction was then transferred to a separatory funnel with EtOAc (35mL) and NaHSO$_3$ (30mL). Organic layer was washed with NaHSO$_3$ (35mL), extracted with EtOAc (1 x 50mL), dried over MgSO$_4$, and concentrated *in vacuo*. Crude solid was first triturated, then recrystallized, but NMR's continued to show minor amounts of impurities, so solid was purified by silica column (3.5cm x 7 cm). Eluted with a graditent of 2:1 Hex:EtOAc (150mL) to 1:2 Hex:EtOAc (150mL) to EtOAc (150mL). Product collected as a white solid (217.6mg 40% yield). ^{1}H NMR (500 MHz, Chloroform-*d*) δ 6.71 (s, 1H), 2.75 (s, 3H), 1.86 (s, 2H), 1.75 (s, 6H), 1.59 (s, 7H); ^{13}C NMR (126 MHz, CDCl$_3$) δ 174.06, 114.83, 37.11, 24.59; ^{11}B NMR (161 MHz, CDCl$_3$) δ 8.21; HRMS (ES+) calculated for C$_{12}$H$_{19}$NO$_4$BBr [M+H]$^+$ *m/z* 331.05905, found 331.05859
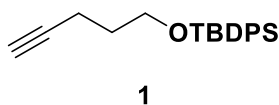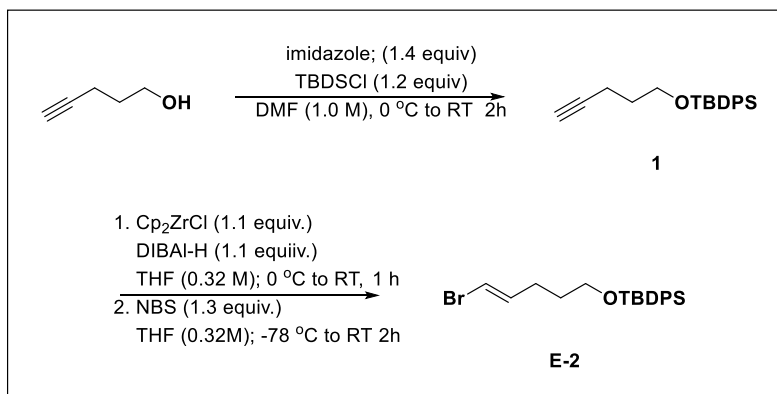
Prep adapted from Armbrust *et al.*[8] A flame dried 500 mL round bottom flask was equipped with stir bar, charged with imidazole (15.28g; 224.68mmol; 1.4 equiv) and backfilled. DMF (SDS; 90mL; 1.75M), was added followed by 4-pentylol (16 mL; 160.49mmol; 1.0 equiv). Reaction was then placed in 0°C for 20 min. TBDPSCl (50mL; 192.59mmol; 1.2 equiv) was added to round bottom flask already under N_2, and cannulated into the reaction flask over 40 min. Reaction mixture solidified preventing stirring, so an additional 40 mL of DMF was added to allow stirring. Reaction was stirred for 25 min in a 0°C and 60 min at room temperature. Reaction was placed in 0°C for 10 min before being quenched with H_2O (60 mL), transferred to separatory funnel. Aqueous layer extracted with Et_2O (2x 30 mL), washed with water (30 mL), and brine (30 mL), dried over $MgSO_4$, and concentrated. Crude oil was purified by silica column (600mL Silica) eluted with hexanes. Product was collected as a colorless oil (49.5063g 85% yield). ^{1}H NMR (500 MHz, Chloroform-*d*) δ 7.69 – 7.65 (m, 4H), 7.45 – 7.36 (m, 6H), 3.74 (t, *J* = 6.0 Hz, 2H), 2.35 (td, *J* = 7.2, 2.7 Hz, 2H), 1.92 (t, *J* = 2.7 Hz, 1H), 1.77 (tt, *J* = 7.1, 5.9 Hz, 2H); ^{13}C NMR (126 MHz, CDCl3) δ 135.75, 134.02, 129.76, 127.81, 84.43, 77.45, 77.20, 76.95, 68.46, 62.46, 31.63, 27.04, 19.43, 15.17; HRMS (ES+) calculated for $C_{21}H_{27}OSi$ [M+H]$^+$ *m/z* 323.1831, found 323.1825

Br⌇⌇⌇⌇OTBDPS

E-2
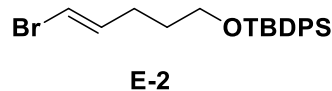
Prep adapted from Pereira *et al.*[9] An oven dried 250 mL round bottom flask with stir bar was taken into the glovebox and charged with Cp_2ZrCl_2 (6.4426g; 22.0 mmol; 1.1 equiv), capped with a septa, removed from glovebox, and connected to a nitrogen line in the hood. THF (SDS; 50 mL; 0.32 M) was added. Flask was lowered into an 0⁰C bath for 10min before DIBALH (1M in hexanes; 22mL; 1.1 equiv) was added dropwise rate over 12min. Reaction was then allowed to stir for 60 min. Alkyne **104-1** (6.48990g; 20 mmol; 1.0 equiv) in THF (SDS, 8 mL) was then added at a fast dropwise rate over 7 min, before the reaction flask was removed from the ice bath and stirred for 85 min. Reaction was the lowered into a -78°C dry ice/ipa bath for 10 min. NBS (7.69458g; 40mmol; 2.0 equiv) was added as a solid in 3 portions over 2 min. The reaction stirred for 45 min. Icebath was then removed and reaction allowed to stir for an additional 65 min at room temp. Reaction was then placed in icebath and quenched with HCl (48 mL, 1M, 2eq compared to Cp_2ZrCl_2) and allowed to stir for 15 min. Reaction was filtered to removed solid, transferred to a separatory funnel, extracted with Et_2O (3 x 45 mL), and washed with brine (1 x 45 mL), dried over $MgSO_4$ and concentrated *in vacuo*. Crude product was purified by silica column (5.5x20 cm). Eluted with a gradient of hexanes (500 mL) to 20:1 hexanes:DCM (400 mL) to 13.3:1 hexanes:DCM (400 mL) to 10:1 hexanes:DCM (800 mL). Product was collected as a colorless oil that became a white solid upon freezing (5.53293g; 69 % yield). ¹H NMR (500 MHz, Chloroform-*d*) δ 8.52 (dp, *J* = 8.2, 1.9 Hz, 4H), 8.30 – 8.21 (m, 6H), 7.04 – 6.96 (m, 1H), 6.84 (dt, *J* = 13.5, 1.6 Hz, 1H), 4.52 (td, *J* = 6.1, 1.7 Hz, 2H), 3.01 (qd, *J* = 7.3, 1.6 Hz, 2H), 2.49 (dt, *J* = 13.2, 6.8 Hz, 2H), 1.91 (s, 6H); ¹³C NMR (126 MHz, Chloroform-*d*) 131.81, 129.69, 127.97, 123.76, 121.80, 98.61, 56.85, 25.53, 23.48, 21.01, 13.37; HRMS (CI+) calculated for $C_{21}H_{28}O_4BrSi$ [M+H]⁺ *m/z* 403.10928, found 403.10762.

An oven dried 300 mL round bottom flask was charged with alkyne **103-1** (9.66304g; 30 mmol; 1,0 equiv) and backfilled before THF (SDS; 48mL; 0.625 M) was added. Flask was then lowered into a -78°C dry ice/acetone bath for 10 min. nBuLi (1.6M in Hexanes; 22mL; 33mmol; 1.1 equiv) was added over 9 min. -78°C bath was then switched out for a 0°C bath and reaction was allowed for stir for 25 min during which time the solution became a bright orange. 0°C bath was switched back to -78°C and reaction was allowed to stir for 7 min before Et₃GeCl (5mL; 30mmol; 1.0 equiv) was added over 3 min. Bath was once again switched to a 0°C bath and reaction was allowed to stir and warm to room temp. After 11.5hrs reaction was quenched with saturated NH₄Cl (6 mL), extracted with Et₂O (2 x 25 mL), washed with brine (20 mL), dried over MgSO₄ and concentrated *in vacuo*. Crude product was purified using silica column (5 x 12 cm) Eluted with 800 mL hexanes followed by 2.5% EtOAc in Hex. Product was collected as colorless oil (9.78762g, 68% yield). ^{1}H NMR (500 MHz, Chloroform-*d*) δ 7.67 (dd, *J* = 7.9, 1.6 Hz, 4H), 7.44 – 7.35 (m, 6H), 3.77 (t, *J* = 6.1 Hz, 2H), 2.41 (t, *J* = 7.1 Hz, 2H), 1.83 – 1.75 (m, 2H), 1.10 – 1.02 (m, 18H), 0.81 (q, *J* = 7.9 Hz, 6H); ^{13}C NMR (126 MHz, CDCl₃) δ 135.67, 134.11, 129.66, 127.74, 107.21, 81.26, 77.41,

77.36, 77.16, 76.91, 62.72, 32.13, 27.00, 19.42, 16.64, 9.12, 5.89; HRMS (ES+) calculated for $C_{27}H_{41}OGeSi$ [M-H]$^+$ *m/z* 483.2138, found 483.2144.

$$GeEt_3$$

4
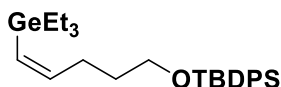
Prep adapted from Pereira *et al.*[9] An oven dried, stir bar equipped 500 mL round bottom flask was taken into the glovebox and charged with Cp_2ZrCl_2 (12.4496g; 42.18 mmol; 2.0 equiv), capped with septa and attached to addition funnel in hood and backfilled 3 times with N_2. THF (SDS; 210mL; 0.10 M) was added before flask was lowered into 0ºC bath for 20 min. DIBALH (1M in hexanes; 42 mL; 42 mmol; 2.0 equiv) was then added over 15 min, and reaction was allowed to stir for 45 min. Alkyne **103-2** (10.15598g; 21.09 mmol; 1.0 equiv) in THF (SDS, 20mL) was added over 10 min, 0ºC bath was removed, and reaction was allowed to stir for 2 hours. Reaction was placed in 0ºC bath for 4 min and quenched with H_2O (14 mL) added over 3 min. Reaction was then allowed to stir for 20min. Pentanes were added and reaction mixture was then filtered through a silica plug. Reaction was purified by silica column (5.5x16cm). Sample was dry loaded on celite. Column eluted with a gradient of hexanes to 1% EtOAc in hexanes to 2% EtOAc in hexanes. Product was isolated as colorless oil (8.01764g 79% yield). ^{1}H NMR (500 MHz, Chloroform-*d*) δ 7.70 – 7.64 (m, 4H), 7.44 – 7.35 (m, 7H), 6.35 (dt, *J* = 12.8, 7.2 Hz, 1H), 5.54 (dt, *J* = 12.8, 1.3 Hz, 1H), 3.67 (t, *J* = 6.3 Hz, 2H), 2.17 (s, 6H), 1.67 – 1.60 (m, 2H), 1.08 – 0.96 (m, 20H), 0.81 (q, *J* = 7.8 Hz, 4H); ^{13}C NMR (126 MHz, CDCl$_3$) δ 147.34, 135.72, 134.16, 129.66, 127.73, 126.86, 77.41, 77.36, 77.16, 76.91, 63.93, 33.04, 31.11, 27.00, 19.36, 9.21, 5.76; HRMS (ES+) calculated for $C_{27}H_{41}OSiGe$ [M-H]$^+$ *m/z* 483.21386, found 483.21466.

Br
OTBDPS
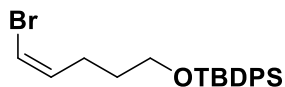
Z-2

Prep adapted from Woerly *et al.*[7] A stir bar and addition funnel equipped, flame dried 1 L flask was charged with alkene **103-3** (8.01264g; 16.55mmol; 1.0 equiv) and backfilled. MeCN (SDS; 250mL; 0.6M) was then added before flask was lowered into a 0°C bath for 15 min. A 100mL flask was charged with NBS (5.43019g; 24.8 mmol; 1.5 equiv) and MeCN (SDS; 50mL). The dissolved NBS was then transferred to the addition funnel and added to the reaction dropwise over 30 min. Reaction was then allowed to stir for 1 hour before being quenched with saturated $Na_2S_2O_3$ (100 mL) and diluted with EtOAc (100 mL). Reaction was then allowed to warm to room temp with vigorous stirring. After 30 min reaction mixture was then transferred to a separatory funnel with 1:1 $Na_2S_2O_3$:H_2O (100 mL) and EtOAc (100 mL). Aqueous layer was then extracted with EtOAc (1 x 50 mL), dried over $MgSO_4$, and concentrated *in vacuo*. Product was purified by silica chromatography (5.5x12 cm) Column was eluted with 400mL hexanes, 400mL 19:1 hexanes:DCM, 400mL 13.3:1 hexanes:DCM, and 200mL 9:1 hexanes:DCM. Product was collected as a colorless oil that became a white solid upon freezing (4.35g 65% yield). ^{1}H NMR (500 MHz, Chloroform-*d*) δ 7.69 – 7.65 (m, 4H), 7.44 – 7.36 (m, 6H), 6.14 (dt, *J* = 6.9, 1.4 Hz, 1H), 6.08 (q, *J* = 6.9 Hz, 1H), 3.68 (t, *J* = 6.2 Hz, 2H), 2.30 (q, *J* = 7.6 Hz, 1H), 1.72 – 1.62 (m, 1H), 1.06 (s, 9H); ^{13}C NMR (126 MHz, CDCl$_3$) δ 135.73, 134.70, 134.07, 129.70, 127.76, 108.05, 77.41, 77.36, 77.16, 76.91, 63.35, 31.21, 27.01, 26.52, 19.37; HRMS (CI+) calculated for $C_{21}H_{28}OSi$ [M+H]$^+$ *m/z* 403.10928, found 403.10847.
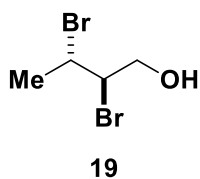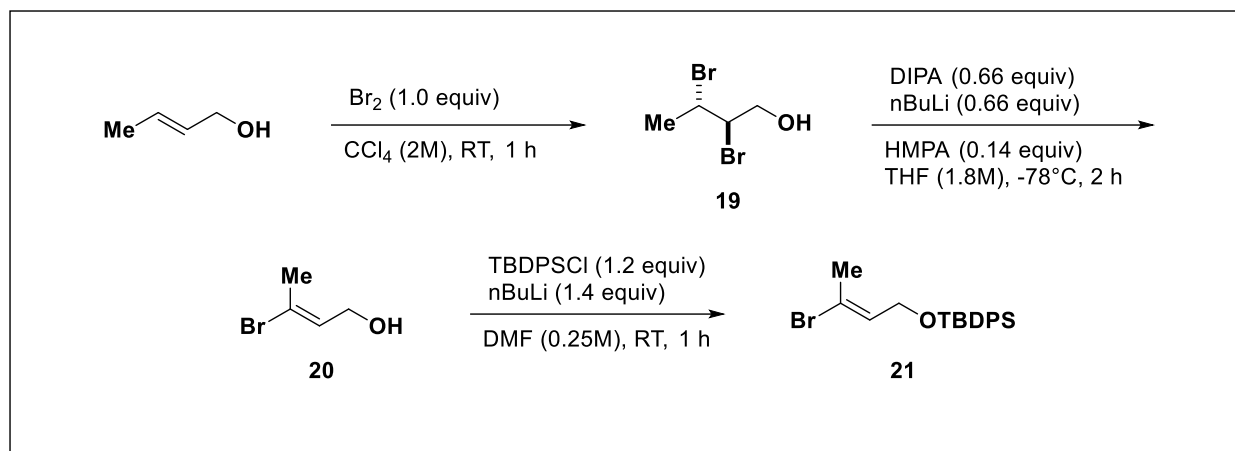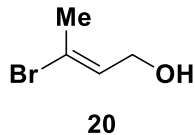
Br₂ (1.0 equiv) Br_2 (1.0 equiv)

CCl₄ (2M), RT, 1 h CCl_4 (2M), RT, 1 h

19

DIPA (0.66 equiv)
nBuLi (0.66 equiv)

HMPA (0.14 equiv)
THF (1.8M), -78°C, 2 h

20

TBDPSCl (1.2 equiv)
nBuLi (1.4 equiv)

DMF (0.25M), RT, 1 h

21

19

Prepared according to literature procedure[27]

20

Prepared according to literature procedure[27]

21
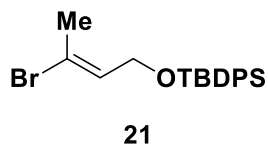
Prepared according to literature procedure[28]

4. REFERENCES

1   Lee, S. J., Anderson, T. M. & Burke, M. D. A Simple and General Platform for Generating Stereochemically Complex Polyene Frameworks by Iterative Cross-Coupling. *Angewandte Chemie International Edition* **49**, 8860-8863, doi:10.1002/anie.201004911 (2010).

2   Ballmer, S. G., Gillis, E. P. & Burke, M. D. B-Protected Haloboronic Acids for Iterative Cross-Coupling. *Organic Syntheses* **86**, 344-359, doi:DOI: 10.15227/orgsyn.086.0344 (2009).

3   Burke, S. J., Gamrat, J. M., Santhouse, J. R., Tomares, D. T. & Tomsho, J. W. Potassium haloalkyltrifluoroborate salts: synthesis, application, and reversible ligand replacement with MIDA. *Tetrahedron Letters* **56**, 5500-5503, doi:https://doi.org/10.1016/j.tetlet.2015.08.012 (2015).

4   *Boronic Acids: Preparation and Applications in Organic Synthesis, Medicine and Materials (*(Wiley-VCH, 2011).

5   Struble, J. R., Lee, S. J. & Burke, M. D. Ethynyl MIDA boronate: a readily accessible and highly versatile building block for small molecule synthesis. *Tetrahedron* **66**, 4710-4718, doi:https://doi.org/10.1016/j.tet.2010.04.020 (2010).

6   Woerly, E. M., Struble, J. R., Palyam, N., O'Hara, S. P. & Burke, M. D. (Z)-(2-bromovinyl)-MIDA boronate: a readily accessible and highly versatile building block for small molecule synthesis. *Tetrahedron* **67**, 4333-4343 (2011).

7   Woerly, E. M., Roy, J. & Burke, M. D. Synthesis of most polyene natural product motifs using just 12 building blocks and one coupling reaction. *Nature chemistry* **6**, 484-491, doi:10.1038/nchem.1947 (2014).

8   Armbrust, K. W., Beaver, M. G. & Jamison, T. F. Rhodium-Catalyzed Endo-Selective Epoxide-Opening Cascades: Formal Synthesis of (−)-Brevisin. *Journal of the American Chemical Society* **137**, 6941-6946, doi:10.1021/jacs.5b03570 (2015).

9   Pereira, A. R. & Cabezas, J. A. A New Method for the Preparation of 1,5-Diynes. Synthesis of (4E,6Z,10Z)-4,6,10-Hexadecatrien-1-ol, the Pheromone Component of the Cocoa Pod Borer Moth Conopomorpha cramerella. *The Journal of Organic Chemistry* **70**, 2594-2597, doi:10.1021/jo048019y (2005).

Rank: 1 Freq: 40954
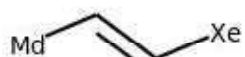
Rank: 2 Freq: 18651

Rank: 3 Freq: 9510

Rank: 4 Freq: 7525
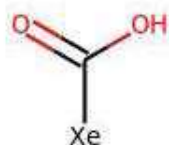
Rank: 5 Freq: 6149
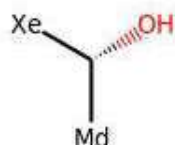
Rank: 6 Freq: 6005
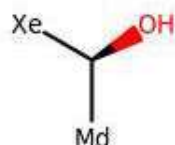
Rank: 7 Freq: 5897
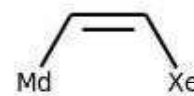
Rank: 8 Freq: 5253
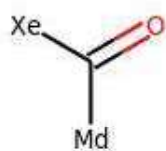
Rank: 9 Freq: 5228
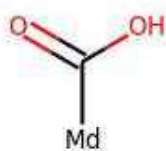
Rank: 10 Freq: 5109
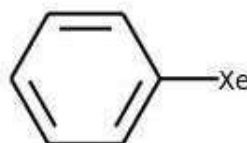
Rank: 11 Freq: 4909

Rank: 12 Freq: 4668

Rank: 13 Freq: 4545

Rank: 14 Freq: 4370
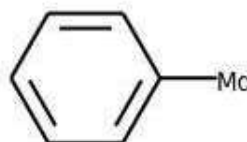
Rank: 15 Freq: 4246

Rank: 16 Freq: 4172
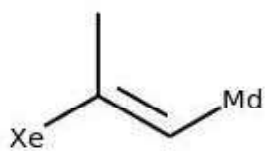
Rank: 17 Freq: 3904
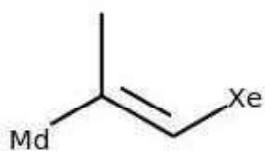
Rank: 18 Freq: 3875

Rank: 19 Freq: 3408

Rank: 20 Freq: 3341

Rank: 21 Freq: 3324
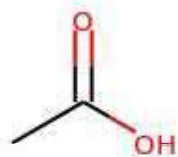
Rank: 22 Freq: 2884
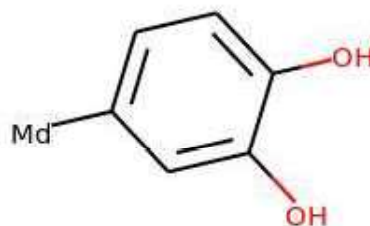
Rank: 23 Freq: 2807
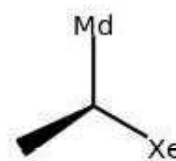
Rank: 24 Freq: 2749
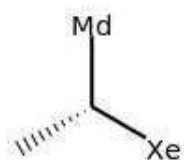
Rank: 25 Freq: 2659

Rank: 26 Freq: 2516

Rank: 27 Freq: 2454

Rank: 28 Freq: 2283

Rank: 29 Freq: 2272

Rank: 30 Freq: 2230
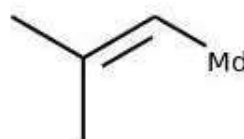
Rank: 31 Freq: 2217
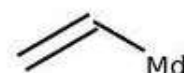
Rank: 32 Freq: 2206

Rank: 33 Freq: 2204
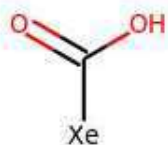
Rank: 34 Freq: 2100
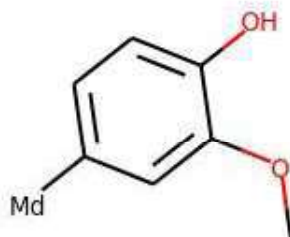
Rank: 35 Freq: 2003
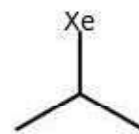
Rank: 36 Freq: 1927
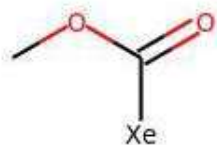
Rank: 37 Freq: 1872
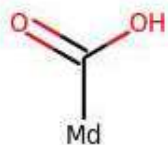
Rank: 38 Freq: 1851

Rank: 39 Freq: 1728
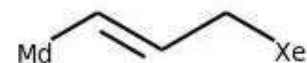
Rank: 40 Freq: 1725
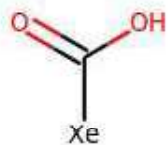
Rank: 41 Freq: 1692
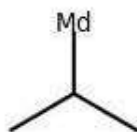
Rank: 42 Freq: 1632
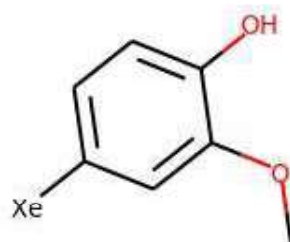
Rank: 43 Freq: 1513
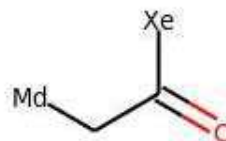
Rank: 44 Freq: 1371
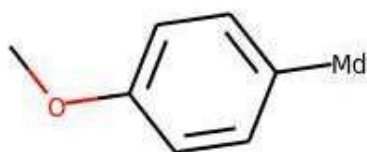
Rank: 45 Freq: 1321
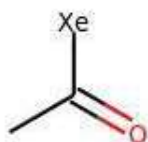
Rank: 46 Freq: 1314

Rank: 47 Freq: 1199
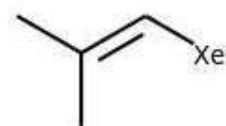
Rank: 48 Freq: 1198
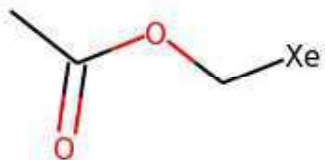
Rank: 49 Freq: 1153
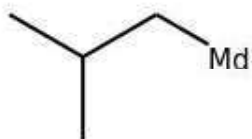
Rank: 50 Freq: 1121
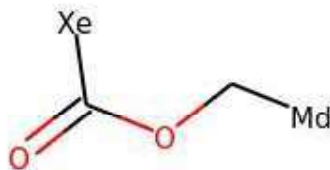
Rank: 51 Freq: 1064
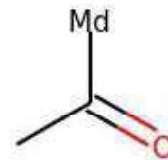
Rank: 52 Freq: 1052
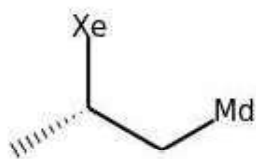
Rank: 53 Freq: 1051
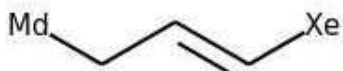
Rank: 54 Freq: 1049
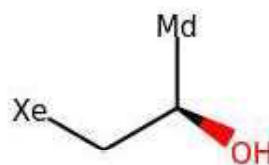
Rank: 55 Freq: 1044
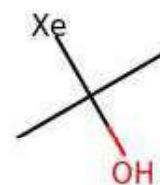
Rank: 56 Freq: 1029
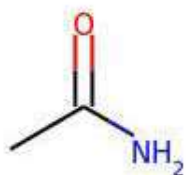
Rank: 57 Freq: 982
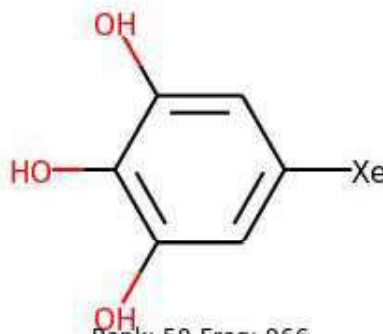
Rank: 59 Freq: 966
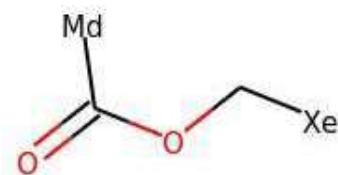
Rank: 60 Freq: 959
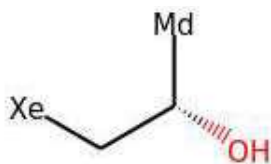
Rank: 61 Freq: 953
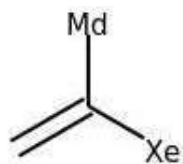
Rank: 62 Freq: 938
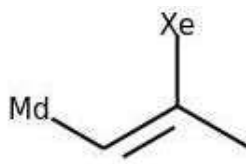
Rank: 63 Freq: 933
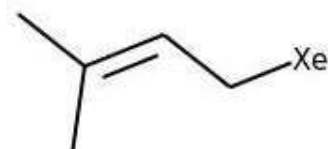
Rank: 64 Freq: 927
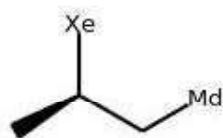
Rank: 65 Freq: 922

Rank: 66 Freq: 892
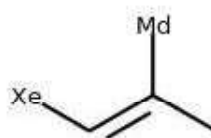
Rank: 67 Freq: 851
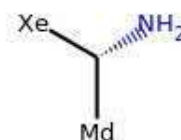
Rank: 68 Freq: 838
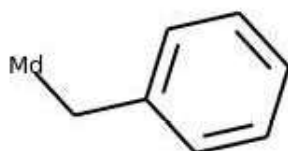
Rank: 69 Freq: 818
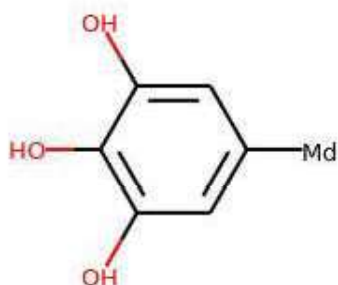
Rank: 70 Freq: 807
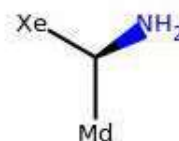
Rank: 71 Freq: 805

Rank: 72 Freq: 792
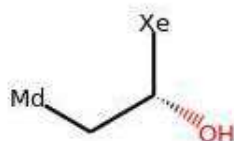
Rank: 73 Freq: 757
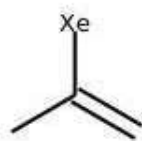
Rank: 74 Freq: 755
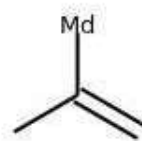
Rank: 75 Freq: 753
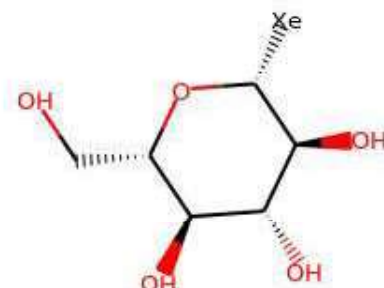
Rank: 76 Freq: 748

Rank: 77 Freq: 731

Rank: 78 Freq: 726
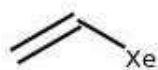
Rank: 79 Freq: 724
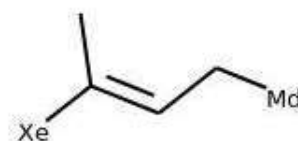
Rank: 80 Freq: 698
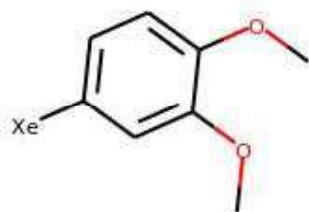
Rank: 81 Freq: 689

Rank: 82 Freq: 683

Rank: 83 Freq: 681

Rank: 84 Freq: 674

Rank: 85 Freq: 666
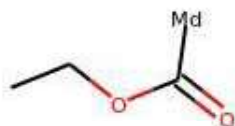
Rank: 86 Freq: 642
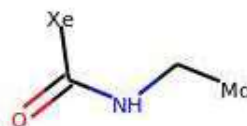
Rank: 87 Freq: 638

Rank: 88 Freq: 636

Rank: 89 Freq: 635

Rank: 90 Freq: 634
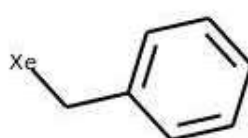
Rank: 91 Freq: 621
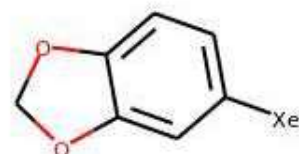
Rank: 92 Freq: 614
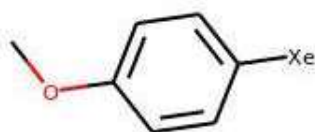
Rank: 93 Freq: 614
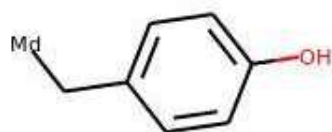
Rank: 94 Freq: 607

Rank: 95 Freq: 605

Rank: 96 Freq: 601
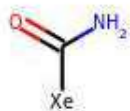
Rank: 97 Freq: 598

Rank: 98 Freq: 598
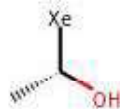
Rank: 99 Freq: 598
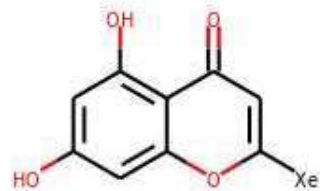
Rank: 100 Freq: 587
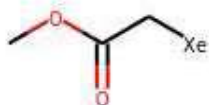
Rank: 101 Freq: 571

Rank: 102 Freq: 568

Rank: 103 Freq: 568
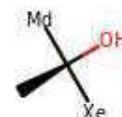
Rank: 104 Freq: 562
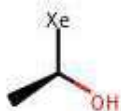
Rank: 105 Freq: 551

Rank: 106 Freq: 548
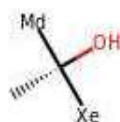
Rank: 107 Freq: 538
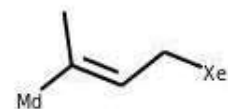
Rank: 108 Freq: 529

Rank: 109 Freq: 527

Rank: 110 Freq: 524
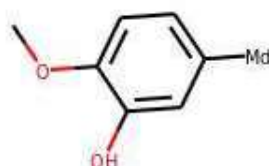
Rank: 111 Freq: 521

Rank: 112 Freq: 517

Rank: 113 Freq: 512
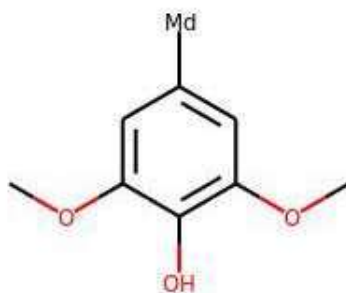
Rank: 114 Freq: 490
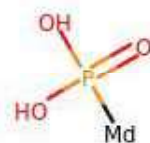
Rank: 115 Freq: 490
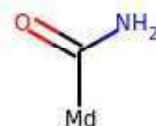
Rank: 116 Freq: 488
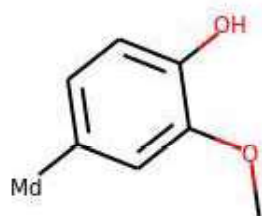
Rank: 117 Freq: 482
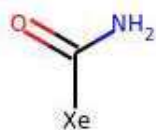
Rank: 118 Freq: 463
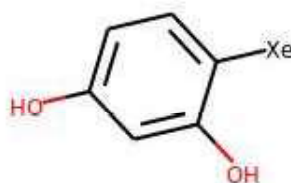
Rank: 119 Freq: 459
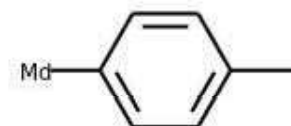
Rank: 120 Freq: 455
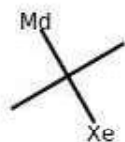
Rank: 121 Freq: 439
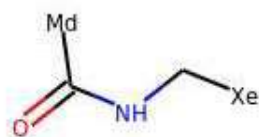
Rank: 122 Freq: 430

Rank: 123 Freq: 422

Rank: 124 Freq: 421

Rank: 125 Freq: 416

Rank: 126 Freq: 407
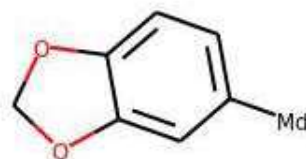
Rank: 127 Freq: 406
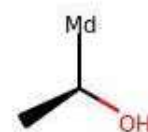
Rank: 128 Freq: 402
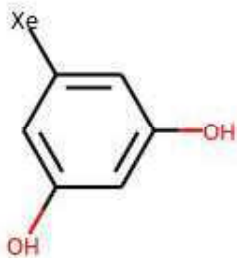
Rank: 129 Freq: 398

Rank: 130 Freq: 396

Rank: 131 Freq: 394

Rank: 132 Freq: 387
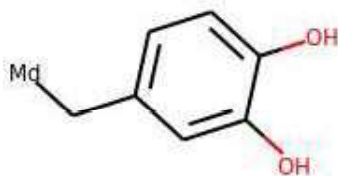
Rank: 133 Freq: 383
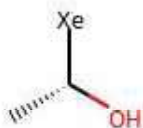
Rank: 134 Freq: 382

Rank: 135 Freq: 381

Rank: 136 Freq: 379

Rank: 137 Freq: 376

Rank: 138 Freq: 374

Rank: 139 Freq: 373
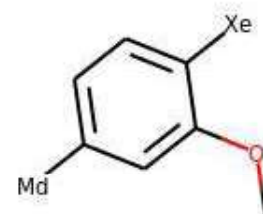
Rank: 140 Freq: 369
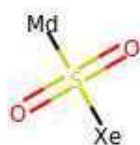
Rank: 141 Freq: 368
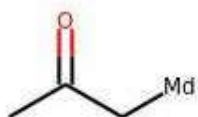
Rank: 142 Freq: 367
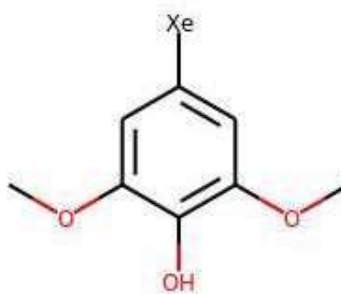
Rank: 143 Freq: 361
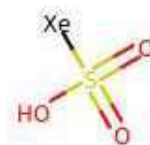
Rank: 144 Freq: 359

Rank: 145 Freq: 359
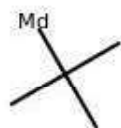
Rank: 146 Freq: 356

Rank: 147 Freq: 353
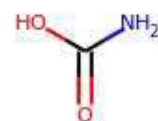
Rank: 148 Freq: 352

Rank: 149 Freq: 349

Rank: 150 Freq: 348
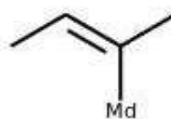
Rank: 151 Freq: 347
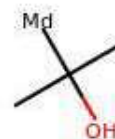
Rank: 152 Freq: 342

Rank: 153 Freq: 342

Rank: 154 Freq: 339

Rank: 155 Freq: 336
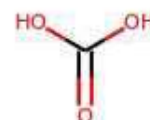
Rank: 156 Freq: 331
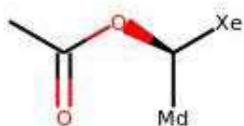
Rank: 157 Freq: 331
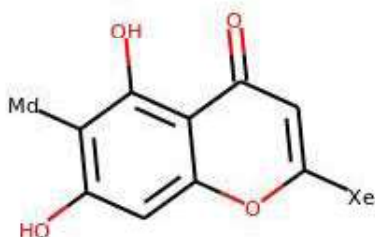
Rank: 158 Freq: 330

Rank: 159 Freq: 326
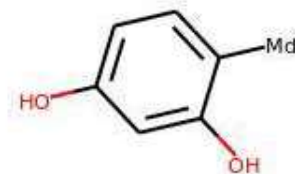
Rank: 160 Freq: 324
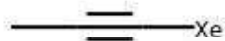
Rank: 161 Freq: 319
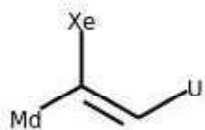
Rank: 162 Freq: 319

Rank: 163 Freq: 318

Rank: 164 Freq: 317

Rank: 165 Freq: 317
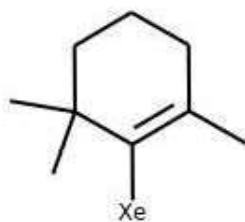
Rank: 166 Freq: 313

Rank: 167 Freq: 312
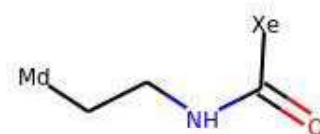
Rank: 168 Freq: 312

Rank: 169 Freq: 311
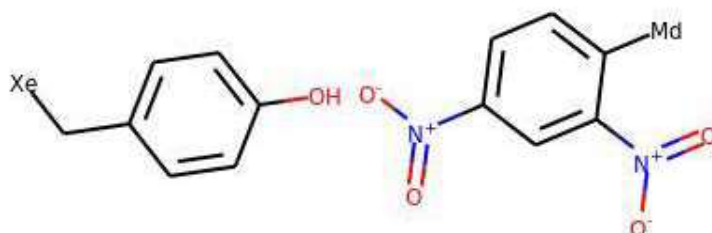
Rank: 170 Freq: 311

Rank: 171 Freq: 302
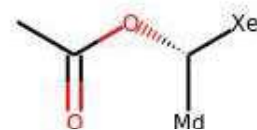
Rank: 172 Freq: 302

Rank: 173 Freq: 292

Rank: 174 Freq: 289

Rank: 175 Freq: 288

Rank: 176 Freq: 286
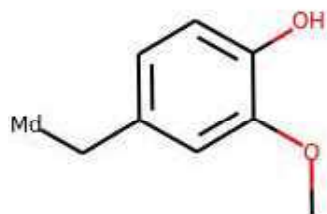
Rank: 177 Freq: 279
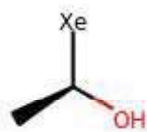
Rank: 178 Freq: 276
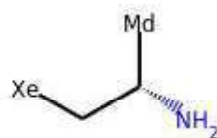
Rank: 179 Freq: 272

Rank: 180 Freq: 271
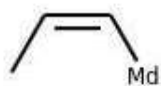
Rank: 181 Freq: 267

Rank: 182 Freq: 267
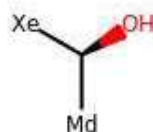
Rank: 183 Freq: 267
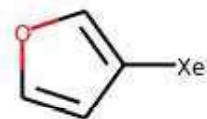
Rank: 184 Freq: 261

Rank: 185 Freq: 261
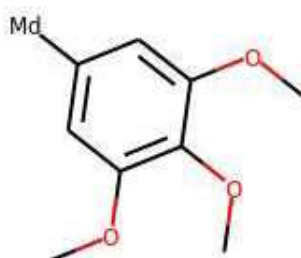
Rank: 186 Freq: 260
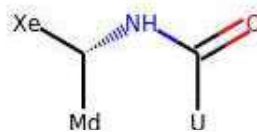
Rank: 187 Freq: 258

Rank: 188 Freq: 256

Rank: 189 Freq: 255
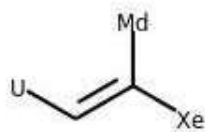
Rank: 190 Freq: 254

Rank: 191 Freq: 253
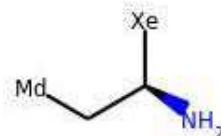
Rank: 192 Freq: 251
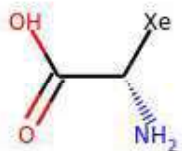
Rank: 193 Freq: 250
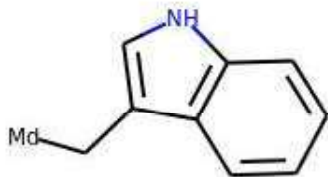


Rank: 194 Freq: 247

Rank: 195 Freq: 241
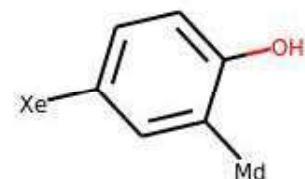
Rank: 196 Freq: 240
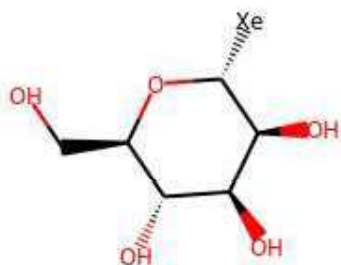
Rank: 197 Freq: 237

Rank: 198 Freq: 236
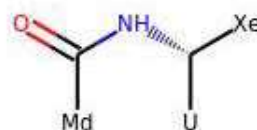
Rank: 199 Freq: 234
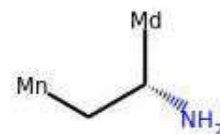
Rank: 200 Freq: 232
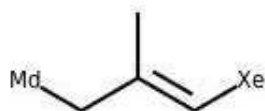
Rank: 201 Freq: 231
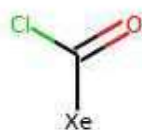
Rank: 202 Freq: 229
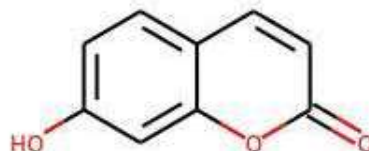
Rank: 203 Freq: 229
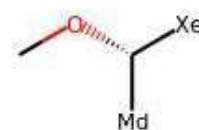
Rank: 204 Freq: 229

Rank: 205 Freq: 227
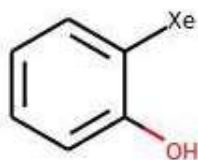
Rank: 206 Freq: 227
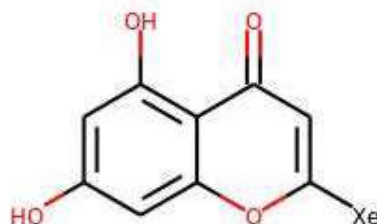
Rank: 207 Freq: 224
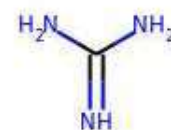
Rank: 208 Freq: 224
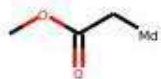
Rank: 209 Freq: 223

Rank: 210 Freq: 220
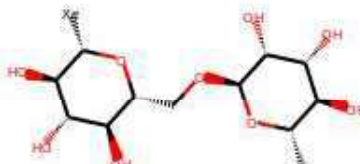
Rank: 211 Freq: 217

Rank: 212 Freq: 212

Rank: 213 Freq: 211
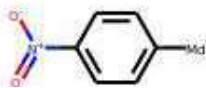
Rank: 214 Freq: 209

Rank: 215 Freq: 208
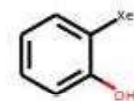
Rank: 216 Freq: 207
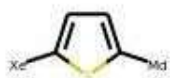
Rank: 217 Freq: 206

Rank: 218 Freq: 206
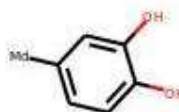
Rank: 219 Freq: 205

Rank: 220 Freq: 199

Rank: 221 Freq: 198

Rank: 222 Freq: 197

Rank: 223 Freq: 194
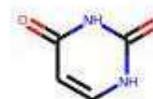
Rank: 224 Freq: 193

Rank: 225 Freq: 191
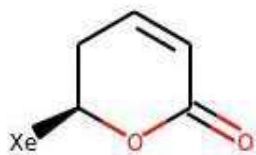
Rank: 226 Freq: 191
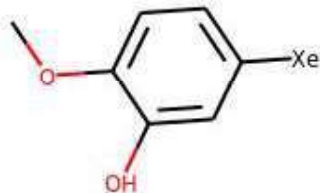
Rank: 227 Freq: 189
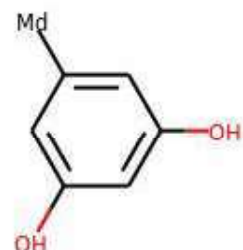
Rank: 228 Freq: 188
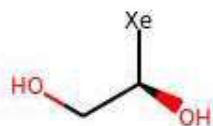
Rank: 229 Freq: 188

Rank: 230 Freq: 186

Rank: 231 Freq: 185
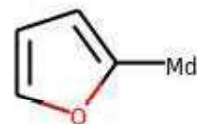
Rank: 232 Freq: 183

Rank: 233 Freq: 181

Rank: 234 Freq: 179

Rank: 235 Freq: 174
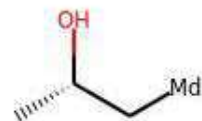
Rank: 236 Freq: 173
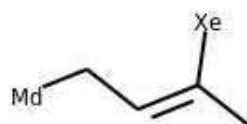
Rank: 237 Freq: 173
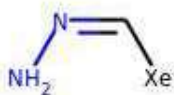
Rank: 238 Freq: 172
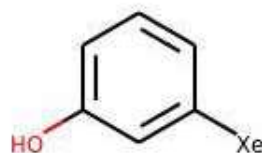
Rank: 239 Freq: 171

Rank: 240 Freq: 170

113

Rank: 241 Freq: 170
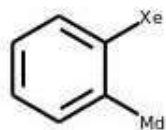
Rank: 242 Freq: 168
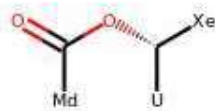
Rank: 243 Freq: 168
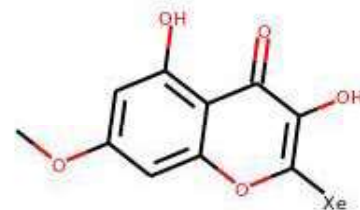
Rank: 244 Freq: 166
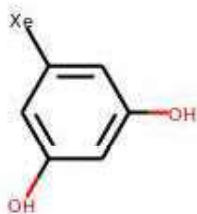
Rank: 245 Freq: 166

Rank: 246 Freq: 165

Rank: 247 Freq: 164
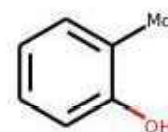
Rank: 248 Freq: 163
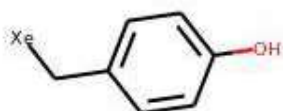
Rank: 249 Freq: 163

Rank: 250 Freq: 161

Rank: 251 Freq: 160

Rank: 252 Freq: 159
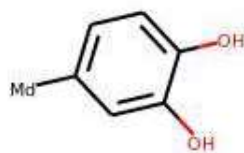
Rank: 253 Freq: 158
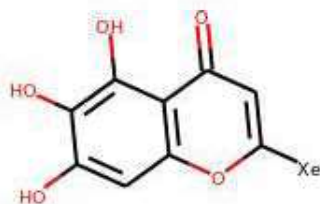
Rank: 254 Freq: 158

Rank: 255 Freq: 156

Rank: 256 Freq: 156

114

Rank: 257 Freq: 156

Rank: 258 Freq: 156
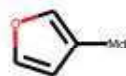
Rank: 259 Freq: 156
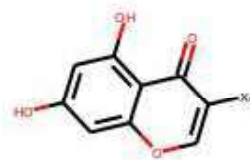
Rank: 260 Freq: 155
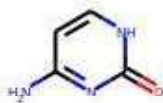
Rank: 261 Freq: 154
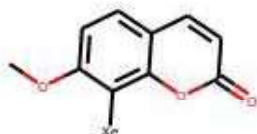
Rank: 262 Freq: 154
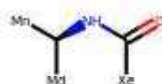
Rank: 263 Freq: 154
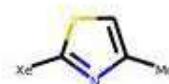
Rank: 264 Freq: 153

Rank: 265 Freq: 153

Rank: 266 Freq: 151
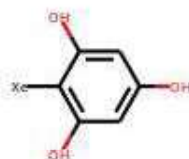
Rank: 267 Freq: 151

Rank: 268 Freq: 151

Rank: 269 Freq: 151
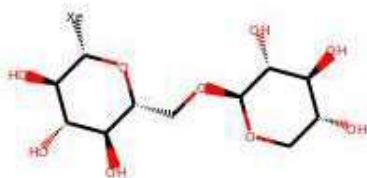
Rank: 270 Freq: 150
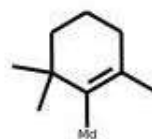
Rank: 271 Freq: 150
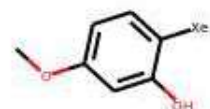
Rank: 272 Freq: 149

Rank: 273 Freq: 149

Rank: 274 Freq: 148

Rank: 275 Freq: 148

Rank: 276 Freq: 148

Rank: 277 Freq: 148

Rank: 278 Freq: 148

Rank: 279 Freq: 147

Rank: 280 Freq: 146

Rank: 281 Freq: 146
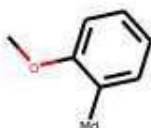
Rank: 282 Freq: 145
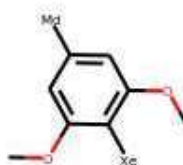
Rank: 283 Freq: 144

Rank: 284 Freq: 142
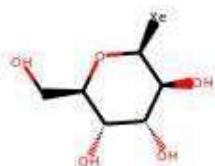
Rank: 285 Freq: 141
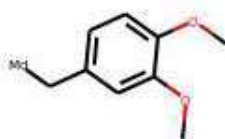
Rank: 286 Freq: 141

Rank: 287 Freq: 140

Rank: 288 Freq: 140
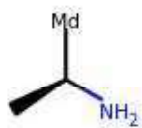
Rank: 289 Freq: 139

Rank: 290 Freq: 138
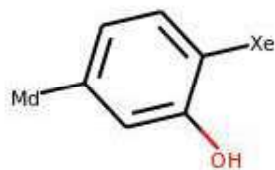
Rank: 291 Freq: 138
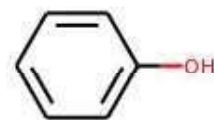
Rank: 292 Freq: 136

Rank: 293 Freq: 136
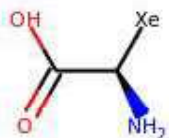
Rank: 294 Freq: 135
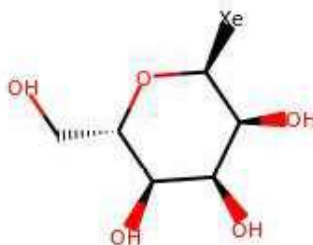
Rank: 295 Freq: 135
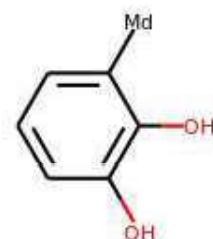
Rank: 296 Freq: 134

Rank: 297 Freq: 133
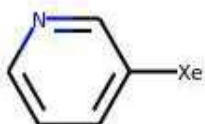
Rank: 298 Freq: 133
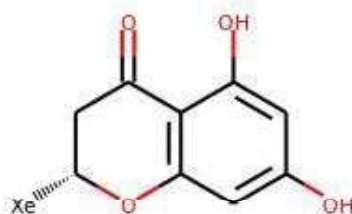
Rank: 299 Freq: 131

Rank: 300 Freq: 131

Rank: 301 Freq: 130

Rank: 302 Freq: 130

Rank: 303 Freq: 130

Rank: 304 Freq: 129
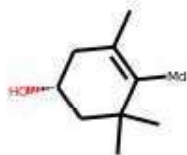
Rank: 305 Freq: 129
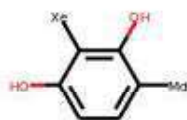
Rank: 306 Freq: 127
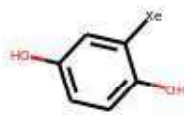
Rank: 307 Freq: 127
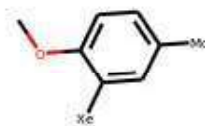
Rank: 308 Freq: 126
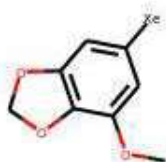
Rank: 309 Freq: 125
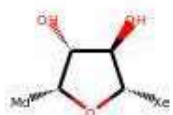
Rank: 310 Freq: 124

Rank: 311 Freq: 123
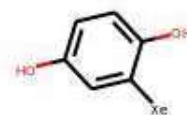
Rank: 312 Freq: 122

Rank: 313 Freq: 122
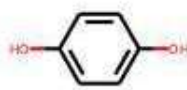
Rank: 314 Freq: 122

Rank: 315 Freq: 121
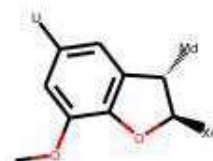
Rank: 316 Freq: 121
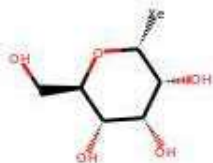
Rank: 317 Freq: 120

Rank: 318 Freq: 120

Rank: 319 Freq: 120
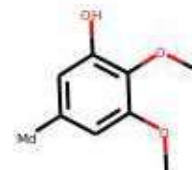
Rank: 320 Freq: 119
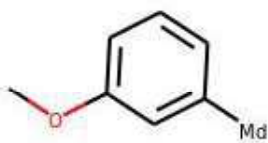
Rank: 321 Freq: 119

Rank: 322 Freq: 119

Rank: 323 Freq: 118

Rank: 324 Freq: 118

Rank: 325 Freq: 117

Rank: 326 Freq: 116

Rank: 327 Freq: 116
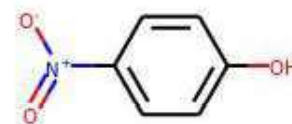
Rank: 328 Freq: 115

Rank: 329 Freq: 115

Rank: 330 Freq: 115

Rank: 331 Freq: 115

Rank: 332 Freq: 114

Rank: 333 Freq: 114

Rank: 334 Freq: 114
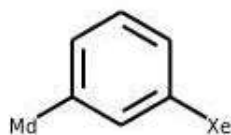
Rank: 335 Freq: 113

Rank: 336 Freq: 112

Rank: 337 Freq: 111
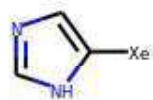
Rank: 338 Freq: 111

Rank: 339 Freq: 111
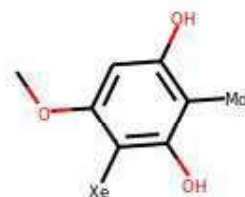
Rank: 340 Freq: 111

Rank: 341 Freq: 110

Rank: 342 Freq: 110

Rank: 343 Freq: 109

Rank: 344 Freq: 109

Rank: 345 Freq: 109

Rank: 346 Freq: 109
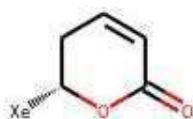
Rank: 347 Freq: 108

Rank: 348 Freq: 108

Rank: 349 Freq: 108

Rank: 350 Freq: 107
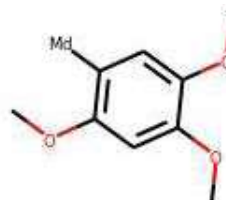
Rank: 351 Freq: 107
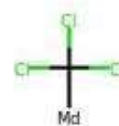
Rank: 352 Freq: 107

Rank: 353 Freq: 106

Rank: 354 Freq: 105
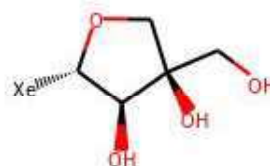
Rank: 355 Freq: 105
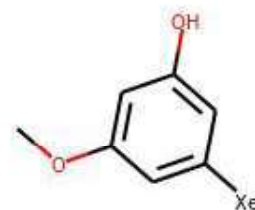
Rank: 356 Freq: 104

Rank: 357 Freq: 104
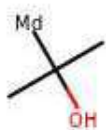
Rank: 358 Freq: 104
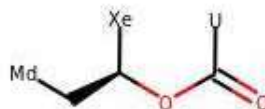
Rank: 359 Freq: 103
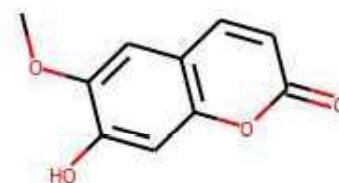
Rank: 360 Freq: 102

Rank: 361 Freq: 102
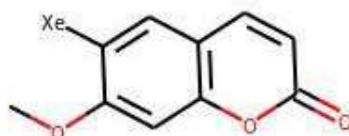
Rank: 362 Freq: 101

Rank: 363 Freq: 101

Rank: 364 Freq: 101

Rank: 365 Freq: 101
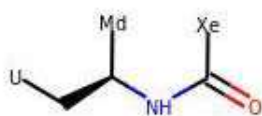
Rank: 366 Freq: 101

Rank: 367 Freq: 100

Rank: 368 Freq: 100
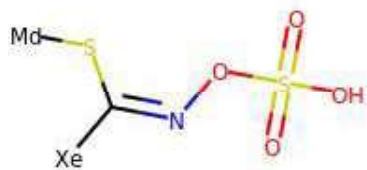
Rank: 369 Freq: 100

Rank: 370 Freq: 99

Rank: 371 Freq: 99
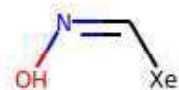
Rank: 372 Freq: 99

Rank: 373 Freq: 99
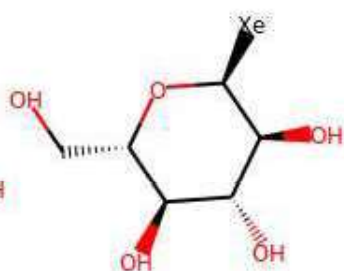
Rank: 374 Freq: 99
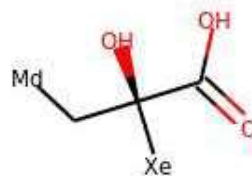
Rank: 375 Freq: 99
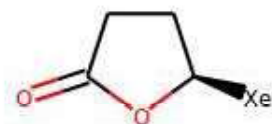
Rank: 376 Freq: 98
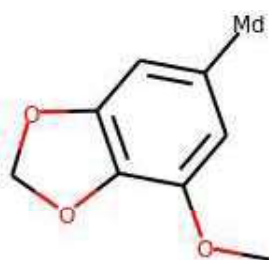
Rank: 377 Freq: 98
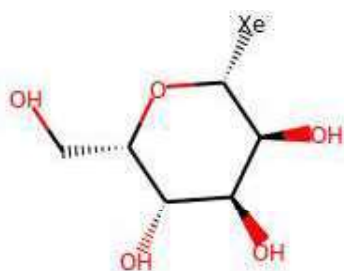
Rank: 378 Freq: 98
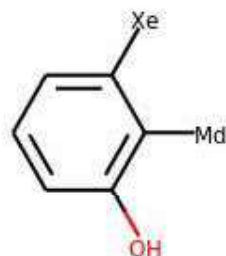
Rank: 379 Freq: 98
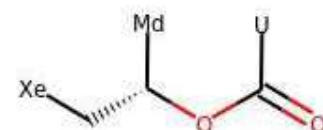
Rank: 380 Freq: 98
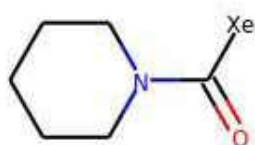
Rank: 381 Freq: 97
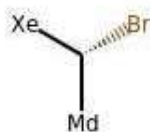
Rank: 382 Freq: 97

Rank: 383 Freq: 96

Rank: 384 Freq: 96
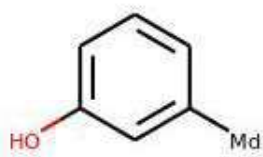
Rank: 385 Freq: 95
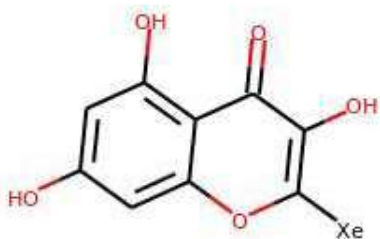
Rank: 386 Freq: 95
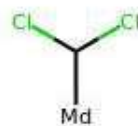
Rank: 387 Freq: 94
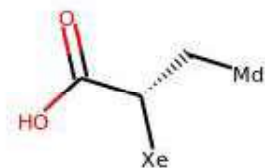
Rank: 388 Freq: 94
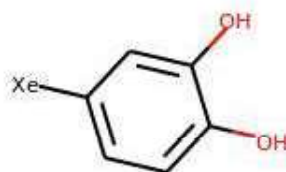
Rank: 389 Freq: 94
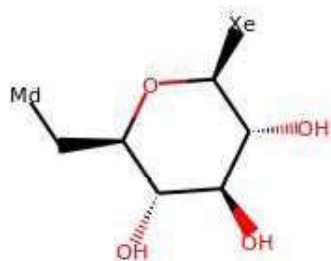
Rank: 390 Freq: 94
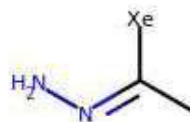
Rank: 391 Freq: 93
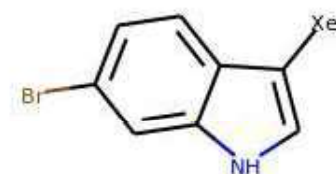
Rank: 392 Freq: 93
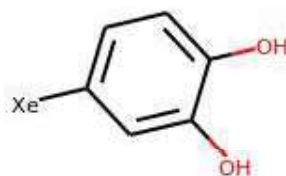
Rank: 393 Freq: 93
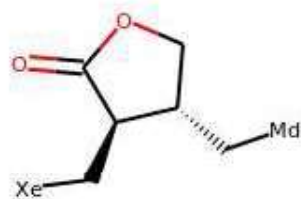
Rank: 394 Freq: 92

Rank: 395 Freq: 92
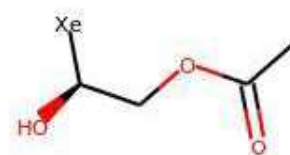
Rank: 396 Freq: 92

Rank: 397 Freq: 92

Rank: 398 Freq: 92

Rank: 399 Freq: 91
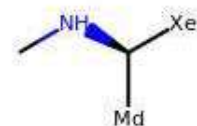
Rank: 400 Freq: 91

Rank: 401 Freq: 90
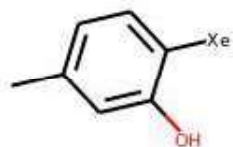
Rank: 402 Freq: 90
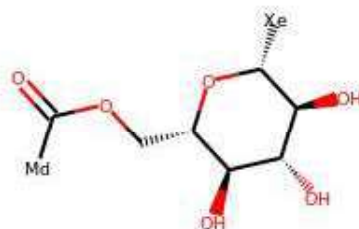
Rank: 403 Freq: 90

Rank: 404 Freq: 89
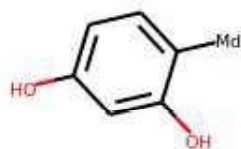
Rank: 405 Freq: 89
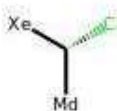
Rank: 406 Freq: 88
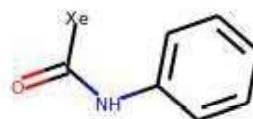
Rank: 407 Freq: 88
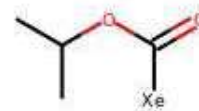
Rank: 408 Freq: 88
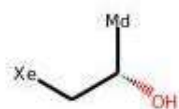
Rank: 409 Freq: 88

Rank: 410 Freq: 87

Rank: 411 Freq: 86

Rank: 412 Freq: 86

Rank: 413 Freq: 86

Rank: 414 Freq: 86
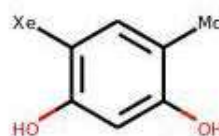
Rank: 415 Freq: 86
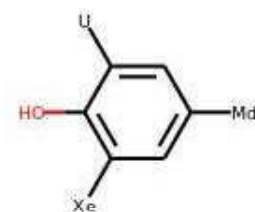
Rank: 416 Freq: 86

Rank: 417 Freq: 85
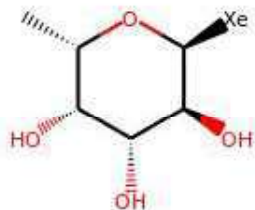
Rank: 418 Freq: 85
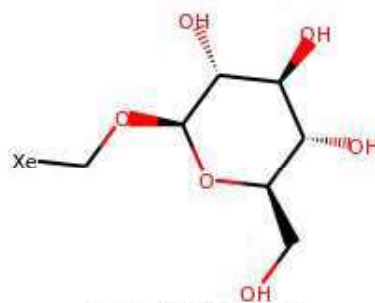
Rank: 419 Freq: 85
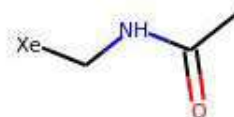
Rank: 420 Freq: 85
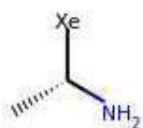
Rank: 421 Freq: 84

Rank: 422 Freq: 84
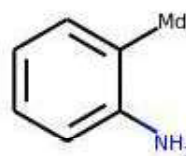
Rank: 423 Freq: 84

Rank: 424 Freq: 84

Rank: 425 Freq: 84
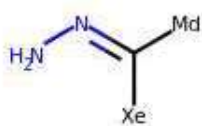
Rank: 426 Freq: 84

Rank: 427 Freq: 84

Rank: 428 Freq: 83

Rank: 429 Freq: 83

Rank: 430 Freq: 82
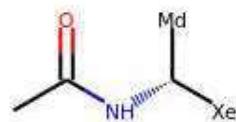
Rank: 431 Freq: 82

Rank: 432 Freq: 81
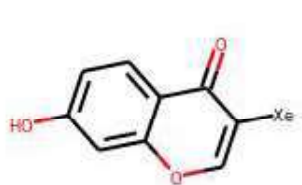
Rank: 433 Freq: 80
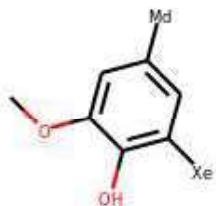
Rank: 434 Freq: 80
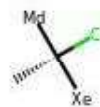
Rank: 435 Freq: 80

Rank: 436 Freq: 79
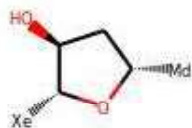
Rank: 437 Freq: 79
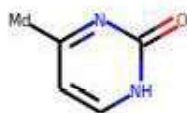
Rank: 438 Freq: 79

Rank: 439 Freq: 78
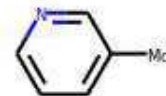
Rank: 440 Freq: 78
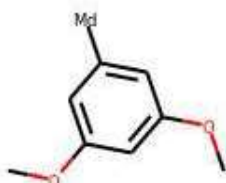
Rank: 441 Freq: 78

Rank: 442 Freq: 78
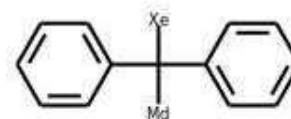
Rank: 444 Freq: 78

Rank: 445 Freq: 77

Rank: 446 Freq: 76
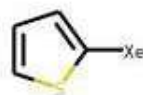
Rank: 447 Freq: 76

Rank: 448 Freq: 76

Rank: 449 Freq: 76

Rank: 450 Freq: 75
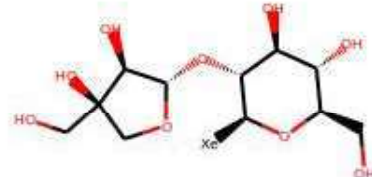
Rank: 451 Freq: 75
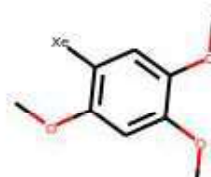
Rank: 452 Freq: 75
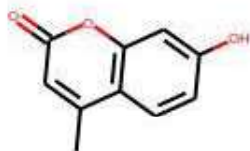
Rank: 453 Freq: 75
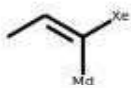
Rank: 454 Freq: 75

Rank: 455 Freq: 74
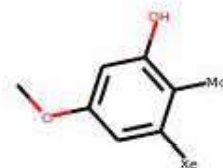
Rank: 456 Freq: 74

Rank: 457 Freq: 74
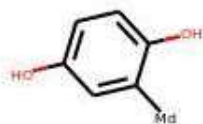
Rank: 458 Freq: 74
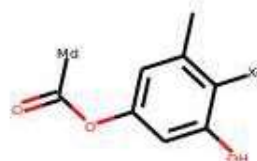
Rank: 459 Freq: 74

Rank: 460 Freq: 74
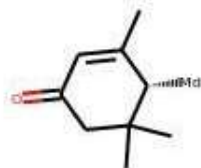
Rank: 461 Freq: 73

Rank: 462 Freq: 73
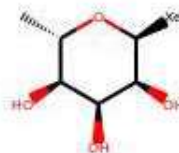
Rank: 463 Freq: 73

Rank: 464 Freq: 72

127
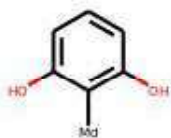
Rank: 465 Freq: 72

Rank: 466 Freq: 72
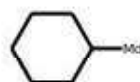
Rank: 467 Freq: 72

Rank: 468 Freq: 72

Rank: 469 Freq: 72

Rank: 470 Freq: 71

Rank: 471 Freq: 71

Rank: 472 Freq: 70
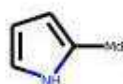
Rank: 473 Freq: 70

Rank: 474 Freq: 70
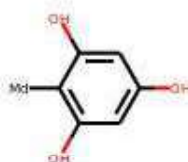
Rank: 475 Freq: 70
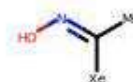
Rank: 476 Freq: 69

Rank: 477 Freq: 69
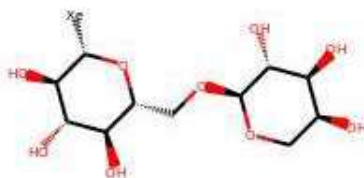
Rank: 478 Freq: 69
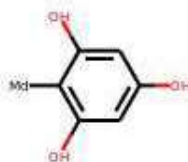
Rank: 479 Freq: 69
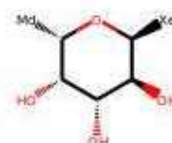
Rank: 480 Freq: 69
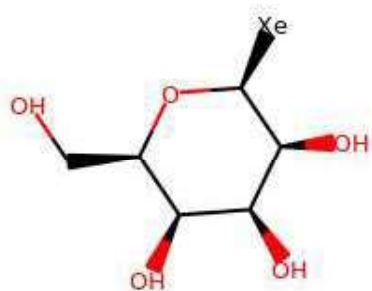
Rank: 481 Freq: 68

Rank: 482 Freq: 67
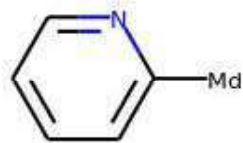
Rank: 483 Freq: 67
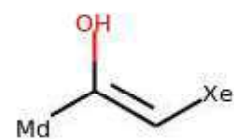
Rank: 484 Freq: 67

Rank: 485 Freq: 67
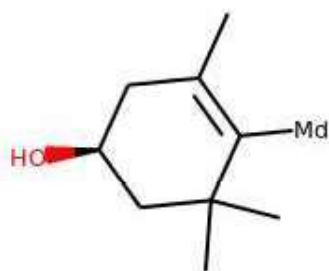
Rank: 486 Freq: 67
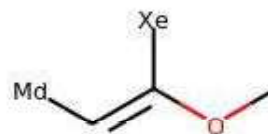
Rank: 487 Freq: 67

Rank: 488 Freq: 67
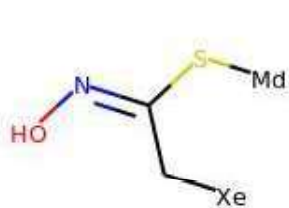
Rank: 489 Freq: 67
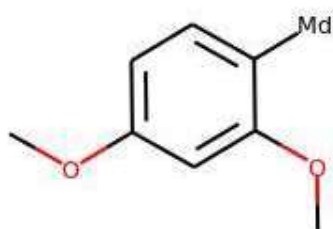
Rank: 490 Freq: 66

Rank: 491 Freq: 66

Rank: 492 Freq: 66
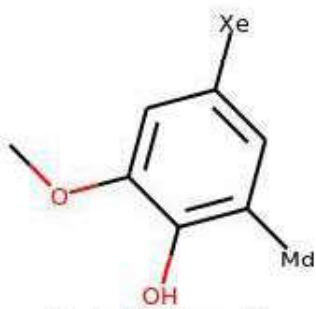
Rank: 493 Freq: 66
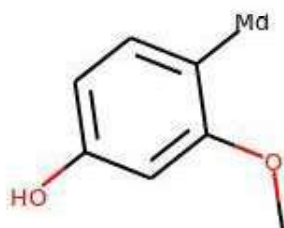
Rank: 494 Freq: 66

Rank: 495 Freq: 66
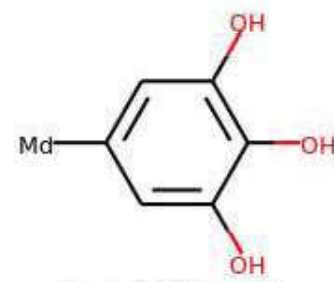
Rank: 496 Freq: 66
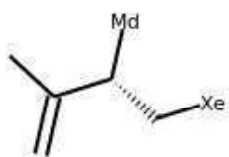
Rank: 497 Freq: 66
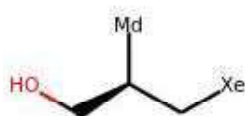
Rank: 498 Freq: 66

Rank: 499 Freq: 65
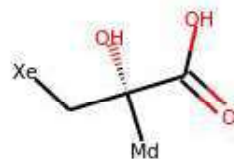
Rank: 500 Freq: 65

Rank: 501 Freq: 65
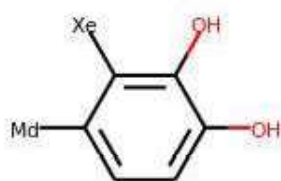
Rank: 502 Freq: 65
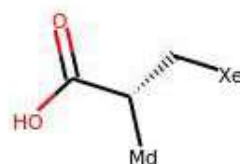
Rank: 503 Freq: 65

Rank: 504 Freq: 64
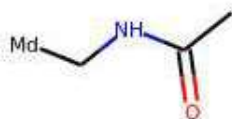
Rank: 505 Freq: 64
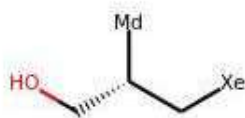
Rank: 506 Freq: 64
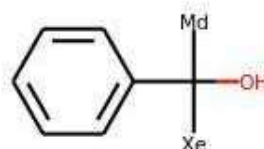
Rank: 507 Freq: 64

Rank: 508 Freq: 64

Rank: 509 Freq: 63
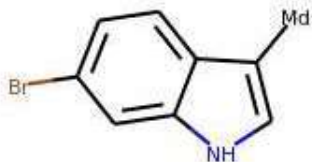
Rank: 510 Freq: 63
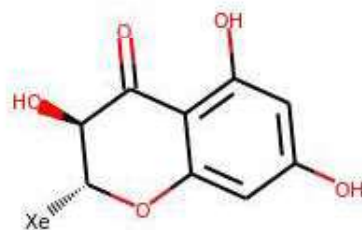
Rank: 511 Freq: 63

Rank: 512 Freq: 63

Rank: 513 Freq: 63

Rank: 514 Freq: 62
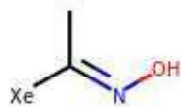
Rank: 515 Freq: 62

Rank: 516 Freq: 62

Rank: 517 Freq: 62
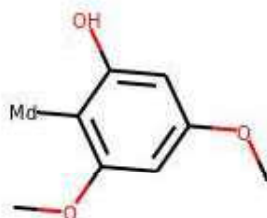
Rank: 518 Freq: 62
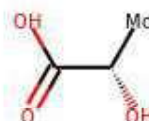
Rank: 519 Freq: 62
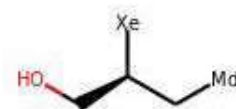
Rank: 520 Freq: 62

Rank: 521 Freq: 62
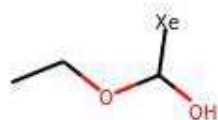
Rank: 522 Freq: 62
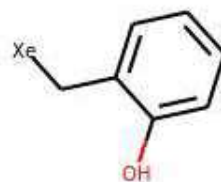
Rank: 523 Freq: 61

Rank: 524 Freq: 61
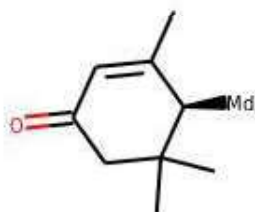
Rank: 525 Freq: 61

Rank: 526 Freq: 61

Rank: 527 Freq: 60

Rank: 528 Freq: 60

Rank: 529 Freq: 60
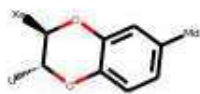
Rank: 530 Freq: 60

Rank: 531 Freq: 60
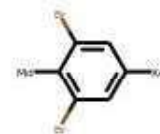
Rank: 532 Freq: 60
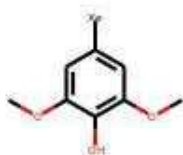
Rank: 533 Freq: 60
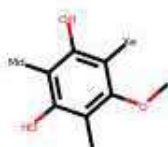
Rank: 534 Freq: 60

Rank: 535 Freq: 60
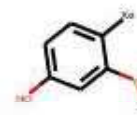
Rank: 536 Freq: 59
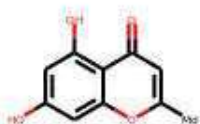
Rank: 537 Freq: 59

Rank: 538 Freq: 59
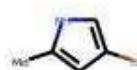
Rank: 539 Freq: 59
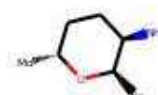
Rank: 540 Freq: 59
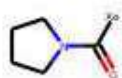
Rank: 541 Freq: 59
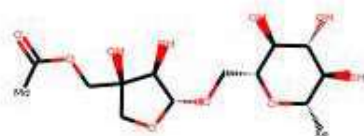
Rank: 542 Freq: 59

Rank: 543 Freq: 58
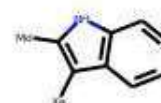
Rank: 544 Freq: 58

Rank: 545 Freq: 58

Rank: 546 Freq: 57

Rank: 547 Freq: 57
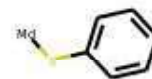
Rank: 548 Freq: 57

Rank: 549 Freq: 57
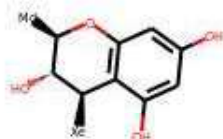
Rank: 550 Freq: 57

Rank: 551 Freq: 57
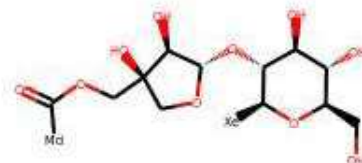
Rank: 552 Freq: 57

Rank: 553 Freq: 57
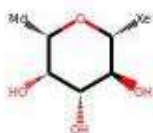
Rank: 554 Freq: 56

Rank: 555 Freq: 56

Rank: 556 Freq: 56

Rank: 557 Freq: 55

Rank: 558 Freq: 55
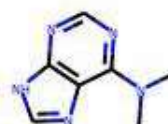
Rank: 559 Freq: 55
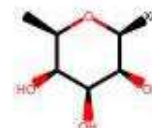
Rank: 560 Freq: 55

Rank: 561 Freq: 55
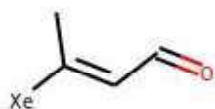
Rank: 562 Freq: 54

Rank: 563 Freq: 54

Rank: 564 Freq: 54
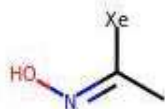
Rank: 565 Freq: 54
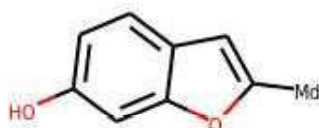
Rank: 566 Freq: 54
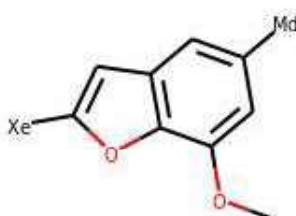
Rank: 567 Freq: 54

Rank: 568 Freq: 54

Rank: 569 Freq: 54
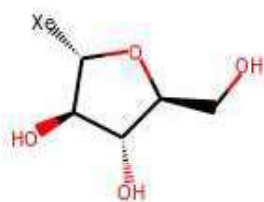
Rank: 570 Freq: 53

Rank: 571 Freq: 53

Rank: 572 Freq: 53

Rank: 573 Freq: 53

Rank: 574 Freq: 53
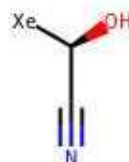
Rank: 575 Freq: 53

Rank: 576 Freq: 53
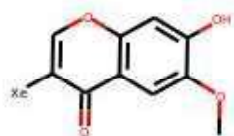
Rank: 577 Freq: 53

Rank: 578 Freq: 53
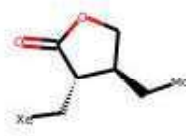
Rank: 579 Freq: 53
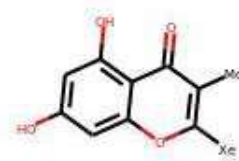
Rank: 580 Freq: 53
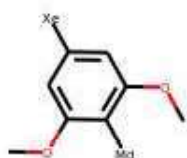
Rank: 581 Freq: 53
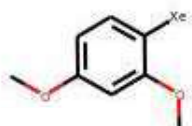
Rank: 582 Freq: 52

Rank: 583 Freq: 52
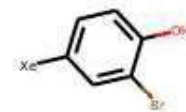
Rank: 584 Freq: 52
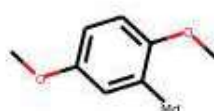
Rank: 585 Freq: 52

Rank: 586 Freq: 52

Rank: 587 Freq: 52
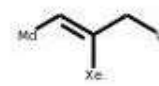
Rank: 588 Freq: 52

Rank: 589 Freq: 52

Rank: 590 Freq: 52
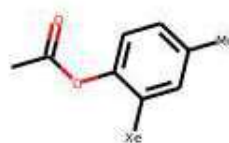
Rank: 591 Freq: 51
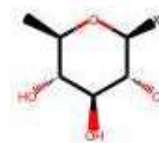
Rank: 592 Freq: 51
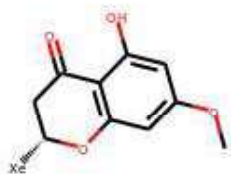
Rank: 593 Freq: 51

Rank: 594 Freq: 51
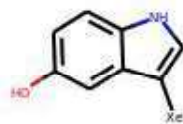
Rank: 595 Freq: 51

Rank: 596 Freq: 51

Rank: 597 Freq: 51
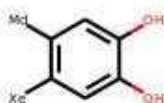
Rank: 598 Freq: 51

Rank: 599 Freq: 51

Rank: 600 Freq: 51

Rank: 601 Freq: 51
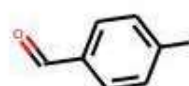
Rank: 602 Freq: 50

Rank: 603 Freq: 50

Rank: 604 Freq: 50

Rank: 605 Freq: 50

Rank: 606 Freq: 50
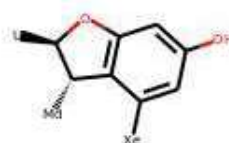
Rank: 607 Freq: 50

Rank: 608 Freq: 49

Rank: 609 Freq: 49
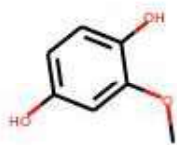

Rank: 610 Freq: 49

Rank: 611 Freq: 49
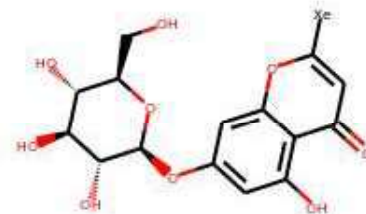
Rank: 612 Freq: 49
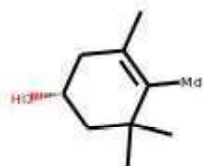
Rank: 614 Freq: 49
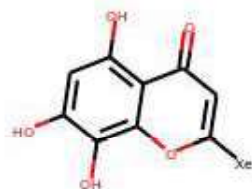
Rank: 615 Freq: 48
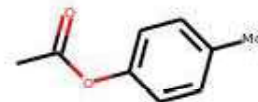
Rank: 616 Freq: 48

Rank: 617 Freq: 48

Rank: 618 Freq: 48

Rank: 619 Freq: 48
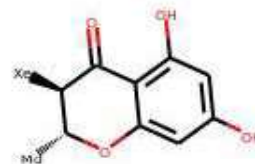
Rank: 620 Freq: 48
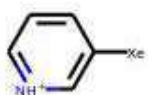
Rank: 621 Freq: 48
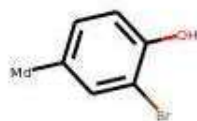
Rank: 622 Freq: 48
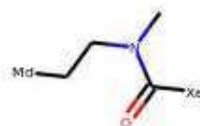
Rank: 623 Freq: 48

Rank: 624 Freq: 48

137
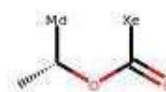
Rank: 625 Freq: 47

Rank: 626 Freq: 47

Rank: 627 Freq: 47
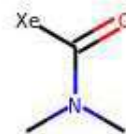
Rank: 628 Freq: 47
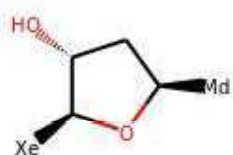
Rank: 629 Freq: 47

Rank: 630 Freq: 47
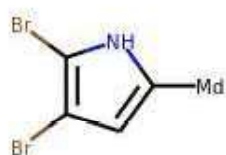
Rank: 631 Freq: 47
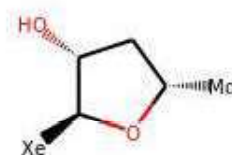
Rank: 632 Freq: 47

Rank: 633 Freq: 47
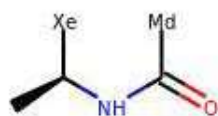
Rank: 634 Freq: 47

Rank: 635 Freq: 46
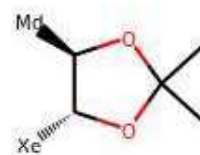
Rank: 636 Freq: 46
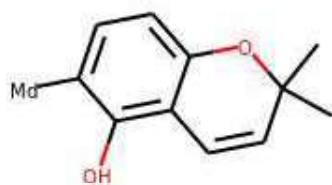
Rank: 637 Freq: 46

Rank: 638 Freq: 46
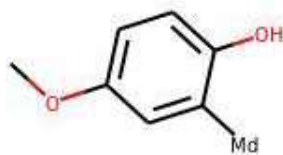
Rank: 639 Freq: 46

Rank: 640 Freq: 46

Rank: 641 Freq: 46

Rank: 642 Freq: 46

Rank: 643 Freq: 46

Rank: 644 Freq: 46
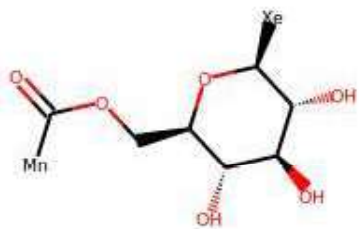
Rank: 645 Freq: 46
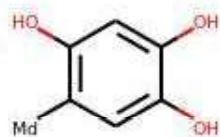
Rank: 646 Freq: 45
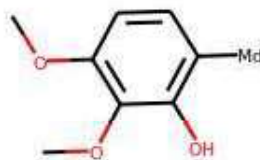
Rank: 647 Freq: 45

Rank: 648 Freq: 45

Rank: 649 Freq: 45
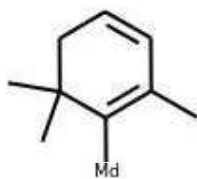
Rank: 650 Freq: 45

Rank: 651 Freq: 45

Rank: 652 Freq: 45

Rank: 653 Freq: 45
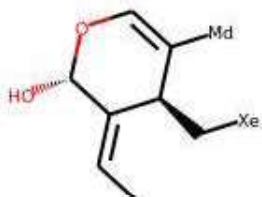
Rank: 654 Freq: 45
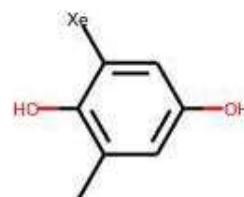
Rank: 655 Freq: 45

Rank: 656 Freq: 45
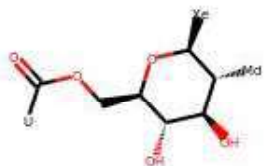
Rank: 657 Freq: 45

Rank: 658 Freq: 44
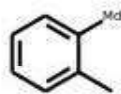
Rank: 659 Freq: 44

Rank: 660 Freq: 44

Rank: 661 Freq: 44

Rank: 662 Freq: 44

Rank: 663 Freq: 44
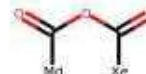
Rank: 664 Freq: 44
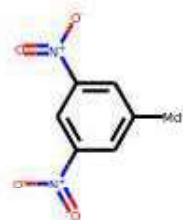
Rank: 665 Freq: 44
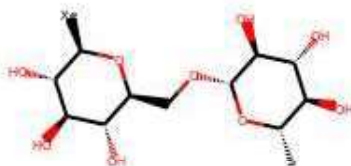
Rank: 666 Freq: 44
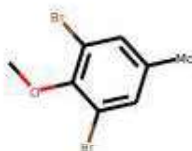
Rank: 667 Freq: 44
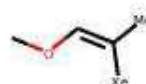
Rank: 668 Freq: 44

Rank: 669 Freq: 44

Rank: 670 Freq: 44
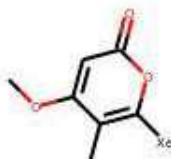
Rank: 671 Freq: 43
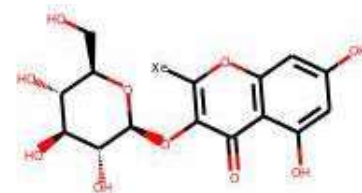
Rank: 672 Freq: 43
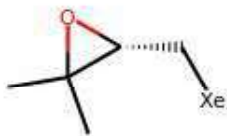
Rank: 673 Freq: 43
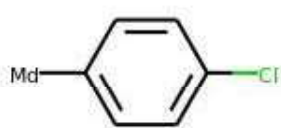
Rank: 674 Freq: 43
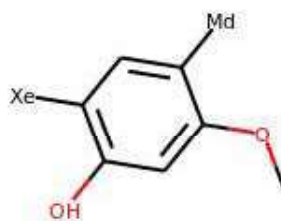
Rank: 675 Freq: 43
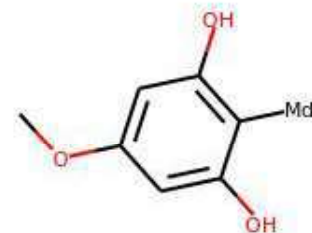
Rank: 676 Freq: 43

Rank: 677 Freq: 43
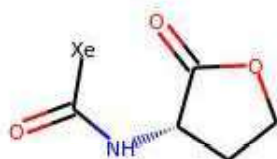
Rank: 678 Freq: 43
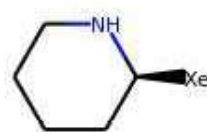
Rank: 679 Freq: 42
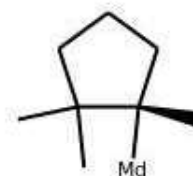
Rank: 680 Freq: 42
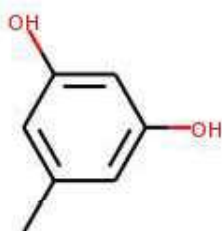
Rank: 681 Freq: 42

Rank: 682 Freq: 42

Rank: 683 Freq: 42

Rank: 684 Freq: 42

Rank: 685 Freq: 42

Rank: 686 Freq: 42
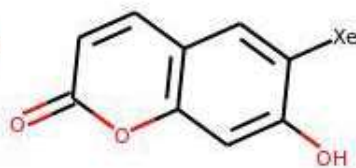
Rank: 687 Freq: 41
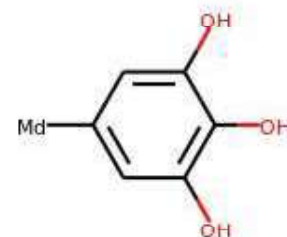
Rank: 688 Freq: 41

Rank: 689 Freq: 41
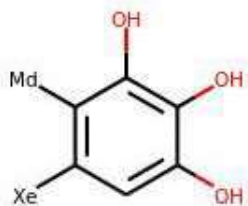
Rank: 690 Freq: 41
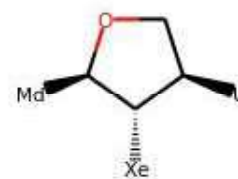
Rank: 692 Freq: 41
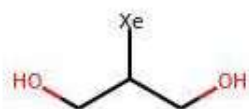
Rank: 693 Freq: 41
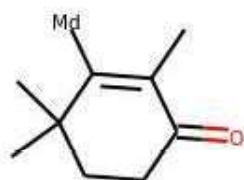
Rank: 694 Freq: 41
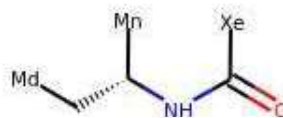
Rank: 695 Freq: 41
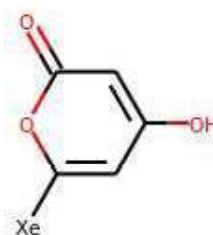
Rank: 696 Freq: 40

Rank: 697 Freq: 40
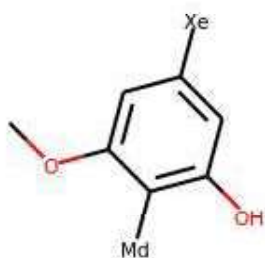
Rank: 698 Freq: 40

Rank: 699 Freq: 40
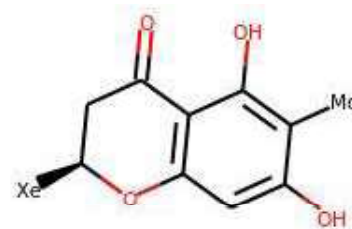
Rank: 700 Freq: 40
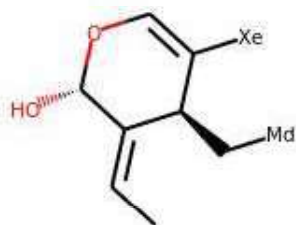
Rank: 701 Freq: 40
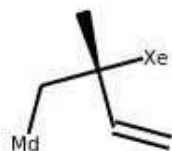
Rank: 702 Freq: 40

Rank: 704 Freq: 39

142
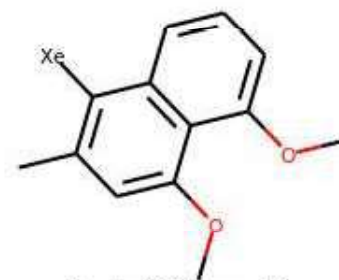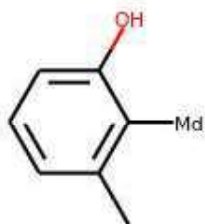
Rank: 705 Freq: 39

Rank: 706 Freq: 39
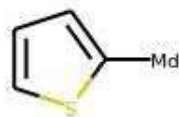
Rank: 707 Freq: 39

Rank: 708 Freq: 39
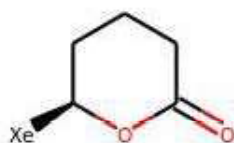
Rank: 709 Freq: 39
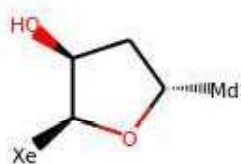
Rank: 710 Freq: 39
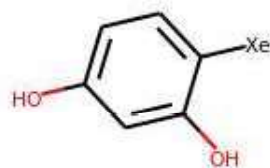
Rank: 711 Freq: 39

Rank: 712 Freq: 39
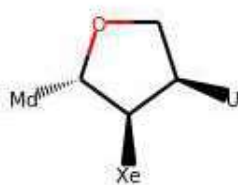
Rank: 713 Freq: 38

Rank: 714 Freq: 38
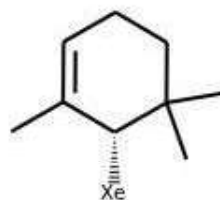
Rank: 715 Freq: 38
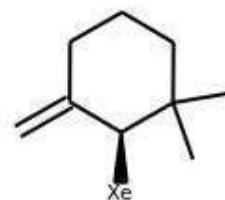
Rank: 716 Freq: 38

Rank: 717 Freq: 38
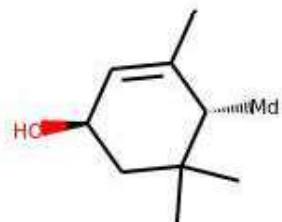
Rank: 718 Freq: 38
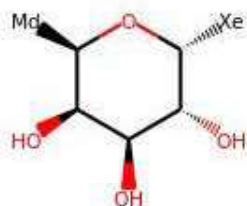
Rank: 719 Freq: 38

Rank: 720 Freq: 38

143

Rank: 721 Freq: 38

Rank: 722 Freq: 38
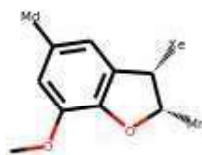
Rank: 723 Freq: 38

Rank: 724 Freq: 38
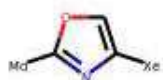
Rank: 725 Freq: 38
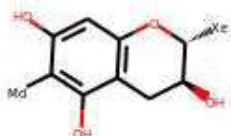
Rank: 726 Freq: 37
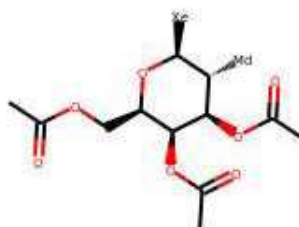
Rank: 727 Freq: 37
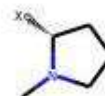
Rank: 728 Freq: 37

Rank: 729 Freq: 37
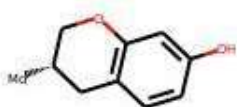
Rank: 730 Freq: 37

Rank: 731 Freq: 37
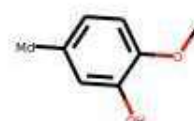
Rank: 732 Freq: 37
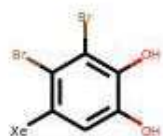
Rank: 733 Freq: 37
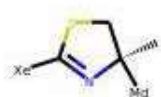
Rank: 734 Freq: 37
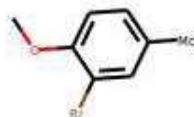
Rank: 735 Freq: 37

Rank: 736 Freq: 37
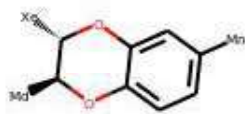
Rank: 737 Freq: 37

Rank: 738 Freq: 37
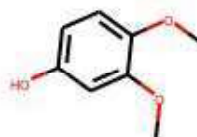
Rank: 739 Freq: 37
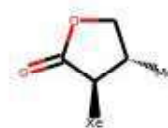
Rank: 740 Freq: 37

Rank: 741 Freq: 37

Rank: 742 Freq: 37
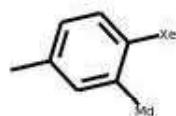
Rank: 743 Freq: 37
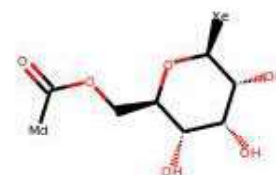
Rank: 744 Freq: 37
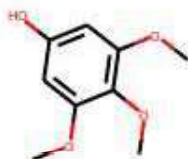
Rank: 745 Freq: 36

Rank: 746 Freq: 36

Rank: 747 Freq: 36

Rank: 748 Freq: 36

Rank: 749 Freq: 36

Rank: 750 Freq: 36

Rank: 751 Freq: 36

Rank: 752 Freq: 36
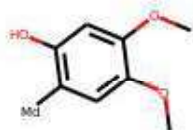
Rank: 753 Freq: 36

Rank: 754 Freq: 36
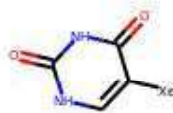
Rank: 755 Freq: 36

Rank: 756 Freq: 36
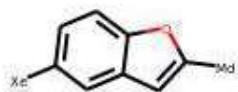
Rank: 757 Freq: 36

Rank: 758 Freq: 36
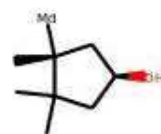
Rank: 759 Freq: 36

Rank: 760 Freq: 36

Rank: 761 Freq: 36
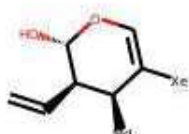
Rank: 762 Freq: 36
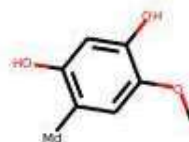
Rank: 763 Freq: 35

Rank: 764 Freq: 35
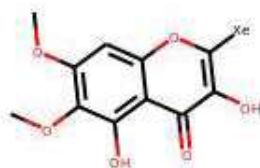
Rank: 765 Freq: 35

Rank: 766 Freq: 35

Rank: 767 Freq: 35
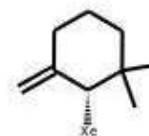
Rank: 768 Freq: 35

Rank: 769 Freq: 35
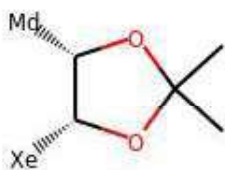
Rank: 770 Freq: 35

Rank: 771 Freq: 35

Rank: 772 Freq: 35
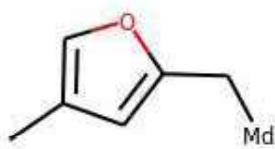
Rank: 773 Freq: 35

Rank: 774 Freq: 35
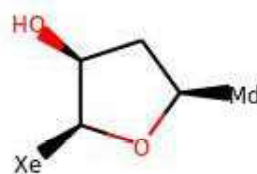
Rank: 775 Freq: 35
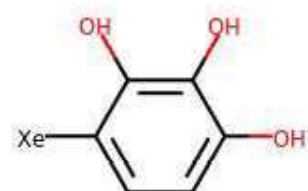
Rank: 776 Freq: 35
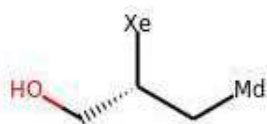
Rank: 777 Freq: 35

Rank: 778 Freq: 35
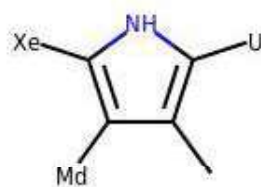
Rank: 779 Freq: 35

Rank: 780 Freq: 34
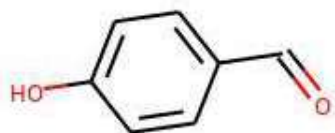
Rank: 781 Freq: 34

Rank: 782 Freq: 34

Rank: 783 Freq: 34

Rank: 784 Freq: 34

147
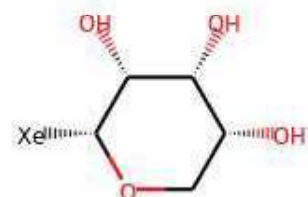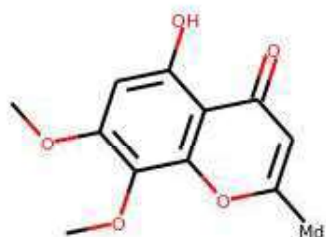
Rank: 785 Freq: 34

Rank: 786 Freq: 34

Rank: 787 Freq: 34

Rank: 788 Freq: 34
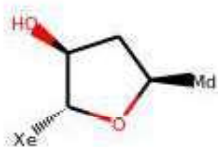
Rank: 789 Freq: 34
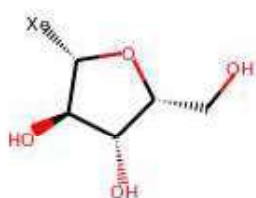
Rank: 790 Freq: 34
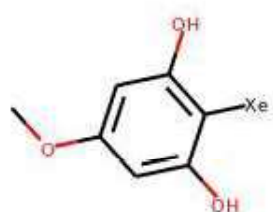
Rank: 791 Freq: 34
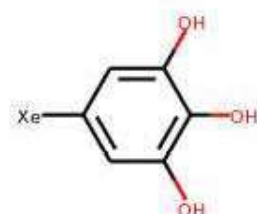
Rank: 792 Freq: 34
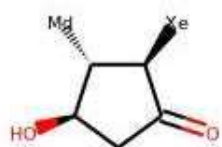
Rank: 793 Freq: 34

Rank: 794 Freq: 34
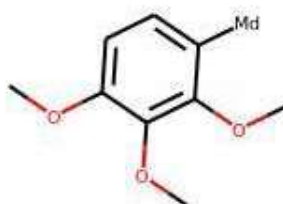
Rank: 795 Freq: 33

Rank: 796 Freq: 33
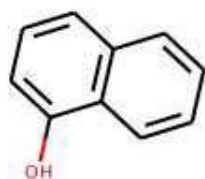
Rank: 797 Freq: 33
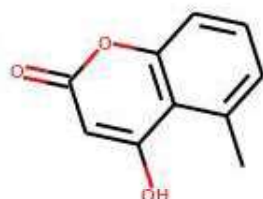
Rank: 798 Freq: 33

Rank: 799 Freq: 33
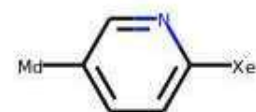
Rank: 800 Freq: 33
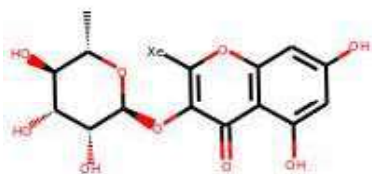
Rank: 801 Freq: 33

Rank: 802 Freq: 33
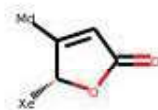
Rank: 803 Freq: 33

Rank: 804 Freq: 33
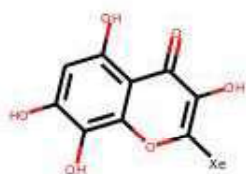
Rank: 805 Freq: 32

Rank: 806 Freq: 32

Rank: 807 Freq: 32

Rank: 808 Freq: 32
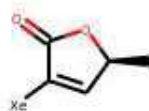
Rank: 809 Freq: 32
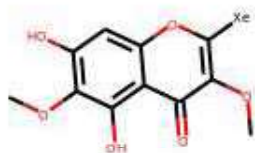
Rank: 810 Freq: 32
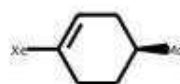
Rank: 811 Freq: 32
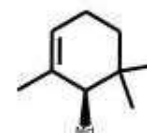
Rank: 812 Freq: 32

Rank: 813 Freq: 32
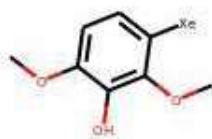
Rank: 814 Freq: 32
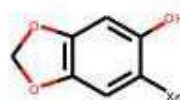
Rank: 815 Freq: 32

Rank: 816 Freq: 32

Rank: 817 Freq: 32
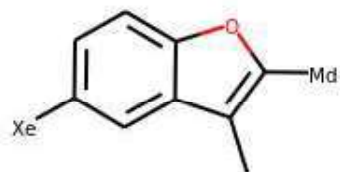
Rank: 818 Freq: 32

Rank: 819 Freq: 32
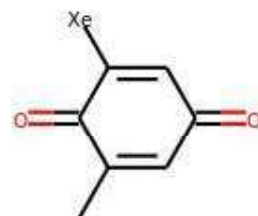
Rank: 820 Freq: 32

Rank: 821 Freq: 32

Rank: 822 Freq: 32

Rank: 823 Freq: 31

Rank: 824 Freq: 31

Rank: 825 Freq: 31
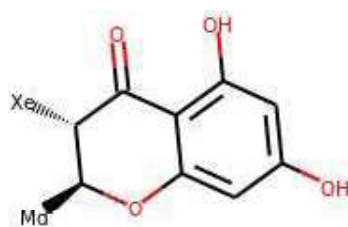
Rank: 826 Freq: 31
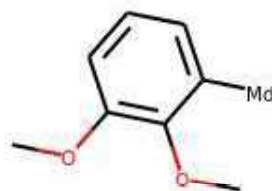
Rank: 827 Freq: 31

Rank: 828 Freq: 31

Rank: 829 Freq: 31
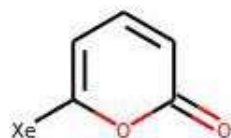
Rank: 830 Freq: 31
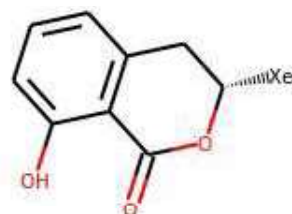
Rank: 831 Freq: 31
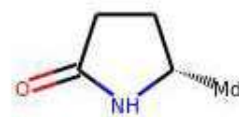
Rank: 832 Freq: 31
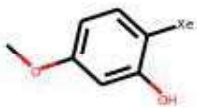
Rank: 833 Freq: 31
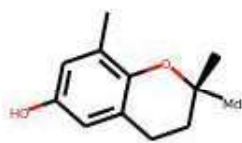
Rank: 834 Freq: 31

Rank: 835 Freq: 31

Rank: 836 Freq: 30
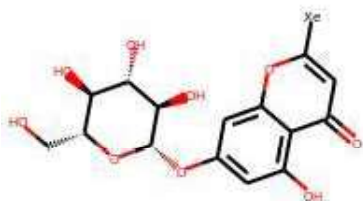
Rank: 837 Freq: 30

Rank: 838 Freq: 30

Rank: 839 Freq: 30
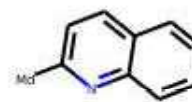
Rank: 840 Freq: 30
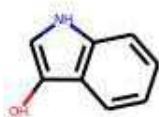
Rank: 841 Freq: 30

Rank: 842 Freq: 30

Rank: 843 Freq: 30
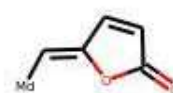
Rank: 844 Freq: 30
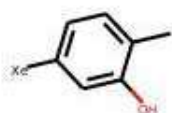
Rank: 845 Freq: 30
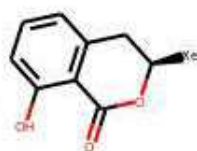
Rank: 846 Freq: 30

Rank: 847 Freq: 30

Rank: 848 Freq: 30

151
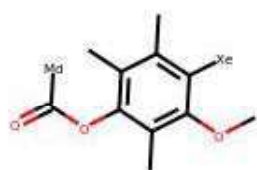
Rank: 849 Freq: 30

Rank: 850 Freq: 30
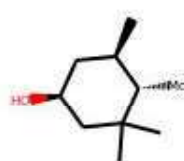
Rank: 851 Freq: 30

Rank: 852 Freq: 30
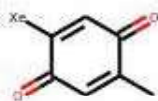
Rank: 853 Freq: 29

Rank: 854 Freq: 29
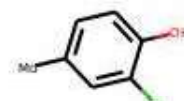
Rank: 855 Freq: 29

Rank: 857 Freq: 29

Rank: 858 Freq: 29

Rank: 859 Freq: 29

Rank: 860 Freq: 29
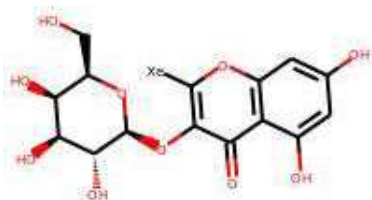
Rank: 861 Freq: 29
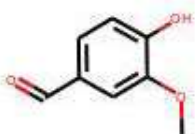
Rank: 862 Freq: 29
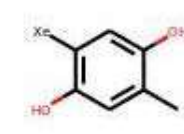
Rank: 863 Freq: 29
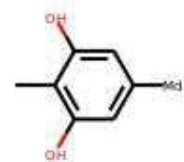
Rank: 864 Freq: 29
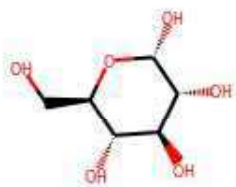
Rank: 865 Freq: 29

Rank: 866 Freq: 29
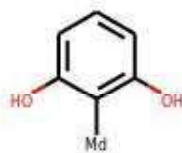
Rank: 867 Freq: 29

Rank: 868 Freq: 29
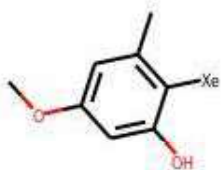
Rank: 869 Freq: 29

Rank: 870 Freq: 29
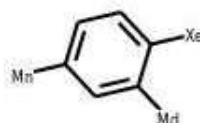
Rank: 871 Freq: 29
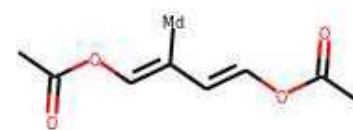
Rank: 872 Freq: 29

Rank: 873 Freq: 29

Rank: 874 Freq: 29

Rank: 875 Freq: 29
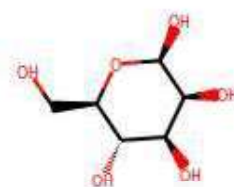
Rank: 876 Freq: 28

Rank: 877 Freq: 28
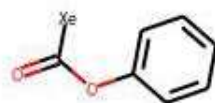
Rank: 878 Freq: 28
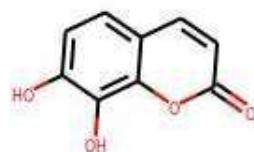
Rank: 879 Freq: 28

Rank: 880 Freq: 28

Rank: 881 Freq: 28

Rank: 882 Freq: 28
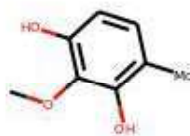
Rank: 883 Freq: 28

Rank: 884 Freq: 28
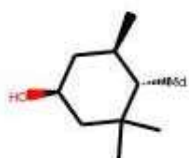
Rank: 885 Freq: 28
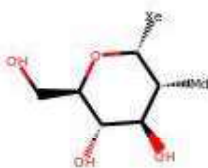
Rank: 886 Freq: 28
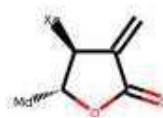
Rank: 887 Freq: 28

Rank: 888 Freq: 28
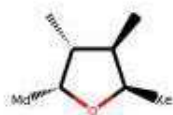
Rank: 889 Freq: 28
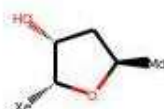
Rank: 890 Freq: 28
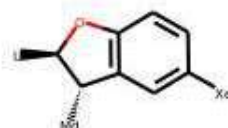
Rank: 891 Freq: 28

Rank: 892 Freq: 28
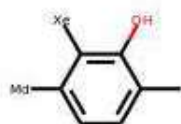
Rank: 893 Freq: 28
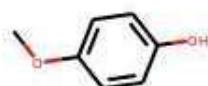
Rank: 894 Freq: 27
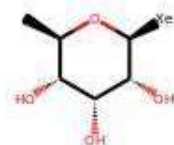
Rank: 895 Freq: 27
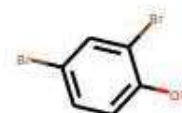
Rank: 896 Freq: 27

Rank: 897 Freq: 27
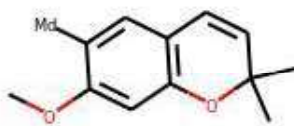
Rank: 898 Freq: 27

Rank: 899 Freq: 27

Rank: 900 Freq: 27
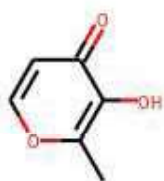
Rank: 901 Freq: 27
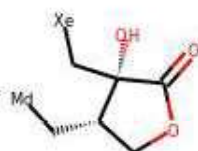
Rank: 902 Freq: 27

Rank: 903 Freq: 27
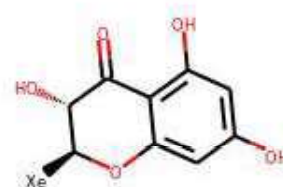
Rank: 904 Freq: 27
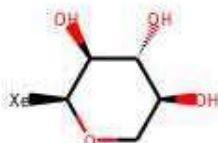
Rank: 905 Freq: 27
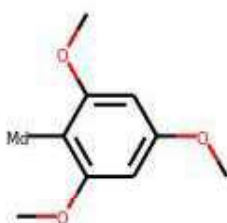
Rank: 906 Freq: 27
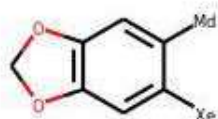
Rank: 907 Freq: 27
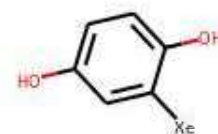
Rank: 908 Freq: 27
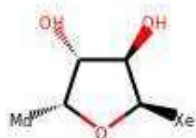
Rank: 909 Freq: 27
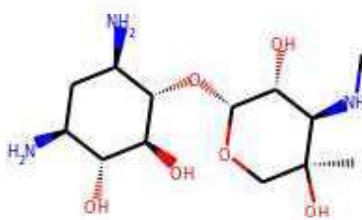
Rank: 910 Freq: 27

Rank: 911 Freq: 27

Rank: 912 Freq: 27

155
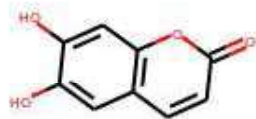
Rank: 913 Freq: 27

Rank: 914 Freq: 26

Rank: 915 Freq: 26

Rank: 916 Freq: 26



Rank: 917 Freq: 26
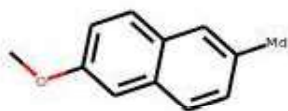

Rank: 918 Freq: 26
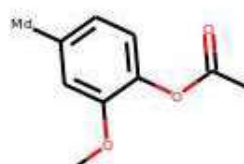
Rank: 919 Freq: 26
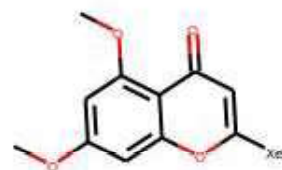
Rank: 920 Freq: 26

Rank: 921 Freq: 26

Rank: 922 Freq: 26
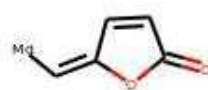
Rank: 923 Freq: 26

Rank: 924 Freq: 26
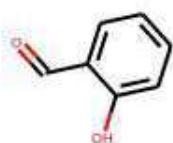
Rank: 925 Freq: 26
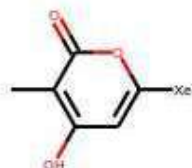
Rank: 926 Freq: 26
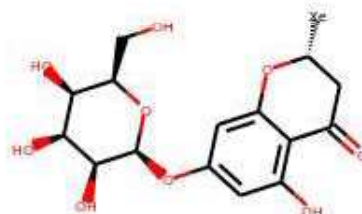
Rank: 927 Freq: 26

Rank: 928 Freq: 26

Rank: 929 Freq: 26

Rank: 930 Freq: 26

Rank: 931 Freq: 26

Rank: 932 Freq: 26
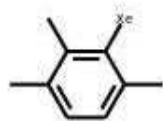
Rank: 933 Freq: 26
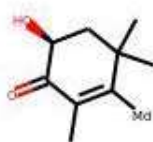
Rank: 934 Freq: 26

Rank: 935 Freq: 26
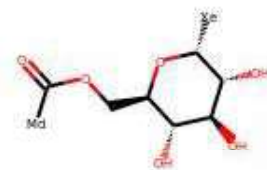
Rank: 936 Freq: 26
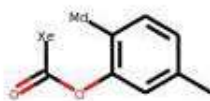
Rank: 937 Freq: 26
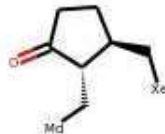
Rank: 938 Freq: 26


Rank: 939 Freq: 26
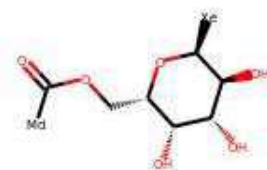
Rank: 940 Freq: 26
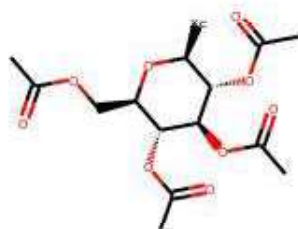
Rank: 941 Freq: 25

Rank: 942 Freq: 25
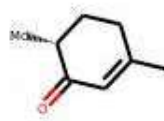
Rank: 943 Freq: 25
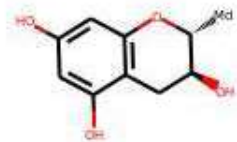
Rank: 944 Freq: 25

Rank: 945 Freq: 25
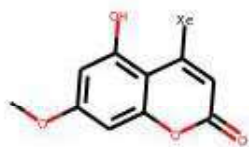
Rank: 946 Freq: 25

Rank: 947 Freq: 25
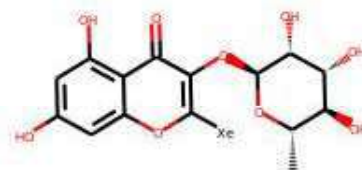
Rank: 948 Freq: 25

Rank: 949 Freq: 25

Rank: 950 Freq: 25
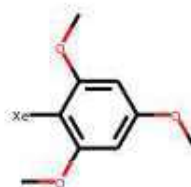
Rank: 951 Freq: 25

Rank: 952 Freq: 25
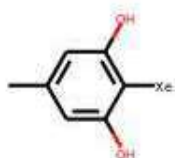
Rank: 953 Freq: 25
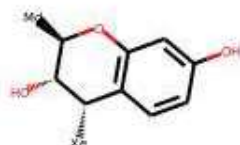
Rank: 954 Freq: 25

Rank: 955 Freq: 25

Rank: 956 Freq: 25

Rank: 957 Freq: 25
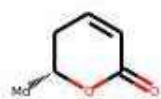
Rank: 958 Freq: 25
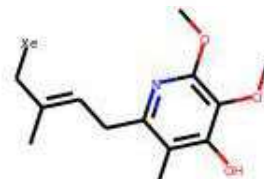
Rank: 959 Freq: 25
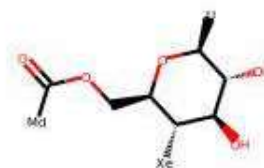
Rank: 960 Freq: 25

Rank: 961 Freq: 25

Rank: 962 Freq: 24
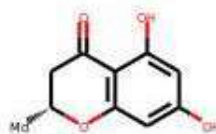
Rank: 963 Freq: 24
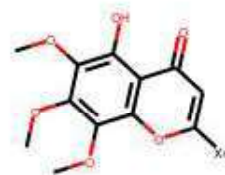
Rank: 964 Freq: 24

Rank: 965 Freq: 24
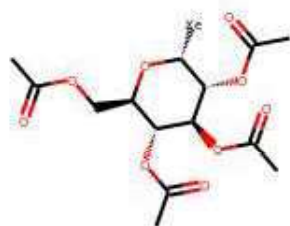
Rank: 966 Freq: 24
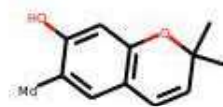
Rank: 967 Freq: 24
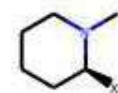
Rank: 968 Freq: 24
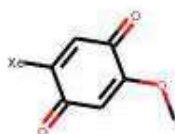
Rank: 969 Freq: 24

Rank: 970 Freq: 24
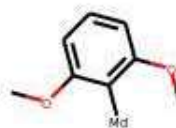
Rank: 971 Freq: 24

Rank: 972 Freq: 24

Rank: 973 Freq: 24
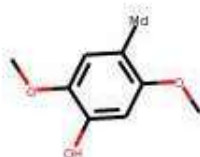
Rank: 974 Freq: 24
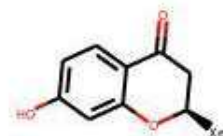
Rank: 975 Freq: 24

Rank: 976 Freq: 24
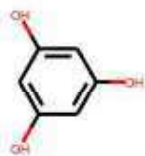
Rank: 977 Freq: 24
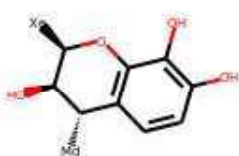
Rank: 978 Freq: 24
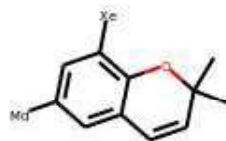
Rank: 979 Freq: 24
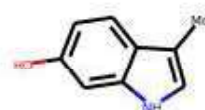
Rank: 980 Freq: 24
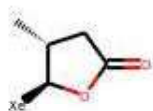
Rank: 981 Freq: 24
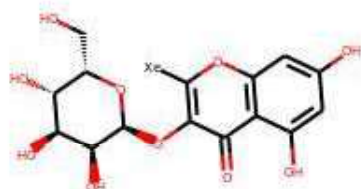
Rank: 982 Freq: 24

Rank: 983 Freq: 24

Rank: 984 Freq: 24

Rank: 985 Freq: 24

Rank: 986 Freq: 24
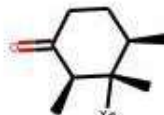
Rank: 987 Freq: 24
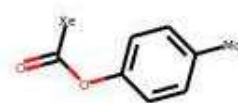
Rank: 988 Freq: 24

Rank: 989 Freq: 23
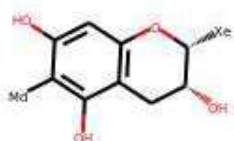
Rank: 990 Freq: 23

Rank: 991 Freq: 23

Rank: 992 Freq: 23

160
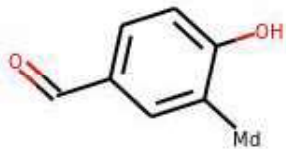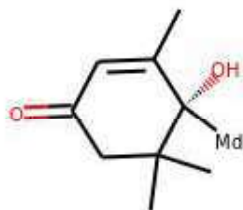
Rank: 993 Freq: 23

Rank: 994 Freq: 23

Rank: 995 Freq: 23
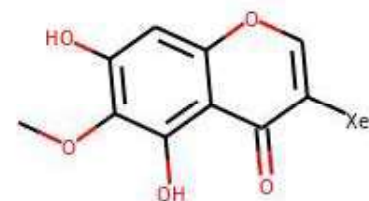
Rank: 996 Freq: 23
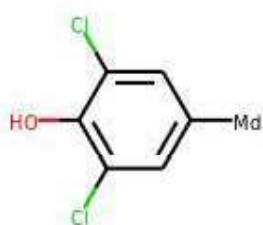
Rank: 997 Freq: 23

Rank: 998 Freq: 23

Rank: 999 Freq: 23

Rank: 1000 Freq: 23
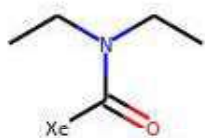
Rank: 1001 Freq: 23

Rank: 1002 Freq: 23
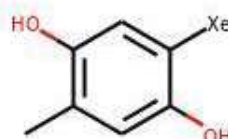
Rank: 1003 Freq: 23

Rank: 1004 Freq: 23
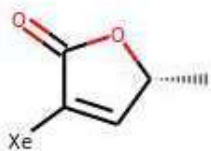
Rank: 1005 Freq: 23

Rank: 1006 Freq: 23

Rank: 1007 Freq: 23
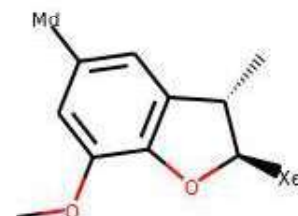
Rank: 1008 Freq: 23

Rank: 1009 Freq: 23

Rank: 1010 Freq: 23

Rank: 1011 Freq: 23

Rank: 1012 Freq: 23
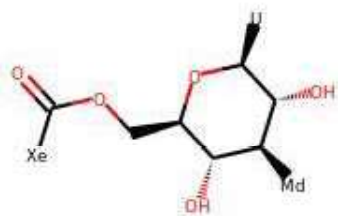
Rank: 1013 Freq: 23

Rank: 1014 Freq: 23
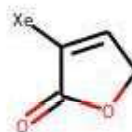
Rank: 1015 Freq: 22
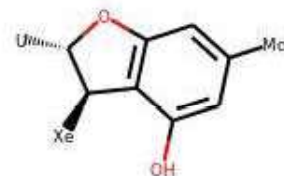
Rank: 1016 Freq: 22
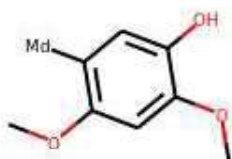
Rank: 1017 Freq: 22
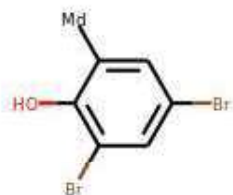
Rank: 1018 Freq: 22

Rank: 1019 Freq: 22

Rank: 1020 Freq: 22

Rank: 1021 Freq: 22

Rank: 1022 Freq: 22
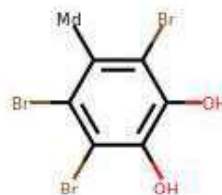
Rank: 1023 Freq: 22

Rank: 1024 Freq: 22
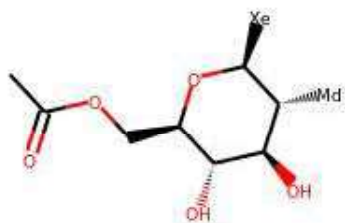
Rank: 1025 Freq: 22

Rank: 1026 Freq: 22

Rank: 1027 Freq: 22
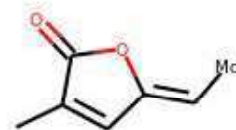
Rank: 1028 Freq: 22

Rank: 1029 Freq: 22
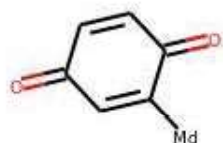
Rank: 1030 Freq: 22
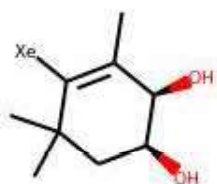
Rank: 1031 Freq: 22
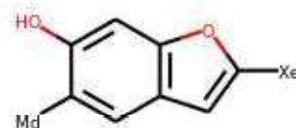
Rank: 1032 Freq: 22

Rank: 1033 Freq: 22

Rank: 1034 Freq: 22

Rank: 1035 Freq: 21
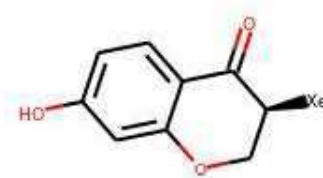
Rank: 1036 Freq: 21
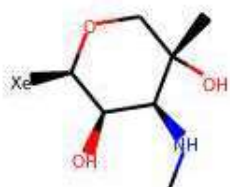
Rank: 1037 Freq: 21

Rank: 1038 Freq: 21
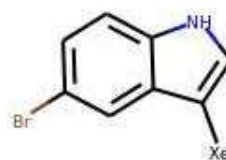
Rank: 1039 Freq: 21

Rank: 1040 Freq: 21
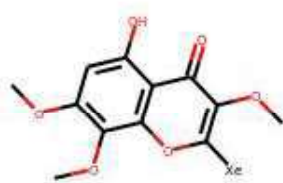
Rank: 1041 Freq: 21

Rank: 1042 Freq: 21
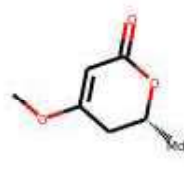
Rank: 1043 Freq: 21

Rank: 1044 Freq: 21

Rank: 1045 Freq: 21
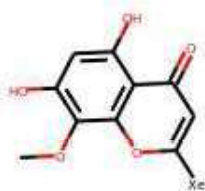
Rank: 1046 Freq: 21
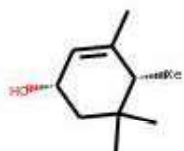
Rank: 1047 Freq: 21
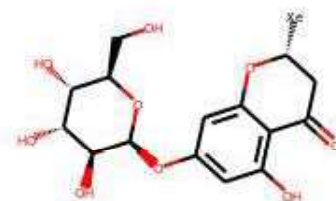
Rank: 1048 Freq: 21

Rank: 1049 Freq: 21

Rank: 1050 Freq: 21

Rank: 1051 Freq: 21
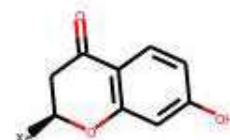
Rank: 1052 Freq: 21
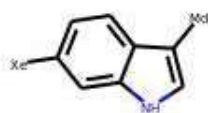
Rank: 1053 Freq: 21
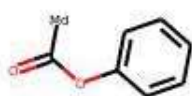
Rank: 1054 Freq: 21

Rank: 1055 Freq: 21

Rank: 1056 Freq: 21

164
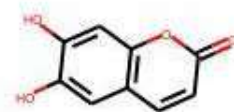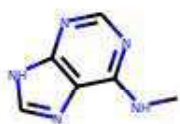
Rank: 1057 Freq: 21

Rank: 1058 Freq: 21
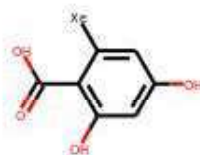
Rank: 1059 Freq: 21
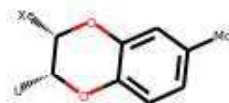
Rank: 1060 Freq: 21

Rank: 1061 Freq: 21
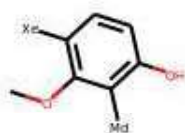
Rank: 1062 Freq: 21
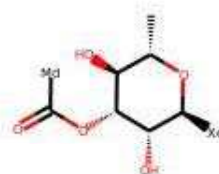
Rank: 1063 Freq: 21
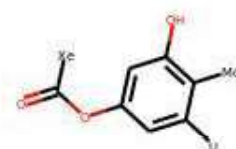
Rank: 1064 Freq: 21
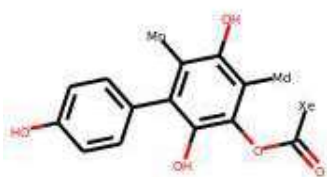
Rank: 1065 Freq: 21

Rank: 1066 Freq: 20

Rank: 1067 Freq: 20
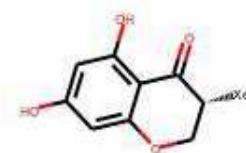
Rank: 1068 Freq: 20

Rank: 1069 Freq: 20
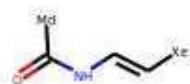
Rank: 1070 Freq: 20
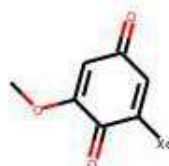
Rank: 1071 Freq: 20
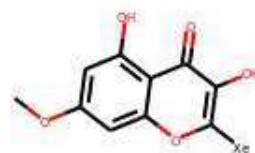
Rank: 1072 Freq: 20

Rank: 1073 Freq: 20

Rank: 1074 Freq: 20
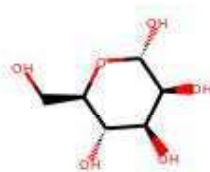
Rank: 1075 Freq: 20
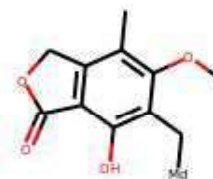
Rank: 1076 Freq: 20

Rank: 1077 Freq: 20

Rank: 1078 Freq: 20

Rank: 1079 Freq: 20
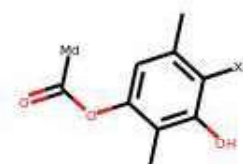
Rank: 1080 Freq: 20
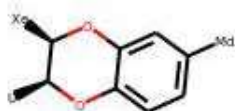
Rank: 1081 Freq: 20

Rank: 1082 Freq: 20

Rank: 1083 Freq: 20

Rank: 1084 Freq: 20
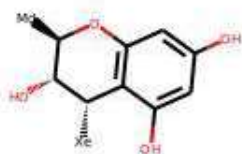
Rank: 1085 Freq: 20

Rank: 1086 Freq: 20

Rank: 1087 Freq: 20
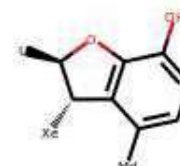
Rank: 1088 Freq: 20
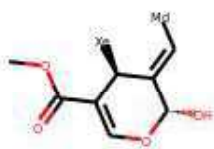
Rank: 1089 Freq: 20
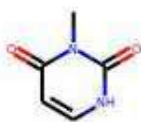
Rank: 1090 Freq: 19
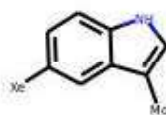
Rank: 1091 Freq: 19

Rank: 1092 Freq: 19
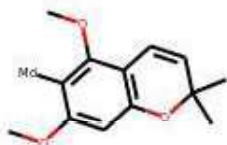
Rank: 1093 Freq: 19
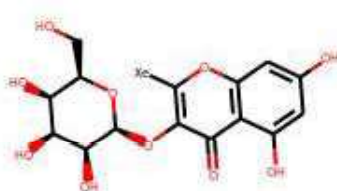
Rank: 1094 Freq: 19
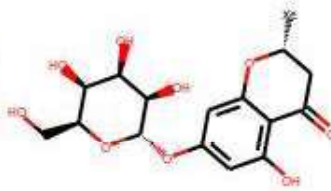
Rank: 1095 Freq: 19

Rank: 1096 Freq: 19
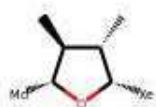
Rank: 1097 Freq: 19

Rank: 1098 Freq: 19

Rank: 1099 Freq: 19
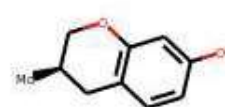
Rank: 1100 Freq: 19

Rank: 1101 Freq: 19
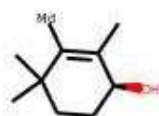
Rank: 1102 Freq: 19
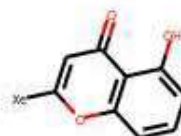
Rank: 1103 Freq: 19

Rank: 1104 Freq: 19

Rank: 1105 Freq: 19
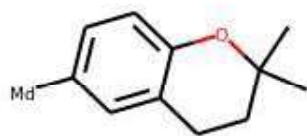
Rank: 1106 Freq: 19
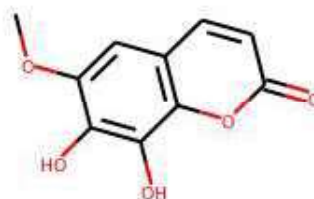
Rank: 1107 Freq: 19

Rank: 1108 Freq: 19

Rank: 1109 Freq: 19

Rank: 1110 Freq: 19
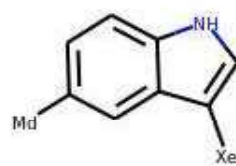
Rank: 1111 Freq: 19

Rank: 1112 Freq: 19
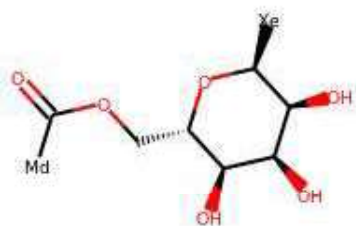
Rank: 1113 Freq: 19

Rank: 1114 Freq: 19

Rank: 1115 Freq: 19

Rank: 1116 Freq: 19

Rank: 1117 Freq: 18

Rank: 1118 Freq: 18

Rank: 1119 Freq: 18

Rank: 1120 Freq: 18

Rank: 1121 Freq: 18
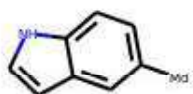
Rank: 1122 Freq: 18
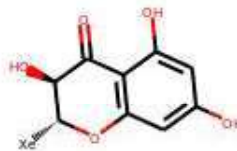
Rank: 1123 Freq: 18

Rank: 1124 Freq: 18

Rank: 1125 Freq: 18

Rank: 1126 Freq: 18
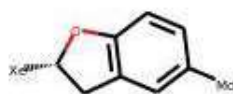
Rank: 1127 Freq: 18

Rank: 1128 Freq: 18

Rank: 1129 Freq: 18
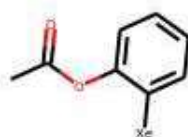
Rank: 1130 Freq: 18
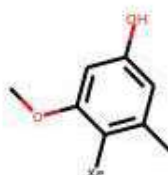
Rank: 1131 Freq: 18

Rank: 1132 Freq: 18
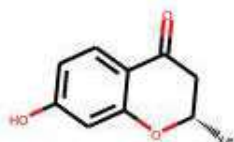
Rank: 1133 Freq: 18
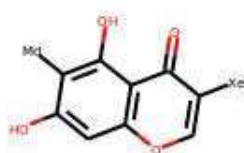
Rank: 1134 Freq: 18

Rank: 1135 Freq: 18
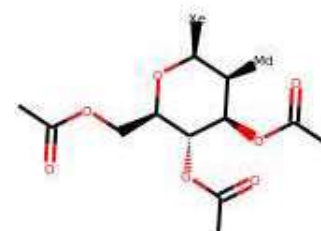
Rank: 1136 Freq: 18

Rank: 1137 Freq: 18

Rank: 1138 Freq: 18

Rank: 1139 Freq: 18
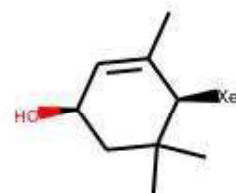
Rank: 1140 Freq: 18

Rank: 1141 Freq: 18

Rank: 1142 Freq: 18

Rank: 1143 Freq: 18
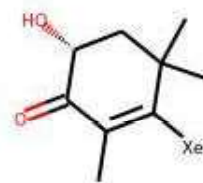
Rank: 1144 Freq: 18
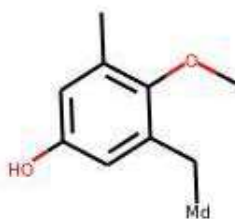
Rank: 1145 Freq: 18
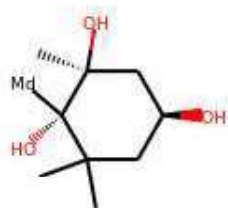
Rank: 1146 Freq: 18

Rank: 1147 Freq: 18
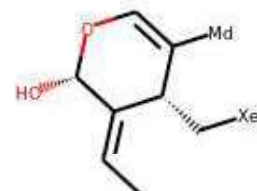
Rank: 1148 Freq: 18
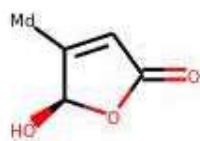
Rank: 1149 Freq: 18
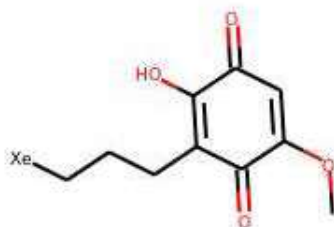
Rank: 1150 Freq: 18

Rank: 1151 Freq: 17
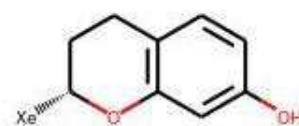
Rank: 1152 Freq: 17

Rank: 1153 Freq: 17

Rank: 1154 Freq: 17

Rank: 1155 Freq: 17
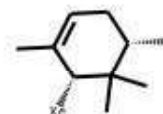
Rank: 1156 Freq: 17
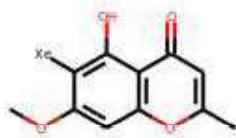
Rank: 1157 Freq: 17
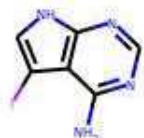
Rank: 1158 Freq: 17
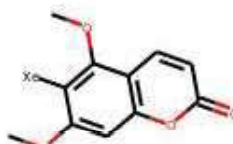
Rank: 1159 Freq: 17

Rank: 1160 Freq: 17
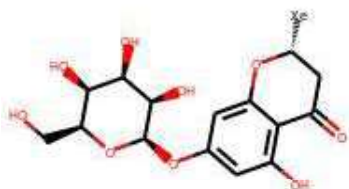
Rank: 1161 Freq: 17
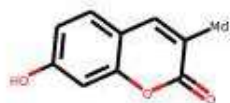
Rank: 1162 Freq: 17

Rank: 1163 Freq: 17

Rank: 1164 Freq: 17

Rank: 1165 Freq: 17

Rank: 1166 Freq: 17

Rank: 1167 Freq: 17

Rank: 1168 Freq: 17

Rank: 1169 Freq: 17
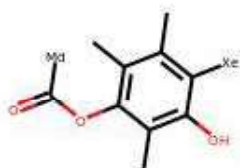
Rank: 1170 Freq: 17

Rank: 1171 Freq: 17
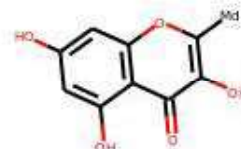
Rank: 1172 Freq: 17
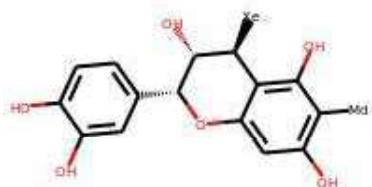
Rank: 1173 Freq: 17
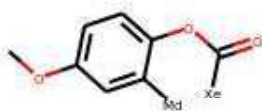
Rank: 1174 Freq: 17
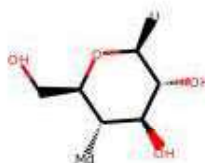
Rank: 1175 Freq: 17

Rank: 1176 Freq: 17

Rank: 1177 Freq: 16
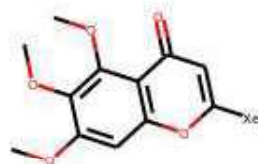
Rank: 1178 Freq: 16
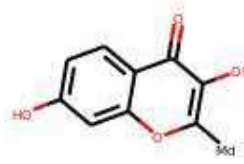

Rank: 1179 Freq: 16

Rank: 1180 Freq: 16

Rank: 1181 Freq: 16
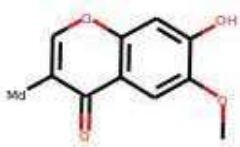
Rank: 1182 Freq: 16

Rank: 1183 Freq: 16
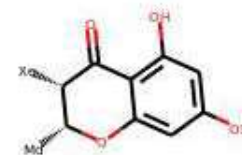
Rank: 1184 Freq: 16
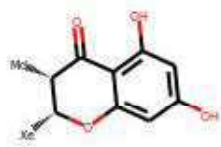
Rank: 1185 Freq: 16


Rank: 1186 Freq: 16

Rank: 1187 Freq: 16
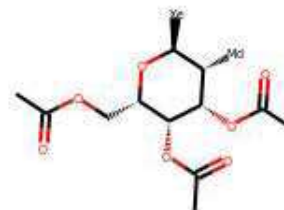

Rank: 1188 Freq: 16
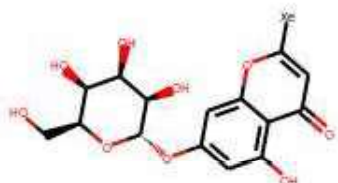
Rank: 1189 Freq: 16
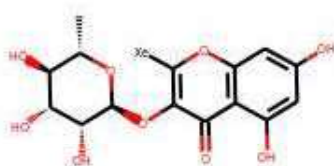
Rank: 1190 Freq: 16


Rank: 1191 Freq: 16

Rank: 1192 Freq: 16
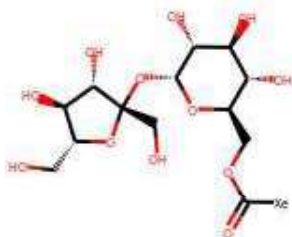
Rank: 1193 Freq: 16

Rank: 1194 Freq: 16
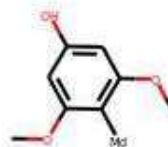
Rank: 1195 Freq: 16
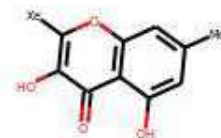
Rank: 1196 Freq: 16

Rank: 1197 Freq: 16

Rank: 1198 Freq: 16

Rank: 1199 Freq: 16
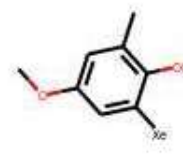
Rank: 1200 Freq: 16

Rank: 1201 Freq: 15
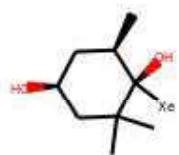
Rank: 1202 Freq: 15

Rank: 1203 Freq: 15
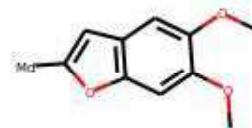
Rank: 1204 Freq: 15
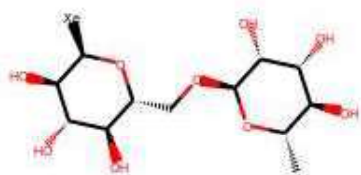
Rank: 1205 Freq: 15

Rank: 1206 Freq: 15
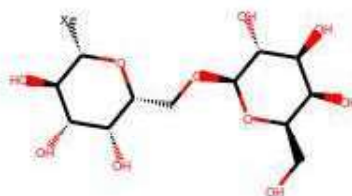
Rank: 1207 Freq: 15

Rank: 1208 Freq: 15

Rank: 1209 Freq: 15

Rank: 1210 Freq: 15

Rank: 1211 Freq: 15

Rank: 1212 Freq: 15
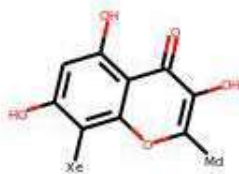
Rank: 1213 Freq: 15

Rank: 1214 Freq: 15

Rank: 1215 Freq: 15

Rank: 1216 Freq: 15

174
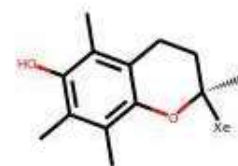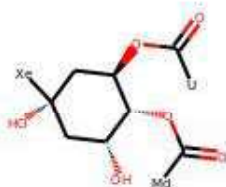
Rank: 1217 Freq: 15

Rank: 1218 Freq: 15

Rank: 1219 Freq: 15
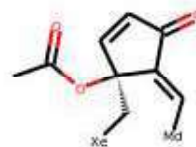
Rank: 1220 Freq: 15
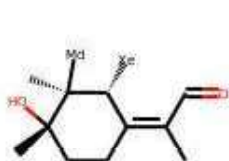
Rank: 1221 Freq: 15

Rank: 1222 Freq: 14
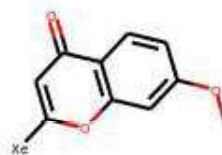
Rank: 1223 Freq: 14
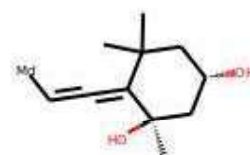
Rank: 1224 Freq: 14
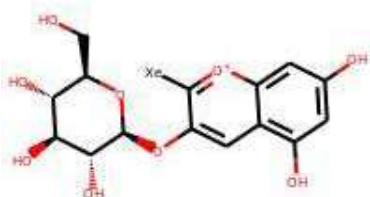
Rank: 1225 Freq: 14

Rank: 1226 Freq: 14
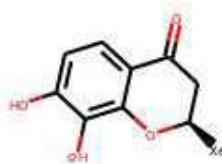
Rank: 1227 Freq: 14

Rank: 1228 Freq: 14

Rank: 1229 Freq: 14
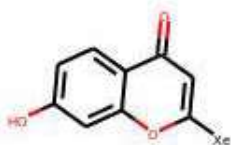

Rank: 1230 Freq: 14
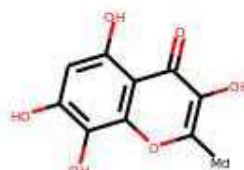
Rank: 1231 Freq: 14

Rank: 1232 Freq: 14

Rank: 1233 Freq: 14
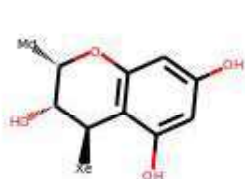
Rank: 1234 Freq: 14
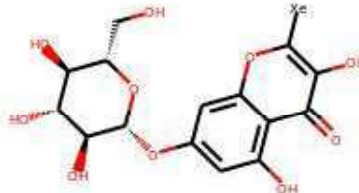
Rank: 1235 Freq: 14

Rank: 1236 Freq: 14

Rank: 1237 Freq: 14
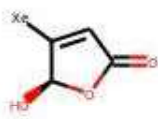
Rank: 1238 Freq: 14
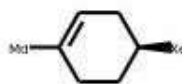
Rank: 1239 Freq: 14
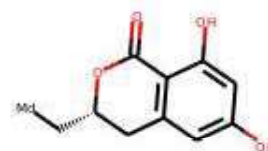
Rank: 1240 Freq: 14

Rank: 1241 Freq: 14

Rank: 1242 Freq: 14

Rank: 1243 Freq: 14

Rank: 1244 Freq: 14

Rank: 1245 Freq: 14
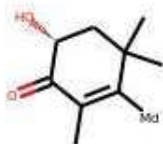
Rank: 1246 Freq: 14

Rank: 1247 Freq: 13

Rank: 1248 Freq: 13
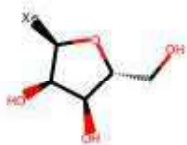
Rank: 1249 Freq: 13
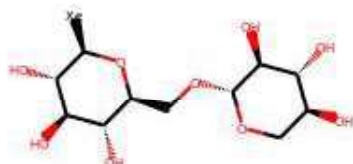
Rank: 1250 Freq: 13

Rank: 1251 Freq: 13
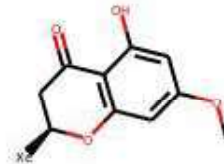
Rank: 1252 Freq: 13

Rank: 1253 Freq: 13

Rank: 1254 Freq: 13
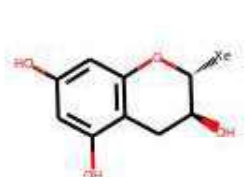
Rank: 1255 Freq: 13

Rank: 1256 Freq: 13

Rank: 1257 Freq: 13

Rank: 1258 Freq: 13
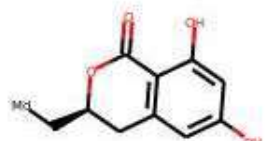
Rank: 1259 Freq: 13
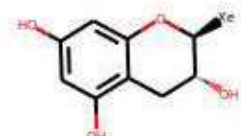
Rank: 1260 Freq: 13
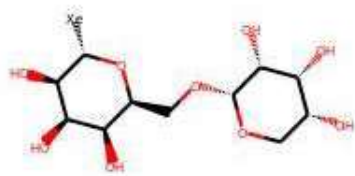
Rank: 1261 Freq: 13


Rank: 1262 Freq: 13

Rank: 1263 Freq: 13
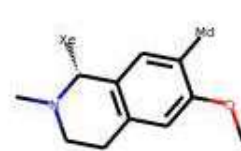
Rank: 1264 Freq: 13
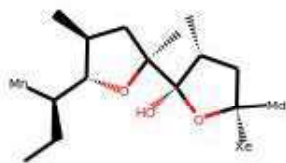
Rank: 1265 Freq: 13
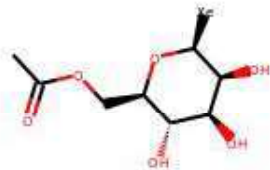
Rank: 1266 Freq: 12
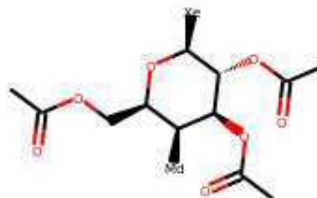
Rank: 1267 Freq: 12
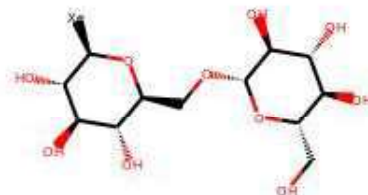
Rank: 1268 Freq: 12
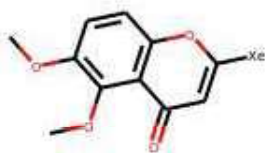
Rank: 1269 Freq: 12
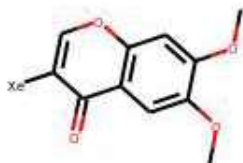
Rank: 1270 Freq: 12

Rank: 1271 Freq: 12
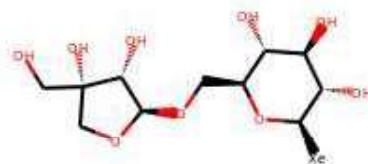
Rank: 1272 Freq: 12
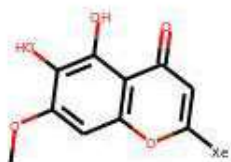
Rank: 1273 Freq: 12

Rank: 1274 Freq: 12

Rank: 1275 Freq: 12

Rank: 1276 Freq: 12
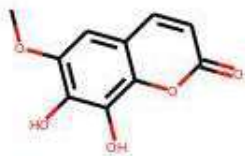
Rank: 1277 Freq: 12

Rank: 1278 Freq: 12

Rank: 1279 Freq: 12
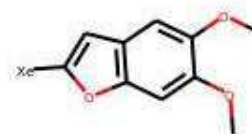
Rank: 1280 Freq: 12

Rank: 1281 Freq: 12
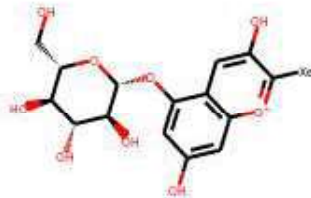
Rank: 1282 Freq: 12
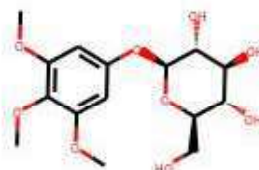
Rank: 1283 Freq: 12

Rank: 1284 Freq: 12

Rank: 1285 Freq: 12

Rank: 1286 Freq: 12

Rank: 1287 Freq: 12


Rank: 1288 Freq: 12
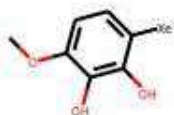
Rank: 1289 Freq: 11

Rank: 1290 Freq: 11
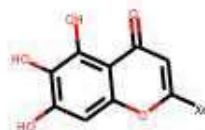
Rank: 1291 Freq: 11

Rank: 1292 Freq: 11
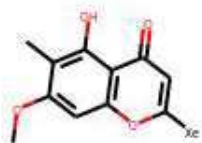
Rank: 1293 Freq: 11
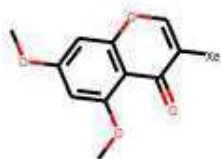
Rank: 1294 Freq: 11
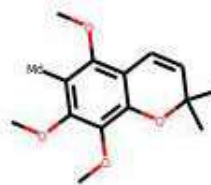
Rank: 1295 Freq: 11
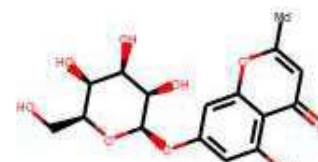
Rank: 1296 Freq: 11

Rank: 1297 Freq: 11

Rank: 1298 Freq: 11

Rank: 1299 Freq: 11

Rank: 1300 Freq: 11
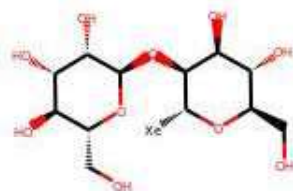

Rank: 1301 Freq: 11

Rank: 1302 Freq: 11

Rank: 1303 Freq: 11

Rank: 1304 Freq: 11

Rank: 1305 Freq: 11
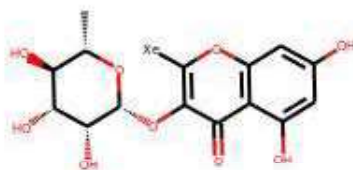
Rank: 1306 Freq: 11
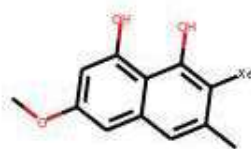
Rank: 1307 Freq: 11

Rank: 1308 Freq: 11
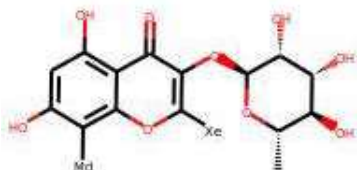
Rank: 1309 Freq: 11

Rank: 1310 Freq: 11
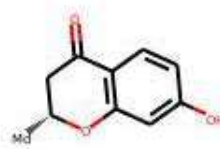
Rank: 1311 Freq: 10
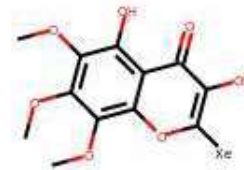
Rank: 1312 Freq: 10

180

Rank: 1313 Freq: 10

Rank: 1314 Freq: 10
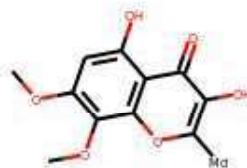
Rank: 1315 Freq: 10

Rank: 1316 Freq: 10

Rank: 1317 Freq: 10

Rank: 1318 Freq: 10
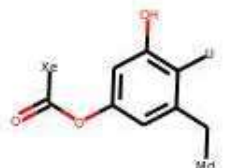
Rank: 1319 Freq: 10

Rank: 1320 Freq: 9
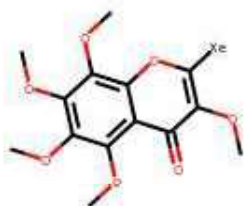
Rank: 1321 Freq: 9
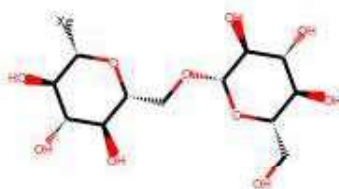
Rank: 1322 Freq: 9

Rank: 1323 Freq: 9
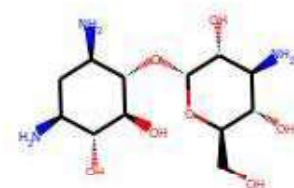
Rank: 1324 Freq: 9

Rank: 1325 Freq: 9

Rank: 1326 Freq: 8
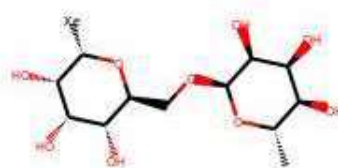
Rank: 1327 Freq: 8

Rank: 1328 Freq: 8

181
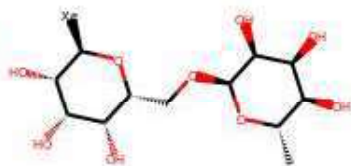
Rank: 1329 Freq: 8

Rank: 1330 Freq: 8
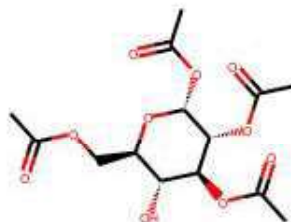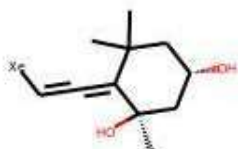
Rank: 1331 Freq: 8
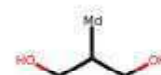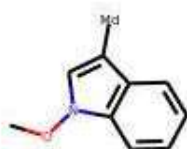
Rank: 1332 Freq: 8
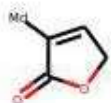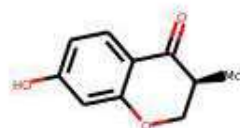
Rank: 1333 Freq: 8
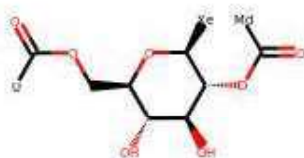
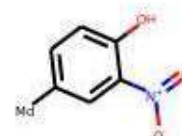Rank: 1334 Freq: 8
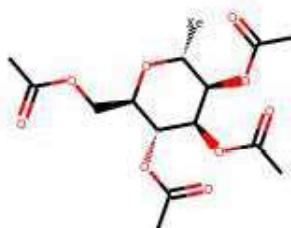
Rank: 1335 Freq: 7
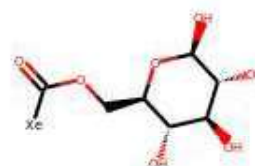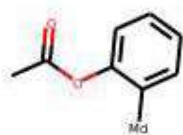
Rank: 1336 Freq: 7

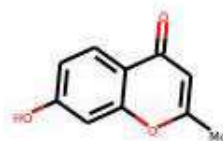Rank: 1337 Freq: 7

Rank: 1338 Freq: 6

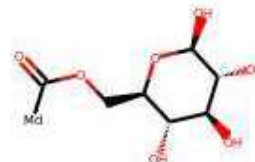Rank: 1339 Freq: 6

Rank: 1340 Freq: 6

Rank: 1341 Freq: 6

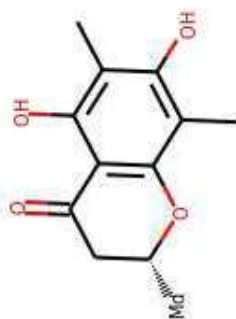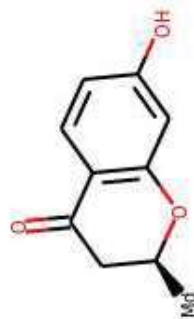Rank: 1342 Freq: 6

Rank: 1343 Freq: 6

Rank: 1344 Freq: 6

Rank: 1348 Freq: 2

Rank: 1346 Freq: 4

Rank: 1350 Freq: 2

Rank: 1345 Freq: 5

Rank: 1349 Freq: 2